

AD _____

Award Number:

W81XWH-12-1-0288

TITLE:

Væ*^cā * Šā æ āÖ^ ^} ā^} ōā ā Šā æ āQā^ ^} ā^} ōā ā! [*^} Ū^&^] q ! Ūā } æā * Ū Ū! • cæ^Á
Ōā &^!

PRINCIPAL INVESTIGATOR:

Ganesh V. Raj MD PhD

CONTRACTING ORGANIZATION:

U) ā^!ā c Ā -Ā^cæ Ū[~ c@ ^•c^!} Ā ^āāÖ^} c!
Dallas TX 75390

REPORT DATE:

October 2014

TYPE OF REPORT:

Annual

PREPARED FOR: U.S. Army Medical Research and Materiel Command
Fort Detrick, Maryland 21702-5012

DISTRIBUTION STATEMENT:

Approved for public release; distribution unlimited

The views, opinions and/or findings contained in this report are those of the author(s) and should not be construed as an official Department of the Army position, policy or decision unless so designated by other documentation.

REPORT DOCUMENTATION PAGE				Form Approved OMB No. 0704-0188	
Public reporting burden for this collection of information is estimated to average 1 hour per response, including the time for reviewing instructions, searching existing data sources, gathering and maintaining the data needed, and completing and reviewing this collection of information. Send comments regarding this burden estimate or any other aspect of this collection of information, including suggestions for reducing this burden to Department of Defense, Washington Headquarters Services, Directorate for Information Operations and Reports (0704-0188), 1215 Jefferson Davis Highway, Suite 1204, Arlington, VA 22202-4302. Respondents should be aware that notwithstanding any other provision of law, no person shall be subject to any penalty for failing to comply with a collection of information if it does not display a currently valid OMB control number. PLEASE DO NOT RETURN YOUR FORM TO THE ABOVE ADDRESS.					
1. REPORT DATE October 2014		2. REPORT TYPE Annual		3. DATES COVERED 30 Sep 2013 - 29 Sep 2014	
4. TITLE AND SUBTITLE Targeting Ligand Dependent and Ligand Independent Androgen Receptor Signaling in Prostate Cancer				5a. CONTRACT NUMBER	
				5b. GRANT NUMBER W81XWH-12-1-0288	
				5c. PROGRAM ELEMENT NUMBER	
6. AUTHOR(S) Ganesh V. Raj MD PhD Email: GANESH.RAJ@UTSouthwestern.edu				5d. PROJECT NUMBER	
				5e. TASK NUMBER	
				5f. WORK UNIT NUMBER	
7. PERFORMING ORGANIZATION NAME(S) AND ADDRESS(ES) . Univeristy of Texas Southwestern Medical Center Dallas , TX 75390				8. PERFORMING ORGANIZATION REPORT NUMBER	
9. SPONSORING / MONITORING AGENCY NAME(S) AND ADDRESS(ES) U.S. Army Medical Research and Materiel Command Fort Detrick, Maryland 21702-5012				10. SPONSOR/MONITOR'S ACRONYM(S)	
				11. SPONSOR/MONITOR'S REPORT NUMBER(S)	
12. DISTRIBUTION / AVAILABILITY STATEMENT Approved for Public Release; Distribution Unlimited					
13. SUPPLEMENTARY NOTES					
14. ABSTRACT We continue to make significant progress in our work with peptidomimetics targeting ligand-dependent and ligand-independent androgen receptor signaling in Prostate Cancer. We have further designed, created, tested and validated over a hundred analogues of our lead compound. We have overcome problems with solubility, off-target effects, toxicity and formulation. We have improved potency of our lead compounds, made some of them more selective for the interaction between the Androgen receptor and select coactivators and are now in the process of optimizing these compounds prior to testing in animal experiments.					
15. SUBJECT TERMS- Prostate cancer, androgen receptor					
16. SECURITY CLASSIFICATION OF:			17. LIMITATION OF ABSTRACT UU	18. NUMBER OF PAGES 56	19a. NAME OF RESPONSIBLE PERSON USAMRMC
a. REPORT U	b. ABSTRACT U	c. THIS PAGE U			19b. TELEPHONE NUMBER (include area code)

Table of Contents

	<u>Page</u>
Introduction.....	4
Body.....	5
Key Research Accomplishments.....	16
Reportable Outcomes.....	17
Conclusion.....	19
References.....	20
Appendices.....	21

Introduction

The androgen receptor (AR) is critical in the normal development and function of the prostate, as well as in prostate carcinogenesis¹. Androgen deprivation therapy is the mainstay in treatment of advanced PCa (PCa); however, after an initial response, the disease inevitably progresses to castration-resistant PCa (CRPC)². Recent evidence suggests that continued AR activation, either in a ligand-dependent (LD) or in a ligand-independent (LI) manner, is commonly associated with CRPC¹. There is an unmet need for novel agents to target both LI and LD AR signaling in CRPC. Our overarching hypothesis is that the disruption of interactions between AR and critical cofactors by targeting structural motifs involved in protein-protein interactions (PPIs) may block both LD and LI activation of AR and represent a novel therapeutic approach for patients with CRPC.

In this grant, we had proposed to design and synthesize peptidomimetics that can more specifically disrupt LD and LI activation of AR. We then wanted to evaluate the mechanism of specific peptidomimetics in blocking AR signaling. Finally, we wanted to evaluate the utility of specific peptidomimetics in animal models and on primary PCa tissue.

In our first year, we had made significant strides in these endeavors. We have created and tested more than 23 variants of the peptidomimetics and have learned to build a better more potent peptidomimetic.

In our second year, we continued on our work from the first year and evaluated pharmacologic properties of our best compounds from year 1. Based on the earlier findings, we have designed and synthesized fifteen second generation peptidomimetic compounds for improving biological activities. We have also synthesized 15- and 20-mer peptides containing WxxLF motif to identify target proteins and to confirm the activities of leading peptidomimetics.

Body

In this grant, our overall goals were to target the androgen receptor in prostate cancer using peptidomimetics for the LxxLL and WxxLF motif using oligo-benzamide scaffolds that are highly specific for and can disrupt the AR-PELP-1 interaction.

We had had a highly productive first year and had made significant strides in our work with peptidomimetics. Towards this end, we had published a critical manuscript in Nature Communications (Ravindranathan et al, Nature Communications 2013) that outlines our work with our leading D2 compound and its remarkable activities on prostate cancer cell lines. This manuscript had been well-received and garnered significant collaborations to further explore these agents. We have further worked on our peptidomimetics and refined their activities.

We had designed tris-benzamide-based molecules to introduce additional functional group from the flanking residues around the LXXLL motif to our lead D2 compound.

* To facilitate the synthesis of tris-benzamide analogues designed to target AR, we had first established the synthetic procedure that allowed us to produce a number of molecules. This standard operating protocol has dramatically enhanced our ability to generate a number of molecules.

* Following the established synthetic protocol, we had synthesized 23 tris-benzamide analogues derived from the leading D2 compound. These compounds were individually evaluated for optimal characteristics by 2-D NMR, stability and toxicity studies prior to full scale studies.

* These tris-benzamide compounds had been examined for their inhibitory activities on cell proliferation and AR function using LNCaP cell line. We found that several molecules had activity comparable to D2: with these modifications, we have gone back to the synthetic procedure to generate more potent modifications.

* To further study these compounds, this year, we started by evaluating the pharmacologic properties of our most promising compounds (within the 23 original compounds and D2). We were struck by the limited solubility of these compounds. While these compounds were biologically active, we could not ascertain the true concentration in vivo that the cells were exposed to. We were unable to reach high enough concentrations to establish a biologically active dose at which 90% of AR activity could be consistently blocked. Since we had established this parameter as the critical step prior to further development, we decided to go back and develop more chemistry to see if we could overcome this primary limitation.

* The simplest option would have been to add a series of polar groups to the D2 peptidomimetic to see if it would increase solubility. However, such an approach would sterically hinder the ability of D2 to fit into the binding pocket of the AR ligand binding domain.

We modeled this using autodock to use which moieties would fit into the helical groove of AR.

Examples of the Autodock modeling is shown below for D2

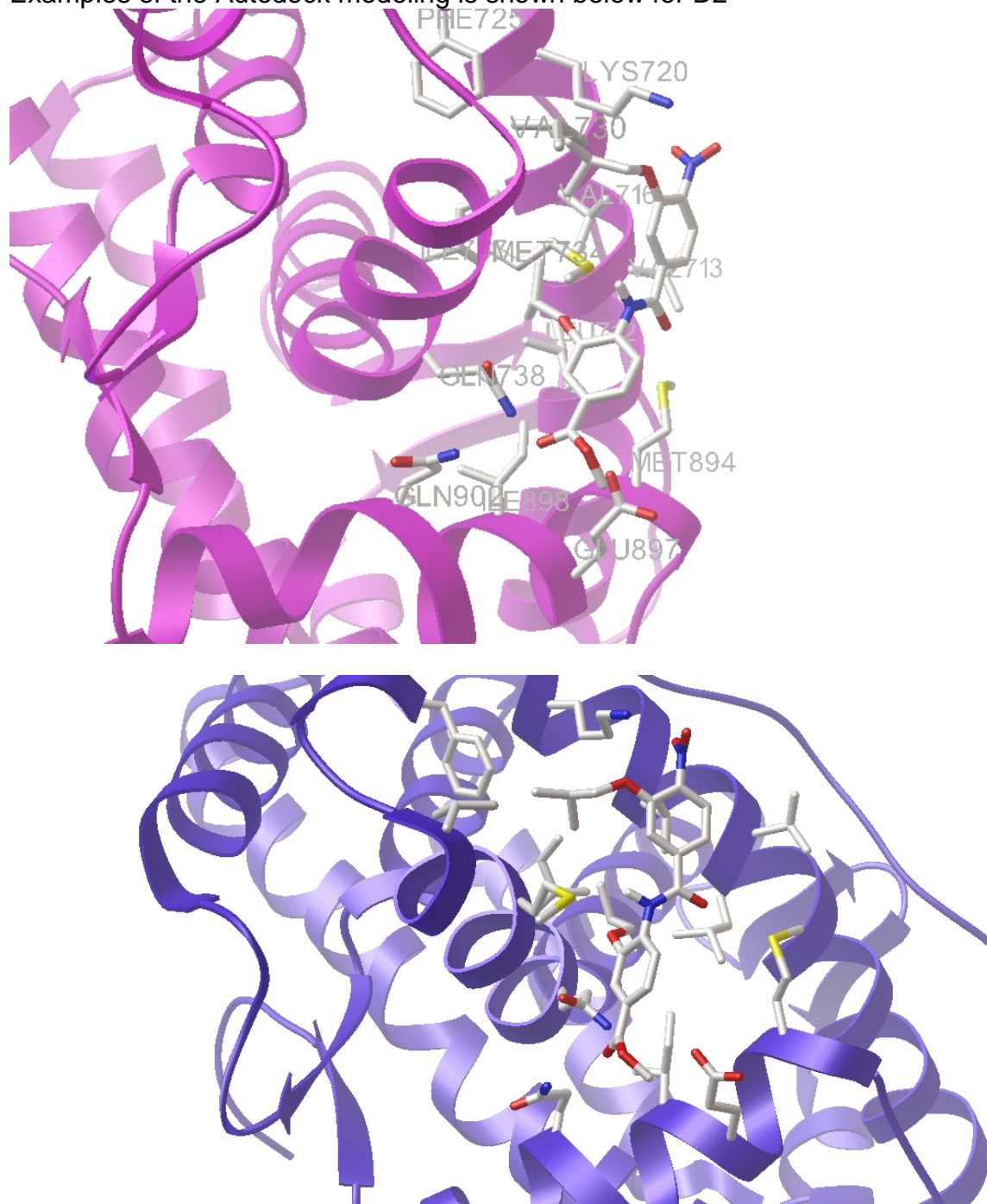


Fig1: D2 autodock structures interacting with the LBD of the androgen receptor. The docking was performed on the androgen receptor (PDB 1XOW). The figures come from the same docking (D2 and 1XOW), only changing molecular presentation (e.g., ribbon or molecular surface).

Based on these results, we decided to systematically evaluate changes in chemistry to optimize a compound that could be more readily translated. We used two distinct approaches. One was a medicinal chemistry approach outlined in the below and the second was a rational structure based drug design.

With the aid of Dr. JungMo Ahn, we evaluated over a hundred compounds that had characteristics of D2, with the goal of improving D2 to a clinically viable candidate. The schematic below represents our approach

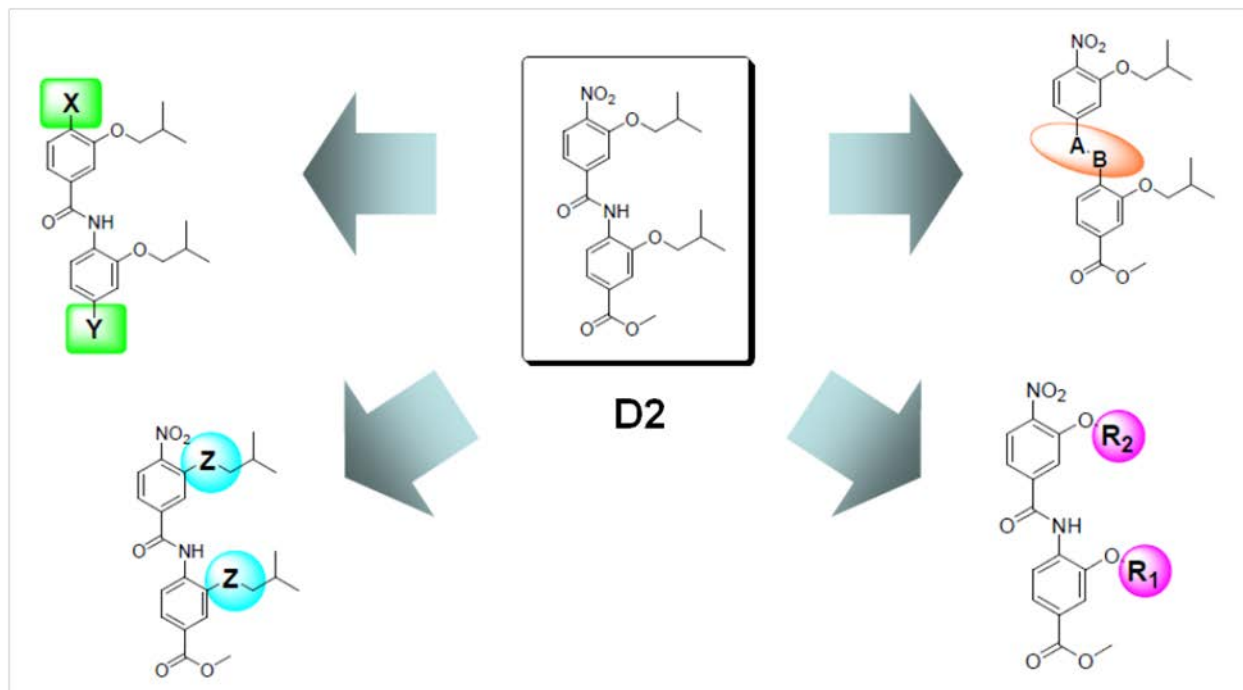


Fig. 2: Derivatization of D2 the medchem approach.

Several compounds were synthesized and evaluated using a systematic medicinal chemistry approach. The readout for these assays included reporter gene assays, endogenous transcripts and effects on DHT-induced proliferation of prostate cancer cells. Representative data from this section is shown below

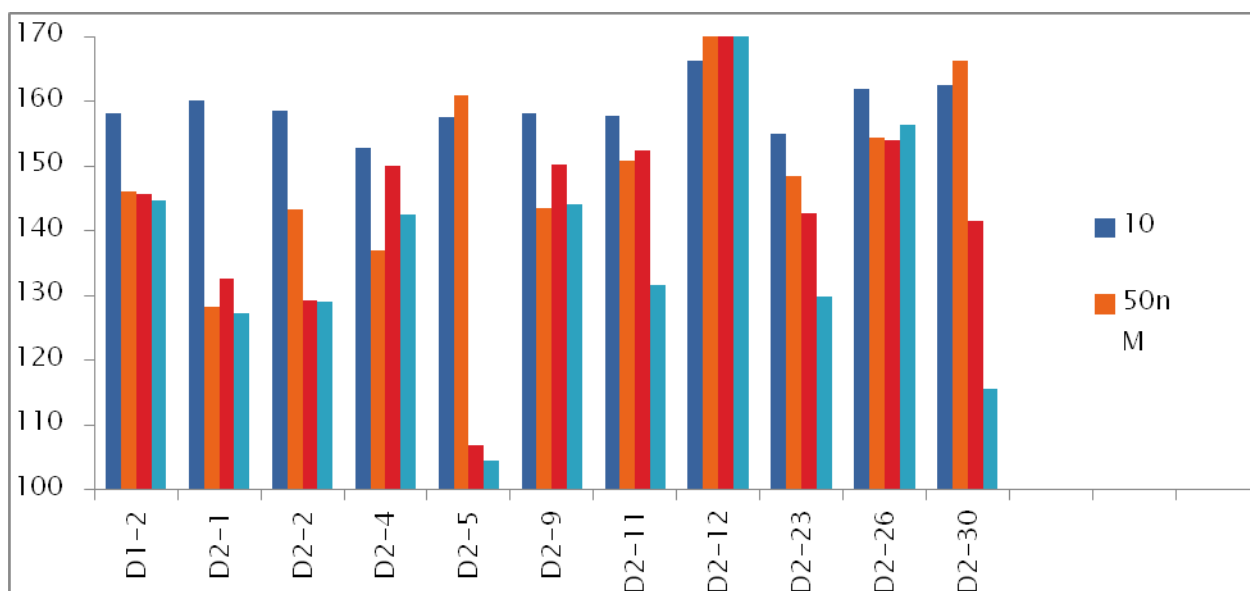
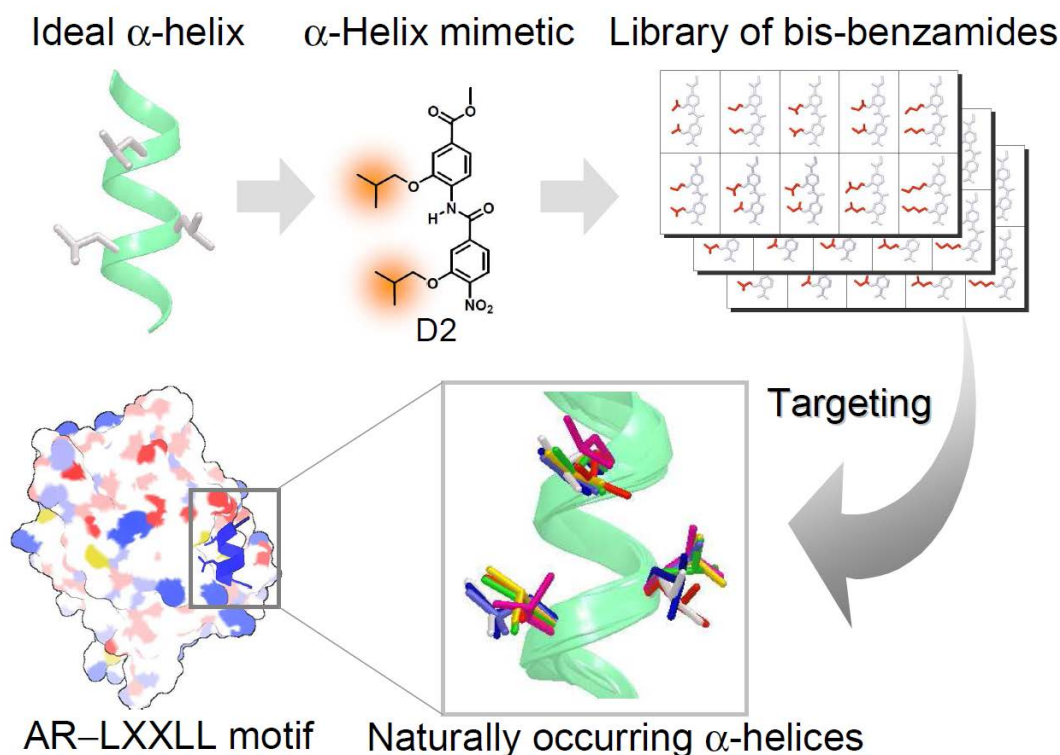


Fig.3 Effect of increasing concentration of D2 derived peptidomimetic on transcription from an androgen-receptor regulated gene in prostate cancer cells. Note D2-5 effectively at 100nM blocks almost 90% of the DHT induced transcript.

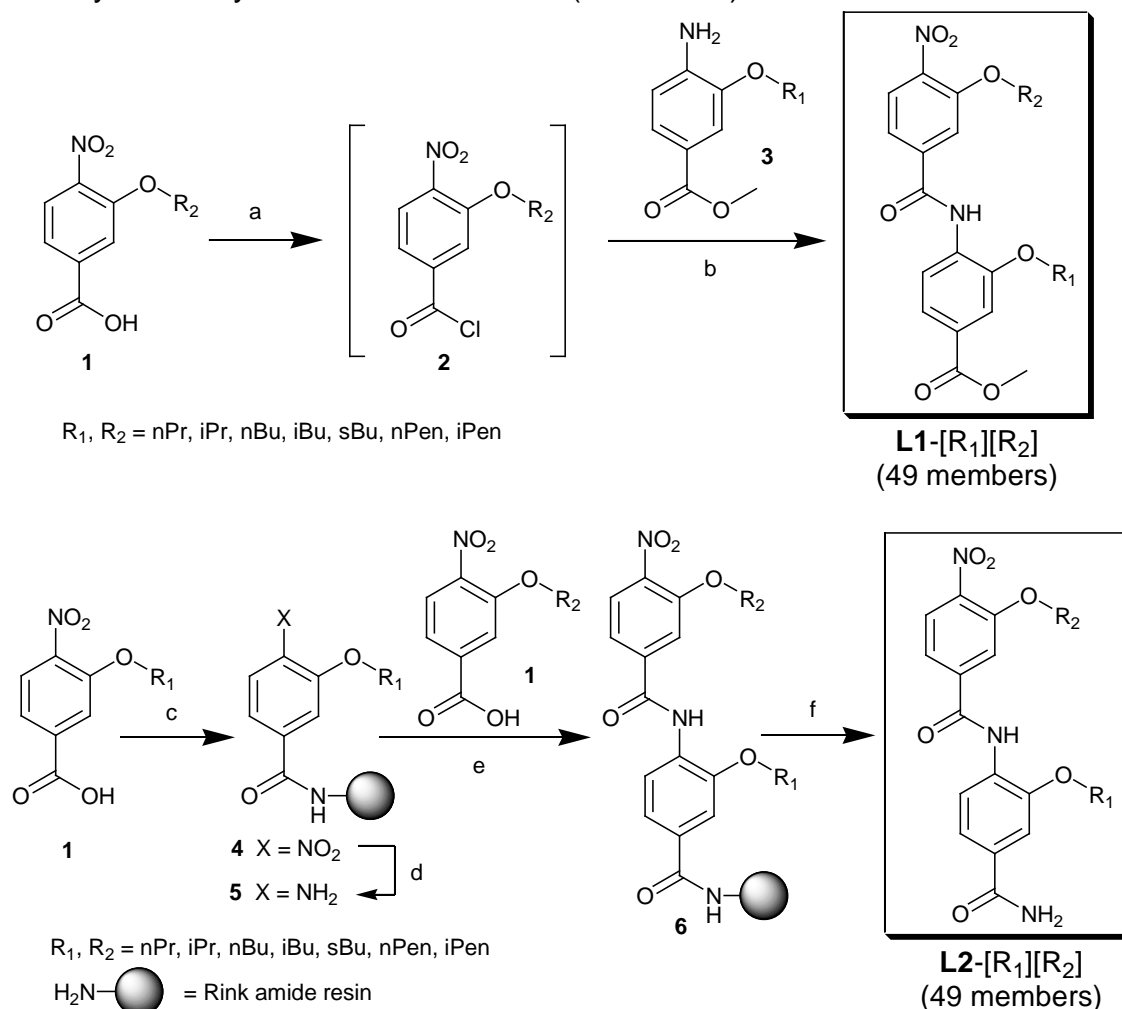
From these analyses in multiple cell lines, multiple assays, we systematically evaluated over a 100 compounds and consistently saw that D2-5 was more potent than D2 and it was worth further evaluating.

In our alternative approach, we rationally looked at the interface between AR and PELP1 and evaluated what an ideal peptidomimetic binding to that site would look like.



Initially, a structural feature of AR was reflected in the library design. Unlike other nuclear receptors, AR has a unique preference for FXXLF (where F is phenylalanine) over LXXLL motifs. In addition to phenylalanine residues of coactivators, AR also binds other related aromatic-rich motifs identified by a phase-display library. Hence, we prepared a series of bis-benzamides containing aromatic groups at the side chains. Surprisingly these compounds, however, showed only modest inhibitory activity in prostate cancer cell growth. Therefore, we used only alkyl groups such as n-propyl, isopropyl, n-butyl, isobutyl, sec-butyl, n-pentyl and isopentyl groups for side chain diversity of the bis-benzamide

We envisioned that screening of these aliphatic chains may find ones which more closely mimic the spatial arrangements of leucine side chains found in the LXXLL motif in complex with AR. Accordingly, a library containing a methyl ester at the C terminus L1-[R₁][R₂] was prepared by reacting 3-alkoxy-4-nitrobenzoyl chlorides **2** with methyl 3-alkoxy-4-aminobenzoates **3** (Scheme 1).²¹



Scheme 1 Syntheses of bis-benzamide libraries. Reagents and conditions: (a) (COCl)₂, cat. DMF, CH₂Cl₂, reflux, 1 h; (b) DIEA, CH₂Cl₂, rt, 4 h; (c) Rink amide resin, HBTU, DIEA, DMF, rt, 12 h; (d) SnCl₂·2H₂O, AcOH/HCl/THF, rt, 24 h; (e) HATU, DIEA, DMF, rt, 24 h; (f) TFA.

The antiproliferative activity of the library L1-[R₁][R₂] were evaluated by MTT assay in prostate cancer cells (Table 1). In a series of compounds containing two identical groups at the side chains, their inhibitory activities changed dramatically. L1-[iBu][iBu] (=D2) showed high potency with the IC₅₀ value of 40 nM, whereas L1-[nBu][nBu] and L1-[sBu][sBu] lost the inhibitory activity. While C5 chains such as n- and isopentyl groups were not active, n- and iso-propyl groups showed modest activity. Among compounds bearing two different substituents, L1-[iPr][iPen], L1-[iBu][iPr], L1-[iBu][nBu] and L1-[iPen][iPr] were found to be potent inhibitors with IC₅₀ values ranging from 57 to 93 nM, which are lower than that of L1-[iBu][iBu] (Table 1). These results suggest that the length of carbon chain as well as substitution pattern of the substituents at the side chains is critical for the ability to suppress the growth of prostate cancer.

In an effort to improve the potency, we constructed a library incorporating a carboxamide at the C-terminus (Scheme 1). The carboxamide is expected to have favorable pharmacological properties such as proteolytic stability and aqueous solubility. The synthesis of the library L2-[R₁][R₂] commenced with the loading of 3-alkoxy-4-nitrobenzoic acids **1** onto Rink amide resin using HBTU. The nitro group in **4** was then reduced with tin (II) chloride under acidic conditions affording the aromatic amine **5**. Examination of coupling agents for the coupling of 3-alkoxy-4-nitrobenzoic acids **1** to the aromatic amine **5** revealed that HATU furnished resin-bound bis-benzamides **6** in high yield, while HBTU and oxalyl chloride were ineffective. After cleavage with TFA, the library of bis-benzamide L2-[R₁][R₂] was obtained with high purity.

Table 1 Inhibitory activity of the library L1-[R₁][R₂] (IC₅₀, nM)^a

R ₁ \ R ₂	nPr	iPr	nBu	iBu	sBu
nPr	115 ^b	NA ^c	NA	NA	114 ^b
iPr	NA	87	NA	106 ^b	NA
nBu	NA	NA	NA	NA	NA
iBu	NA	93	59 ^b	40	133 ^b
sBu	NA	NA	NA	NA	NA
nPen	NA	NA	NA	NA	NA
iPen	NA	63 ^b	NA	120 ^b	NA

^a MTT assay in LNCaP cells. ^b Partial antagonist. ^c NA: not active. Maximum concentration tested is 200 nM.

The library L2-[R₁][R₂] members were also investigated for their inhibitory effects on LNCaP cells (Table 2). In general, bis-benzamides with a carboxamide showed higher potency than those containing a methyl ester suggesting that functional groups at the C-terminus also affect the antitumoral activity and the binding mode of carboxamides to AR would be different from that of methyl esters. Among the compounds tested, L2-[nPr][iBu] and L2-[iBu][sBu] proved to be highly potent with IC₅₀ values of 16 and 24 nM, respectively. These compounds are more active than

the lead compound L1-[iBu][iBu]. Besides, L2-[nPr][nBu], L2-[nBu][nBu], L2-[nBu][sBu] and L2-[iBu][nBu] exhibited the inhibitory activity comparable to L1-[iBu][iBu] with IC₅₀ values of 40–57 nM. In addition to isobutyl group which was found to be a critical substituent in the methyl ester library, n-propyl, n-butyl, and sec-butyl groups from the the carboxamide library showed significant inhibitory activity in LNCaP cells.

Table 2 Inhibitory activity of the library L2-[R₁][R₂] (IC₅₀, nM)^a

R ₁ \ R ₂	nPr	iPr	nBu	iBu
nPr	118	97	50	16
iPr	70	175	74	81
nBu	76	66	51	125 ^c
iBu	NA	68	44	67
sBu	NA	NA	NA	NA
nPen	71	NA	88 ^c	NA
iPen				

^a MTT assay in LNCaP cells. ^b NA: not active. ^c Partial antagonist. Maximum concentration tested is 200 nM.

On the other hand, the order of substituents at the side chain is also crucial for the antitumor activity. For instance, L2-[nPr][iBu], L2-[nBu][sBu] and L2-[iBu][sBu] are highly potent inhibitors, whereas when the order is reversed (e.g., L2-[iBu][nPr], L2-[sBu][nBu] and L2-[sBu][iBu]), their inhibitory activity was lost. However, iso-propyl/n-butyl and n-butyl/n-pentyl groups are interchangeable without a considerable loss in cytotoxicity.

In a genomic pathway, the cellular growth of LNCaP cells is enhanced through the transactivation mediated by AR within the nucleus. Thus to see the effect of bis-benzamides on the transcriptional activity, we performed a androgen-responsive luciferase reporter gene assay (Fig 2). The compounds that showed the high potency were tested (i.e., L2-[nPr][iBu], L2-[iBu][sBu], and L2-[nBu][nBu]) and effectively inhibited DHT-induced transcription from a ARE-luciferase promoter with IC₅₀ values in the nanomolar range. These results demonstrate that the suppression of AR transactivation is responsible for the antiproliferative activities of bis-benzamides.

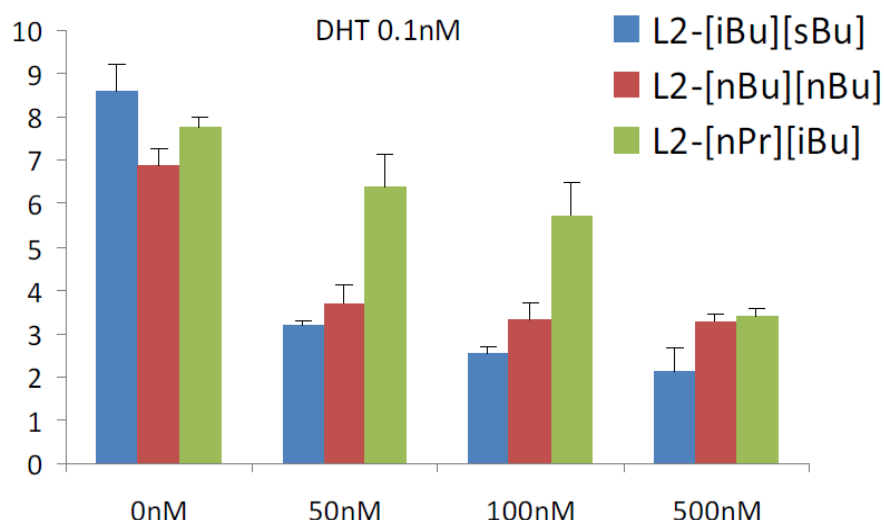


Fig. 2 Effect of bis-benzamides on the AR transactivation. Luciferase activity was measured after treatment with bis-benzamides in the presence of 0.1 nM DHT in LNCaP cells.

Next, we performed co-immunoprecipitation with a coactivator to define the mechanism of the bis-benzamide-induced suppression of AR transactivation (Fig 3). L2-[nPr][iBu] indeed blocked the interaction between AR and PELP1, in which α -helical LXXLL motifs are involved. Therefore, inhibition of the AR–PELP1 interaction by L2-[nPr][iBu] in part accounts for the antitumoral activity in LNCaP cells. On the other hand, L2-[iBu][sBu] and L2-[nBu][nBu] were unable to disrupt the AR–PELP1 interaction in spite of their inhibitory activity in cell growth and AR transcription, indicating that the compounds might target other AR coactivators.

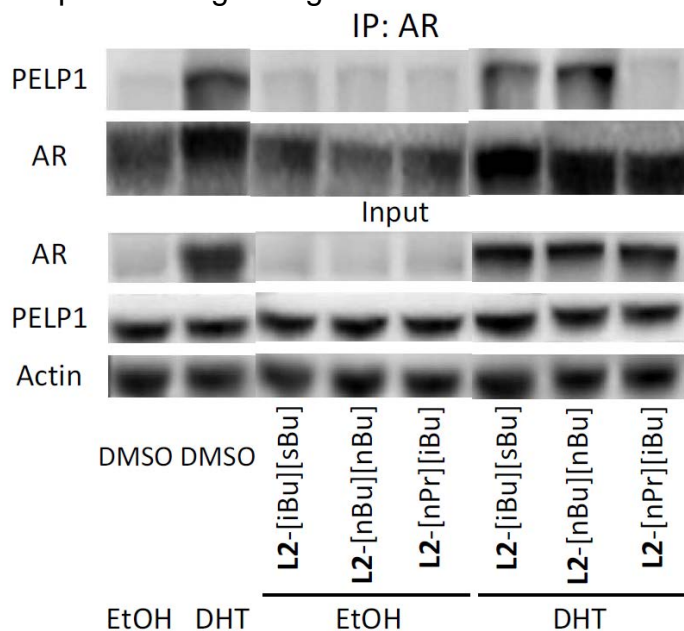


Fig. 3 Effect of bis-benzamides on the AR-PELP1 interactions. LNCaP cells were treated with bis-benzamides in the presence of 10 nM DHT. Cell lysates were then

immunoprecipitated with specific antibody for AR and immunocomplexes were subjected to Western blotting with AR and PELP1 antibodies.

In conclusion, we have generated libraries of bis-benzamides which was designed to target the α -helical LXXLL motif of AR coactivators. To explore the optimal substituents at the side chains, various alkyl groups which differ in substitution pattern and the length of carbon chain were incorporated to the libraries. Their evaluation for the antiproliferative activity against prostate cancer cells identified several potent compounds with IC₅₀ values in the nanomolar range. Among them, L2-[nPr][iBu] was found to suppress the AR transactivation by disrupting the interaction. Impressively, this compound was the same as D2-5 identified from our medicinal chemistry approach.

We are currently further examining this compound using primary tumor explants and will then evaluate it in xenograft models.

Our proposed SOW for each specific aim is shown below along with the progress performed for each SA

Proposed Specific Aim#1 To improve the design and synthesis of peptidomimetics for the LxxLL and WxxLF motif by using oligo-benzamide scaffolds that are highly specific for and can disrupt the AR-PELP-1 interaction, including

Development of LxxLL and WxxLF peptidomimetics by using a tris-benzamide scaffold

- Months 1-3 Designing and synthesizing trisbenzamide variants
- Months 3-12 Testing trisbenzamide variants *in vitro* and confirmation *in vivo* using co-immunoprecipitation experiments
- Months 13-18 Testing trisbenzamide variants on AR genomic signaling, proliferation
- Months 19-24 Evaluation of the data and publication of results

Work Performed to date: As shown above, we have evaluated several trisbenzamide peptidomimetics using coIP experiments, tested them *in vitro* and confirmed their effects on AR genomic signaling and proliferation. We have improved our medicinal chemistry efforts and have identified D2-5 as a prototypical LxxLL compound. A manuscript outlining this data is being readied for publication. Essentially, most of this aim has been performed.

Proposed work for Specific Aim #1 in year 3: We will continue to improve our peptidomimetics and optimize them prior to publication

Proposed Specific Aim #2: To mechanistically characterize the ability of the peptidomimetics to modulate AR signaling in PCa cells, including the

Effect on genomic signaling and AR-modulated gene expression signatures

- Months 1-9 Testing peptidomimetics on LD and LI activity in Q PCR analyses
- Months 10-18 Microarray evaluation and analyses
- Months 19-24 Evaluation of the data and publication of results

Effect on nuclear translocation of AR

- Months 1-9 Optimization of nuclear translocation assays using confocal microscopy
- Months 10-14 Evaluation of effect of peptidomimetics on AR nuclear translocation
- Months 15-24 Biochemical validation of results from confocal experiments
- Months 25-27 Evaluation of the data and publication of results

Work Performed to date: As shown above, we have evaluated several trisbenzamide peptidomimetics using Q-PCR experiments and have set up more detailed studies for testing effect on gene expression signatures. Given that RNA-Seq may offer more information than microarray studies, we will use RNA-Seq rather than microarray analyses and are in the process of setting this up.

Additionally, we have focused our studies on the effect of peptidomimetics targeting AR nuclear translocation towards the biochemical experiments with validation with confocal experiments. We believe that this approach enables more rapid analyses of the effect of these agents on AR nuclear translocation.

Proposed work for Specific Aim #2 in year 3: Given the cost and labor involved in RNA-Seq and confocal experiments, we will perform these once we have isolated lead compounds. We anticipate that we will validate the findings from Q-PCR and biochemical studies.

Proposed Specific Aim #3: To study the effect of peptidomimetics on AR signaling in PCa cells in vivo, including the

Effect on CWR22v1 xenografts

- Months 7-12 Animal experiments with LD pathway
- Months 13-18 validation of LD pathway with biochemical studies
- Months 19-24 Animal experiments with LI pathway
- Months 25-33 validation of LI pathway with biochemical studies
- Months 33-36 Evaluation of the data and publication of results

Effect on human explants

- Months 1-32 Explant experiments
- Months 1-18 validation of LD pathway with biochemical studies
- Months 7-24 validation of LI pathway with biochemical studies
- Months 25-36 Evaluation of genetic signatures induced by LD and LI pathways
- Months 33-36 Evaluation of the data and publication of results

Work Performed to date: To optimize our resources and studies, we have performed explant experiments with several peptidomimetics and are in the process of validating these studies. We will reserve the xenograft studies for the lead compounds in each arm

Proposed work for Specific Aim #2 in year 3: Given the cost and labor involved in xenograft experiments, we will perform these once we have isolated lead compounds. We anticipate that we will validate the findings from explant studies.

Key Research Accomplishments

1. We have systematically designed, synthesized and evaluated over a 100 compounds to improve pharmacologic properties of D2
2. We have created a lead compound that appears to be active at 10nM
3. Both our medicinal chemistry efforts and rational design efforts lead to the identification of the same molecule. Further work is ongoing

Reportable Outcomes

1. We have published our approach to peptidomimetic design
Tailoring peptidomimetics for targeting protein-protein interactions. Akram ON¹, DeGraff DJ², Sheehan JH³, Tilley WD⁴, Matusik RJ⁵, Ahn JM⁶, Raj GV⁷. *Mol Cancer Res.* 2014 Jul;12(7):967-78. doi: 10.1158/1541-7786.MCR-13-0611. Epub 2014 Mar 18
2. We have published on our understanding of PELP1 as a central target
Gonugunta VK, Miao L, Sareddy GR, Ravindranathan P, Vadlamudi R, Raj GV. The social network of PELP1 and its implications in breast and prostate cancer. *Endocr Relat Cancer.* 2014 May 23. pii: ERC-13-0502. [Epub ahead of print] PMID: 24859989
3. We have worked to extend the peptidomimetics to AR-NF1 complexes
Grabowska MM¹, Elliott AD, DeGraff DJ, Anderson PD, Anumanthan G, Yamashita H, Sun Q, Friedman DB, Hachey DL, Yu X, Sheehan JH, Ahn JM, Raj GV, Piston DW, Gronostajski RM, Matusik RJ. NFI transcription factors interact with FOXA1 to regulate prostate-specific gene expression *Mol Endocrinol.* 2014 Jun;28(6):949-64. doi: 10.1210/me.2013-1213. Epub 2014 May 6.
4. We have obtained further peer-reviewed funding from the DOD
Raj, co PI
DOD transformative grant W81XWH-13-2-0093
5. We have overcome potentially fatal solubility issues with our agents with two distinct approaches that pointed to the same type of compound
6. We have published extensively using the explant model
Daniel AR, Gaviglio AL, Knutson TP, Ostrander JH, D'Assoro AB, Ravindrathan P, Peng Y, Raj GV, Yee D, Lange CA. Progesterone receptor-B enhances estrogen responsiveness of breast cancer cells via scaffolding PELP1- and estrogen receptor-containing transcription complexes. *Oncogene* 2014 Jan 27. [Epub ahead of print] PMID: 24469035.

Wang S, Kollipara RK, Srivastava N, Li R, Ravindranathan P, Hernandez E, Freeman E, Humphries CG, Kapur P, Lotan Y, Fazli L, Gleave ME, Plymate R, Raj GV, Hsieh JT, Kittler R. Ablation of the oncogenic transcription factor ERG by deubiquitinase inhibition in prostate cancer. *Proc Natl Acad Sci U S A.* 2014 Mar 18; 111(11): 4251-6. Epub 2014 Mar 3. PMID: 24591637.

Centenera MM, Raj GV, Knudsen KE, Tilley WD, Butler LM. Ex vivo culture of human prostate tissue and drug development. *Nat Rev Urol* 2013 Aug; 10(8): 483-7. Epub 2013 Jun 11. PMID: 23752995

Schiewer MJ, Goodwin JF, Han S, Brenner JC, Augello MA, Dean JL, Liu F, Planck JL, Ravindranathan P, Chinnaiyan AM, McCue P, Gomella LG, Raj GV, Dicker AP, Brody JR, Pascal JM, Centenera MM, Butler LM, Tilley WD, Feng FY, Knudsen KE. Dual roles of PARP-1 promote cancer growth and progression. *Cancer Discov.* 2012 (12):1134-49

Ravindranathan P, Lee TK, Yang L, Centenera MM, Butler L, Tilley WD, Hsieh JT, Ahn JM, Raj GV. Peptidomimetic targeting of critical androgen receptor-coregulator interactions in prostate cancer. *Nat Commun* 2013; 4:1923. PMID: 23715282.

Centenera MM, Gillis JL, Hanson AR, Jindal S, Taylor RA, Risbridger GP, Sutherland PD, Scher HI, Raj GV, Knudsen KE, Yeadon T; Australian Prostate Cancer BioResource, Tilley WD, Butler LM. Evidence for efficacy of new Hsp90 inhibitors revealed by ex vivo culture of human prostate tumors. *Clin Cancer Res.* 2012 Jul 1;18(13):3562-70.

Conclusion

We continue to make progress in our work with peptidomimetics targeting ligand-dependent and ligand-independent androgen receptor signaling in prostate Cancer. We have now identified a potential lead compound and intend to study it in animal experiments.

References

1. Centenera MM, Raj GV, Knudsen KE, Tilley WD, Butler LM. Ex vivo culture of human prostate tissue and drug development. *Nat Rev Urol*. 2013 Aug;10(8):483-7
2. Ravindranathan P, Lee TK, Yang L, Centenera MM, Butler L, Tilley WD, Hsieh JT, Ahn JM, Raj GV. Peptidomimetic targeting of critical androgen receptor-coregulator interactions in prostate cancer. *Nat Commun*. 2013;4:1923
3. Schiewer MJ, Goodwin JF, Han S, Brenner JC, Augello MA, Dean JL, Liu F, Planck JL, Ravindranathan P, Chinnaiyan AM, McCue P, Gomella LG, Raj GV, Dicker AP, Brody JR, Pascal JM, Centenera MM, Butler LM, Tilley WD, Feng FY, Knudsen KE. Dual roles of PARP-1 promote cancer growth and progression. *Cancer Discov*. 2012 Dec;2(12):1134-49
4. Centenera MM, Gillis JL, Hanson AR, Jindal S, Taylor RA, Risbridger GP, Sutherland PD, Scher HI, Raj GV, Knudsen KE, Yeadon T; Australian Prostate Cancer BioResource, Tilley WD, Butler LM. Evidence for efficacy of new Hsp90 inhibitors revealed by ex vivo culture of human prostate tumors. *Clin Cancer Res*. 2012 Jul 1;18(13):3562-70
5. Chung PH, Gayed BA, Thoreson GR, Raj GV. Emerging drugs for prostate cancer. *Expert Opin Emerg Drugs*. 2013 Dec;18(4):533-50.

Molecular Cancer Research



Tailoring Peptidomimetics for Targeting Protein–Protein Interactions

Omar N. Akram, David J. DeGraff, Jonathan H. Sheehan, et al.

Mol Cancer Res 2014;12:967-978. Published OnlineFirst March 18, 2014.

Updated version Access the most recent version of this article at:
doi:[10.1158/1541-7786.MCR-13-0611](https://doi.org/10.1158/1541-7786.MCR-13-0611)

Cited Articles This article cites by 101 articles, 27 of which you can access for free at:
<http://mcr.aacrjournals.org/content/12/7/967.full.html#ref-list-1>

E-mail alerts [Sign up to receive free email-alerts](#) related to this article or journal.

Reprints and Subscriptions To order reprints of this article or to subscribe to the journal, contact the AACR Publications Department at pubs@aacr.org.

Permissions To request permission to re-use all or part of this article, contact the AACR Publications Department at permissions@aacr.org.

Review

Tailoring Peptidomimetics for Targeting Protein–Protein Interactions

Omar N. Akram¹, David J. DeGraff⁶, Jonathan H. Sheehan⁴, Wayne D. Tilley⁵, Robert J. Matusik³, Jung-Mo Ahn², and Ganesh V. Raj¹

Abstract

Protein–protein interactions (PPI) are a hallmark of cellular signaling. Such interactions occur abundantly within the cellular milieu and encompass interactions involved in vital cellular processes. Understanding the various types, mechanisms, and consequences of PPIs with respect to cellular signaling and function is vital for targeted drug therapy. Various types of small-molecule drugs and targeted approaches to drug design have been developed to modulate PPIs. Peptidomimetics offer an exciting class of therapeutics as they can be designed to target specific PPIs by mimicking key recognition motifs found at critical points in the interface of PPIs (e.g., hotspots). In contrast to peptides, peptidomimetics do not possess a natural peptide backbone structure but present essential functional groups in a required three-dimensional pattern complimentary to the protein-binding pocket. This design feature overcomes many limitations of peptide therapeutics including limited stability toward peptidases, poor transport across biologic membranes, and poor target specificity. Equally important is deciphering the structural requirements and amino acid residues critical to PPIs. This review provides an up-to-date perspective of the complexity of cellular signaling and strategies for targeting PPIs in disease states, particularly in cancer, using peptidomimetics, and highlights that the rational design of agents that target PPIs is not only feasible but is of the utmost clinical importance. *Mol Cancer Res*; 12(7): 967–78. ©2014 AACR.

Introduction

Protein–protein interactions (PPI) play a fundamental role in cellular signaling pathways. Such interactions are necessary for cell maintenance and healthy metabolic function, which together combine to ensure proper functioning of an organism. Metabolic diseases, and in particular cancer, form a complex network of PPIs that change not only at the initiation and temporarily during disease progression but also in the presence of exogenous therapeutic modulators (1). Understanding the mechanisms behind PPIs, how and why various protein subunits interact under specific conditions, and the consequences of these interactions are fundamental to drug development. Thus, it can be beneficial to either inhibit or promote certain PPIs to realign a system

toward homeostasis. However PPIs are complex. Research has recently found that downregulation of a key cellular regulator by treatment with specific siRNAs can lead to reprogramming of gene expression pathways elicited by that protein by redirecting associated proteins to new chromatin-binding sites (1). This demonstrates that modulating a PPI may not necessarily result in realignment to homeostasis but may exacerbate the perturbation by activating alternative signaling pathways. Thus, a more subtle approach, which aims to attenuate a PPI, may prove more effective than completely silencing a given function of a protein (2). Various small-molecule drugs including small synthetic organic molecules, peptides, and proteins have been designed to target specific PPIs. Each possesses advantages and disadvantages with respect to efficacy, specificity, bioavailability, and process of synthesis. Gaining specificity and efficacy is improved in our view by designing molecules based on structural knowledge of PPI interfaces. The effective development and testing of these molecules requires a high-throughput approach. One approach, which addresses robustness, avoids siRNA strategies, and is amenable to high-throughput synthesis and evaluation, is peptidomimetics. These are a valuable class of therapeutic agents, which can be rationally designed to block specific PPIs.

Peptidomimetics (also called peptide mimics) are small organic molecules bearing an identifiable resemblance to peptides or peptide segments of proteins. They can be designed by either modification of an existing peptide or introduction of similar molecules that mimic α -amino acids

Authors' Affiliations: ¹Department of Urology, University of Texas Southwestern Medical Center, Dallas; ²Department of Chemistry, University of Texas at Dallas, Richardson, Texas; ³Department of Urologic Surgery, Vanderbilt University Medical Center; ⁴Department of Biochemistry (Center for Structural Biology), Vanderbilt University, Nashville, Tennessee; ⁵Dame Roma Mitchell Cancer Research Laboratories and the Adelaide Prostate, Cancer Research Centre, School of Medicine, Hanson Institute Building, University of Adelaide, Adelaide, Australia; and ⁶Penn State College of Medicine, Milton S. Hershey Medical Center, Hershey, Pennsylvania

Corresponding Author: Ganesh V. Raj, Department of Urology, University of Texas Southwestern Medical Center, 5323 Harry Hines Blvd. J8130, Dallas, TX 75390. Phone: 214-648-8532; Fax: 214-648-8786; E-mail: ganesh.raj@utsouthwestern.edu

doi: 10.1158/1541-7786.MCR-13-0611

©2014 American Association for Cancer Research.

such as peptoids and β -peptides. Peptidomimetics overcome the disadvantages of pure peptide-based drugs, which include limited stability toward proteolysis by peptidases, poor transport properties through biologic membranes such as the intestines and cell membranes, low oral bioavailability, rapid excretion, and poor target specificity resulting from the flexible nature of peptides. In contrast, peptidomimetics offer conformationally restricted structures potentially minimizing cross-target interactions, better transport properties through biologic membranes, improved resistance to degradation by peptidases and other enzymes, and resistance to immune responses (3, 4). To achieve these properties, peptides have been chemically modified to include unnatural amino acid substitutions, backbone amide bond modifications, or rigid scaffolds or addition of hydrophobic residues (5–7). Whereas peptidomimetics do not possess a natural peptide backbone structure, they retain the capability to interact with the same target protein of interest by arranging essential functional groups (i.e., pharmacophores) in a required 3-dimensional (3D) pattern complementary to a binding pocket in a protein. Thus, a peptidomimetic can be rationally designed to achieve desired effects on cellular signaling pathways by targeting specific PPI motifs. This review focuses on current strategies for using peptidomimetics to target PPIs in disease states, with an emphasis on cancer, as well their potential use as next-generation therapeutic agents.

Targeting PPIs in Biology

Understanding PPIs is fundamental to deciphering molecular signaling phenotypes of disease (8), as PPIs regulate critical cellular functions such as cell growth, repair, gene transcription, translation, intra- and extracellular signaling (9). PPIs take place when 2 or more proteins bind together to carry out specific cellular functions or to initiate a cascade of events, which facilitates downstream cellular functions within specific tissues of organs.

Complexity of PPIs in biology

More than 5,000 PPIs have been demonstrated to occur using full-length human open reading frames (ORF; ref. 10) and a combination of ORF-based clones and cDNA libraries (11). The recent use of a high-throughput immunoprecipitation combined with mass spectrometry revealed more than 300,000 protein interactions involved in gene transcription and signaling (12) indicating the abundance of PPIs.

Fundamentally, all disease states have roots in aberrant cellular signaling, from cancer, cardiovascular disease, diabetes mellitus, inflammatory disorders, and infectious diseases. Cancer arguably represents the most complex metabolic and genetic disease, with each type displaying unique cellular events in its initiation, progression, and metastases. For instance, tumorigenic B cells in human lymphoma are aided and abetted by Bcl-2 and Bcl-xL proteins, which act to block cell apoptosis by inhibiting pro-apoptotic proteins Bax and Bak (13). In prostate cancer, the androgen receptor (AR) signaling is persistent despite absence of ligand, due to its

interaction with a myriad of transcription factors and signaling proteins (14, 15). In each case, the mode of PPI may differ significantly and each interaction potentially forms part of a transient, stable, specific, or nonspecific complex (12). For instance, is it possible for the antiapoptotic actions of Bcl-2 and Bcl-xL to be replaced by other proteins, which bind Bak and Bax. Downregulation of BAG1 (Bcl-2-associated AthanoGene-1), a putative coregulator of Bcl-2, decreases Bcl-2 protein expression, but the expression of the proapoptotic protein Bax is not affected. Further analysis shows that BAG3 expression is upregulated to compensate for the deregulation of BAG1, thus stabilizing the protumorigenic activity of Bcl-2 (16).

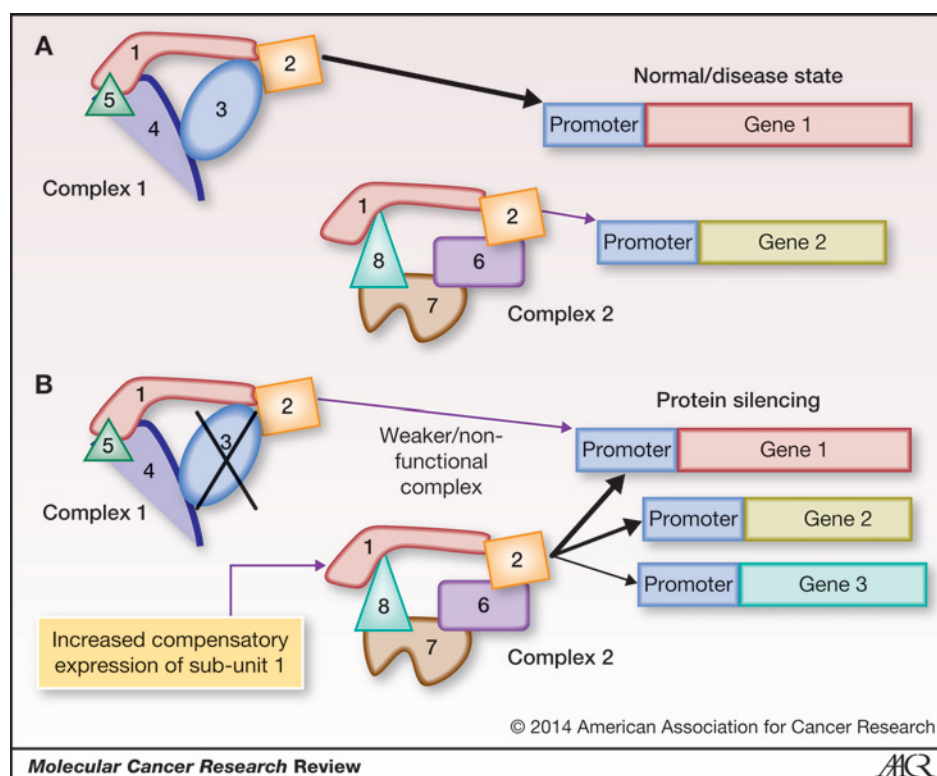
In prostate cancer, AR is the critical driver, even under conditions of androgen ablation. Maintenance of AR activity following androgen ablation can occur due to amplification of AR, deregulation of the expression of AR coregulators, intratumoral production of androgens, gain-of-function AR mutations, and indirect AR activation by growth factors, cytokines (15). Recently, it was also shown that AR can be activated via estrogen receptor- α (ER α) signaling by binding to the PELP1/ER α complex, thus bypassing its requirement for binding of its cognate ligand (17). In addition, the recent identification of AR variants (ARVs), which form heterodimers with the full-length AR (18, 19), in advanced prostate cancer provides a mechanism whereby PPIs contribute to the progression of this lethal disease. Furthermore, the PPIs between AR and critical coregulators, such as SRC-3, may enable control of additional cellular functions (12). For example, SRC-3, a multifunctional transcriptional coregulator involved in cellular growth programs (20–23) including adipogenesis and energy balance (24) as well as control of mRNA translation of pro-inflammatory cytokines (25), also associates with multiple other coregulators including CBP/p300 and nuclear receptors such as AR and ER α (12).

Cistrome (genome-wide chromatin binding) analysis aided by high-throughput chromatin immunoprecipitation (ChIP) sequencing experiments of various transcription factors shows the genomic location of transcription factor-binding sites is altered when expression of specific protein factors (i.e., pioneer factors required for chromatin accessibility) are enhanced or suppressed (1, 26). Intriguingly, when specific PPIs are disrupted, alternative PPIs may compensate and enable activation of the associated signaling pathway (Fig. 1). Understanding these unique events within disease states is fundamental to designing organic molecules for therapeutic targeting. Rather than completely ablating a protein, it may be beneficial to target a critical surface area that acts as a focal point of interaction between specific proteins to modulate its function. Such an approach could prevent inappropriate proteins being recruited to replace critical "disease-promoting" factors present in a PPI complex.

Druggable pathways in cancer

Delineation of signaling pathways involved in the development of cancerous phenotypes, including decreased cell apoptosis, rapid cell proliferation, and increased cell survival,

Figure 1. Cellular signaling adaptation to protein silencing. Cellular signaling is a complex process involving a cascade of PPIs. The depicted schematic represents a view of the complexity of targeting protein interactions for disease therapy. A, within a normal cellular or disease state, protein subunit 1 (such as a transcriptional cofactor) may exhibit promiscuous binding to form separate complexes, which bind different gene promoter sequences with different affinities. B, when a protein subunit in complex 1 is silenced (e.g., subunit 3), subunit 1 is overexpressed as a compensatory mechanism, which in turn activates complex 2 to bind gene 1 with higher affinity or indeed another gene promoter, thus altering the transcriptional program of complexes 1 and 2.



have enabled development of therapeutic agents targeting critical drivers (27–32). Traditional (and relatively nonspecific) "catch-all" therapies have focused on DNA chelating agents (e.g., cisplatin) and radiotherapy aimed at targeting rapidly dividing cells (33–35). However, poor specificity, a severe side effect profiles, and often poor outcomes, particularly in late-stage cancers (33, 36), require re-evaluation of these approaches and the identification of more specific targeted therapies. Identification of a specific target or signaling pathway in cancer can be frustrating, as signaling networks can be inconsistently involved, characterized by promiscuous and overlapping pathways or redundant. The complexity in targeting specific proteins is highlighted by the examples of MSL (responsible for histone H4 lysine 16 acetylation) and NSL (responsible for histone H4 lysine 5 and 6 acetylation) protein complexes, both of which contain the transcriptional coregulator MYST1 but with divergent substrate specificities (37). Thus, targeting MSLs may not affect the cellular or cancer phenotype. Other targets for therapeutic modulation include PPIs found in several of the common pathways linked to cancer (Table 1; ref. 38). Consideration should be given to the existence of alternative pathways to counteract the effect of their therapeutic modulation.

Categories of PPIs

There are several types of PPIs, each with unique binding characteristics and functionalities. Each type requires analysis and deconvolution of signaling effects after altering a specific PPI, either by downregulation of the protein or disruption using synthetic organic molecules. Knowledge of these bind-

ing mechanisms with respect to their occurrence in specific PPIs will provide better approaches to targeted therapy. PPIs can be classified broadly into 4 different categories:

1. Protein–protein docking interactions, which occur between similar sized proteins or protein domains and are generally more rigid due to steric constraints (e.g., seen in heterodimers where binding strength is relatively than homodimers; ref. 39).
2. Protein receptor–ligand docking, characterized by tighter binding due to binding pockets within the interaction sites, which can render the interaction rigid. However, the interaction can change conformation to allow induced fit of the ligand within the receptor (40).
3. Rigid ligand with a flexible receptor allows for a larger-than-usual ligand to bind the receptor by virtue of the receptors flexibility. Under normal circumstances, energy penalties are incurred if the ligand–receptor interface requires additional binding (e.g., via van der Waals) due to the large size of the ligand. This is avoided by the rigid nature of the ligand allowing for a more energetically favorable binding conformation (41).
4. Flexible ligand with a rigid receptor is characterized by a smaller ligand compared with the receptor docking site, resulting in a less rigid binding conformation. The flexible nature of the ligand allows numerous binding conformations with the receptor (42). Thus, in such a binding interaction, the challenge is to determine the most energetically favorable conformation (43).

Table 1. Potential targets for peptidomimetic modulation in common tumorigenic pathways

Pathway	Target protein(s)	Cancers	Examples of desired signaling effect
JAK/STAT	EGF receptor, STAT	Head, neck, breast, lung	STAT-STAT homodimer disruption. Decreased STAT-mediated gene activation
Notch	Notch receptors	Breast, melanoma, medulloblastoma	Notch/ER α complex or other Notch cofactor complex disruption. Decreased ER α signaling
MAPK/ERK	RAS	Colon, pancreatic, others	RAS-SOS complex disruption. Decreased JUN/FOS-mediated gene activation
PI3K/AKT	AKT/C-RAF	Glioblastomas, lung, melanomas/breast ovarian, thyroid, others	RAS-RAF complex disruption. Decreased JUN/FOS-mediated gene activation
NF- κ B	REL-A, p50	B-cell, Hodgkin, T-cell lymphomas	p50/REL-A complex disruption. Decreased NF- κ B gene activation
Wnt	Tcf-Lef	Intestinal adenocarcinomas, myeloid leukemia, prostate	β -Catenin/Tcf-Lef complex disruption. Decreased Tcf-Lef-mediated gene activation
TGF β	SMAD	Lung, pancreatic ductal adenocarcinoma, colon, prostate	SMAD cofactor complex disruption
AR	AR coregulators	Prostate, breast	AR-PELP1 complex disruption. Decreased AR-mediated gene activation
ER α	ER coregulators	Prostate, breast	A1B1-HER complex disruption. Decreased ER α -mediated gene activation

Utility and Limitations of Peptide-Based Therapy

Peptides are short chains of amino acid monomers linked by peptide (amide) bonds. The peptide bond is a covalent bond made of the backbone carboxylic acid group of one amino acid and the backbone amino group of another. Peptide therapy was initially based on mimicking an endogenous peptide found to be lacking within a disease state, designed to enhance or replace the effect of a natural peptide. A classic example is the human analogue of insulin, administered to patients with insulin-dependent diabetes. Initially purified from bovine and porcine (44), insulin is now routinely manufactured via recombinant methods as pro-insulin (45). However, critical limitations of insulin and exogenous peptide administration in general, including instability in water and low bioavailability (e.g., poor cell permeability and susceptibility to metabolic degradation), are apparent when administered orally (46). For this reason, injectable pro-insulin is a more efficacious approach. Research is focused on developing less invasive delivery routes including inhalation, transdermal, buccal, and intranasal routes (45).

Other forms of peptide therapy include protein-based hormone administration for cancer treatment. A commonly used strategy for prostate cancer treatment is synthetic luteinizing hormone releasing hormone (LHRH) administration to inhibit androgen biosynthesis in the testes. This occurs via negative feedback when overexposure to LHRH causes lowered LHRH receptor expression, leading to decreased luteinizing hormone (LH) and follicle-stimulating hormone (FSH) secretion from the anterior pituitary gland, ultimately resulting in decreased androgen synthesis (47, 48). Commercially available forms of LHRH antagonists include abarelix and degarelix (49, 50). However, this form

of treatment is limited in its clinical outcomes with respect to castrate-resistant prostate cancer treatment (51). An ideal treatment is tissue- and cell-specific targeted therapy, which allows blockade of critical protumor signaling pathways.

Peptides represent an exciting form of next-generation therapeutic agents as they can be deployed in multiple ways for targeted therapy and implemented to treat malignant tumors. These include using peptides as radionuclide carriers (52–54), vaccines (55), cytotoxic drug carriers (56), or directly as antitumor agents (e.g., inhibiting PPIs). Somatostatin analogues are used in treatment of various tumors as a target for overexpressed somatostatin receptor. The peptide is coupled with a DNA chelator and a radioactive element (e.g., ^{111}In , ^{90}Y , or ^{177}Lu) such that when injected, the radiolabeled peptide targets somatostatin receptor overexpressing cells, delivering the radioactive element directly to tumorigenic cells for eradication (52). Similarly, peptides targeted toward specific receptors can be conjugated with cytotoxic agents aimed at cancerous cells. Classical peptide drugs like LHRH analogues have been conjugated with doxorubicin, a chemotherapeutic agent, which selectively targets cells overexpressing LHRH receptors (57, 58). A corollary to peptide carriers are homing peptides, which are independent of tumor type and target specific molecules in either normal or diseased tissues (59, 60). Targeting angiogenesis may include targeting peptides including RGD and NGR peptides, which home in on α_v integrin receptors and aminopeptidase N, respectively (48), which are overexpressed in the neovasculature surrounding the tumors (59). A major drawback of peptide-based drugs is bioavailability. Short synthetic peptides, exclusive of unnatural amino acids, render the molecule unstable *in vivo*. Peptides are susceptible to degradation by enzymes (e.g., trypsin) or

gastric acids in the stomach, peptidases in the blood and organs like the liver and kidney and poor membrane permeability through the intestine and cell membrane, all of which can contribute to poor half-lives of these molecules. Other considerations include immune response to peptides as well as scaling-up costs for viable commercial use (61).

Finally, in the current climate of drug design, a class of compounds that are mostly targeted toward cancer cells are rationally designed peptide mimics, which are developed on the basis of target-specific binding motifs of PPIs. Such an approach has been tested with respect to prostate cancer, leukemia, and other cancers, in which secondary structural motifs (mostly α -helices) are mimicked to block critical PPIs involved in aberrant cell growth. For instance, AR coregulator interactions recently were targeted to inhibit the interaction between PELP1 and AR in prostate cancer (2). The peptidomimetic D2 was able to inhibit androgen-induced proliferation of prostate cancer cells, block AR nuclear translocation, activation of AR target genes and prostate cancer cell growth *in vivo*. To develop these agents, non-peptidic scaffolds are synthesized and further modified using a rational design approach to achieve desired specificity, potency, efficacy, and stability. The advantages and disadvantages of protein, peptide, and peptidomimetic drug therapy approaches are summarized in Table 2.

Converting Peptides to Peptidomimetics

Identifying PPI surfaces

Identifying interaction motifs between proteins can be a laborious task for rational drug design. Ideally, analysis of crystal structures by X-ray crystallography provides accurate and visual confirmation of amino acid residues involved at the binding interface. However, obtaining crystal structures is slow and cumbersome and not suitable for detecting PPIs in a high-throughput manner (9, 62–64). Binding interac-

tions can be determined by co-immunoprecipitation experiments, pull-down assays (bait protein used instead of an antibody), tandem-affinity purification coupled mass spectrometry (TAP-MS; complex orientated, i.e., multi-subunits), 2-hybrid protein interaction systems, and protein arrays/protein chips (binary orientated). Verifying the identity of interacting proteins is necessarily accomplished using a combination of molecular techniques. For example, PPIs detected via co-immunoprecipitation can be further probed using LC/MS techniques to verify the identity of protein sequences and matched to an online database (e.g., SWISS-PROT). Once identified, sequence analysis may be used to predict contact surfaces and verified by mutational analysis. cDNAs encoding mutated sequences of the protein of interest can be cloned, transfected into host cell lines *in vitro*, and queried for binding hits using the techniques mentioned above. In addition, mutational complementation analysis can be used to verify chemical properties of amino acids involved in PPIs. Predicting likely interacting protein surface residues can be achieved by scanning potential hydrophobic surfaces (65), proline brackets (66), and areas of potential van der Waals interactions using sequence information and computational methods (9). Other methods include multiple sequence alignment (67, 68), structure-based multimeric threading, and analysis of amino acid characteristics of spatial neighbors of a target residue using a neural network (69). Even with the availability of these techniques, there remain major structural issues in deciphering contactable surfaces between proteins. A notable consideration includes deciphering the most conformationally stable PPI complex given that all biologic interactions are in dynamic equilibrium (70). X-ray structures often do not reveal deep pockets that mark binding. Moreover, a single crystal structure may only reveal one binding conformation amidst multiple that occur at equilibrium (71) or between

Table 2. Targeting PPIs

Therapeutic approach	Advantages	Disadvantages
Proteins	Mimic endogenous function Target-specific Can be synthesized by recombinant methods Low immunogenicity	Bulky Unstable in solution (storage and protein folding problems) Limited biologic function (unlikely to be used as template) Some require posttranslational mods (e.g., glycosylation)
Peptides	Small size Multiple uses (delivery agents, antagonists, agonists) PPI-specific	Low cell permeability Susceptible to enzymatic degradation (short half-life) Unstable in solution High immunogenicity
Peptidomimetics	Rationally designed Specific to core PPI hot spots (amphiphilic nature) Stable in solution Resistant to proteases High cell permeability Low immunogenicity	Potentially cross-reactive to other PPIs bearing similar conformational hotspots Based on mimicking generic secondary structures

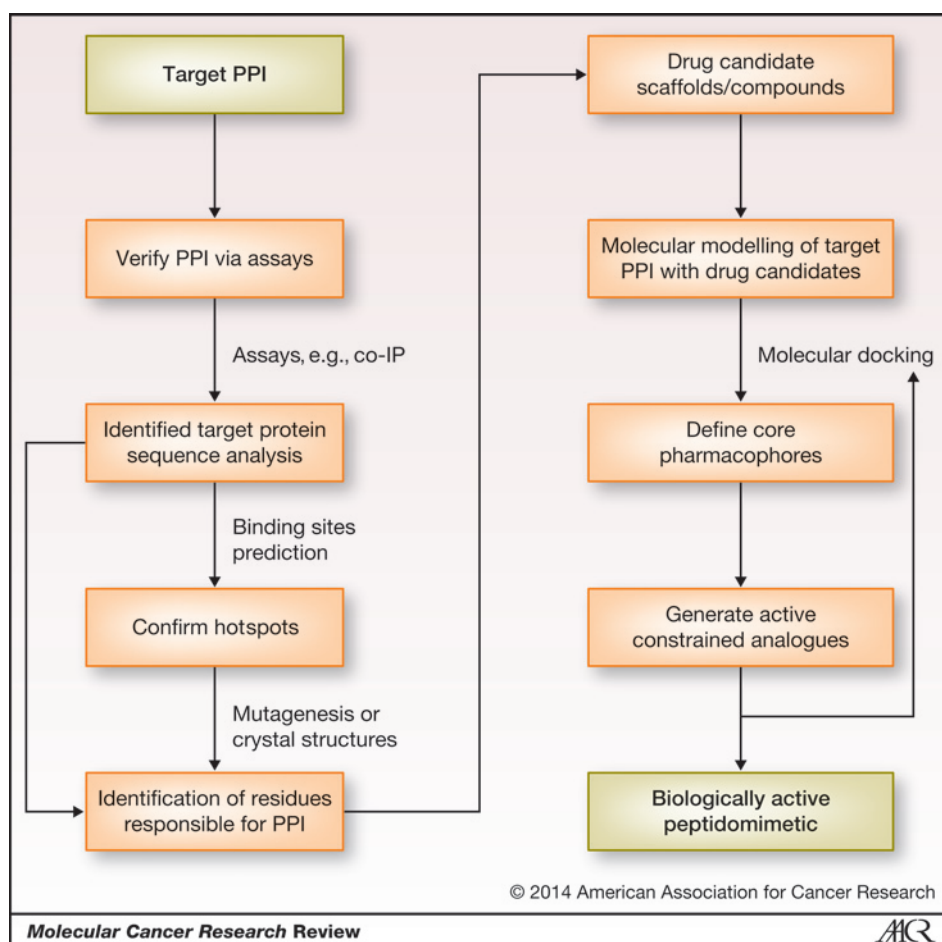


Figure 2. A systematic approach to peptidomimetic design.

transient PPIs. Identifying binding pocket hotspots—small areas of bumps and holes that largely determine binding—can become complicated with respect to multimeric binding interactions. Another problem is that interacting surfaces of proteins typically are many times larger than a small molecule and interactions observed *in vitro* may not be paralleled *in vivo*. Therefore, identifying "hotspots" that act as important mediators of PPIs is in essence a trial and error process. Nevertheless, key recognition motifs in a PPI may be verified using targeted mutagenesis of suspected interacting domains and tested via several of the aforementioned assays (Fig. 2).

Peptidomimetic subtypes

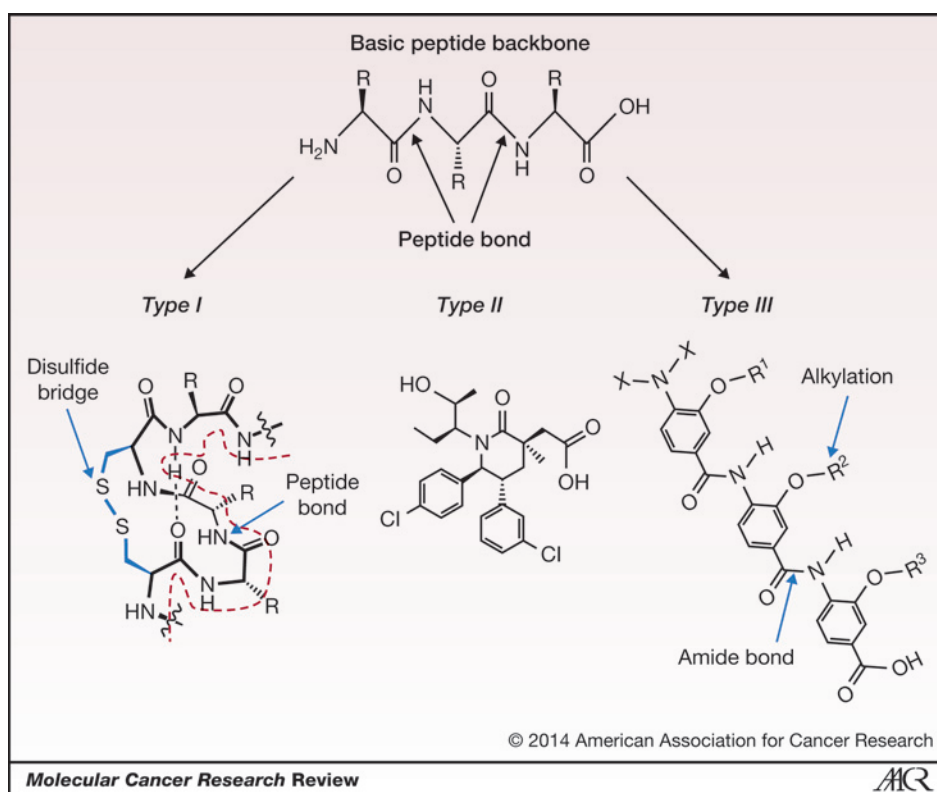
Conversion of peptides to peptidomimetics is one method to use peptide sequences that have potential as therapeutic agents. Peptides can be converted to stable peptide mimics that display comparable effects to their peptide counterparts but exhibit increased rigidity in structure, improving target specificity, stability, and cell membrane permeability. There are 3 major classes of peptidomimetics (types I–III; Fig. 3), each of which is categorized according to specific chemical modifications such as lactam, spiro, bicyclic bridges, or secondary protein structure mimics (e.g., β -turns and α -helices). However, the current discussion will be based on type I and type III mimetics, which are designed to mimic and

target PPIs. Type II mimetics do not mimic PPIs but are likely to be receptor antagonists (6) and are structurally characterized as small non-peptide molecules (72).

Type I. Type I mimetics (although not technically classified as peptidomimetics) are short-peptide oligomers designed to replicate the local topography of an α -helical motif found in PPIs (73). Type I mimetics are akin to parent peptides as they may suffer from poor stability and cell permeability. However, type I mimetics differ from parent peptides by exhibiting substitutions such as salt bridges and metal chelators as well as covalent cyclization motifs such as lactam and disulfide bridges to stabilize the secondary structural motif (72). As such, type I mimetics can be thought of as conformationally restricted peptides. Modifications which enable the classification of type I as peptidomimetics are the ones made at the amide backbone structure (e.g., amide bond isosteres). Type I mimetics have been used as inhibitors for aspartic proteases (74), cysteine protease (75), renin (76, 77), and the critical p53/MDM2 interaction present in many cancers (78).

Walensky and colleagues have developed a method for synthesizing stapled α -helical cross-links to mimic interaction peptide motifs of BID (BH3; Bcl-2 homology containing member). The strategy relies on inserting nonnatural olefinic amino acids into peptide sequences, followed by

Figure 3. Examples of the 3 different types of peptidomimetics. Type I: Basic amino acid backbone is altered to include basic stabilization substitutions such as disulfide bridges to stabilize helical functional mimetic (red dotted line traces peptide backbone). Type II: Piperidinone. Little resemblance to amino acid backbone or secondary structural motifs. Type III: Tris-benzamide scaffold. Altered peptide backbone structure consisting of benzene residues linked via amide bonds. Alkylation position on the benzene rings can vary to tweak compound efficacy. Backbone does not resemble any of the 20 natural known amino acids but is customized to resemble α -helical structure. Type I-III structures adapted from Azzarito et al. (72).



ruthenium-catalyzed metathesis to form an all hydrocarbon "staple" (79). BID is a proapoptotic BH3-only protein that when activated triggers activation of the multidomain proapoptotic proteins Bax and Bak, resulting in apoptosis (79). However, even with modifications (e.g., lactam bridges) that improve stability of type I mimetics, bioavailability and efficacy issues still exist (72).

Type III. Type III mimetics are characterized by highly modified structures that may not contain the basic peptide backbone structure but still retain functional groups necessary for key binding site recognition. In addition, they may represent key characteristics of secondary structures (3, 72). The 2 most common protein secondary motifs are α -helices and β -pleated sheets. In rod-like α -helices, the amino acids arrange themselves in a regular helical conformation whereby the carbonyl oxygen of each peptide bond is hydrogen bonded to the hydrogen on the amino group of the $i+4$ amino acid residues from the original amino acid. An α -helix is characterized by 3.4 amino acid residues per turn, a rise of 0.54 nm and defined by backbone dihedral angles θ and ψ of -60° and -45° , respectively. A unique feature in the α -helix is that the hydrogen bonds run nearly parallel to the axis of the helix. In β -pleated sheets, hydrogen bonds form between the peptide bonds either in different polypeptide chains or in different sections of the same polypeptide chain. The planarity of the peptide bond forces the polypeptide to be pleated with the side chains of amino acids protruding above and below the sheet. The α -helices are frequently found at the interface of PPIs. More than 30% of protein secondary structures are helical in nature (72). Not

surprisingly, strategies have been developed to synthesize helical peptides containing key recognition features of helices as inhibitors of specific PPIs. Type III-based α -helix mimetics can be designed using drastic modifications to the peptide backbone and amino acid side chains and consequently are described as non-peptidic-based peptidomimetics. One approach to designing such α -helix mimetics is via structural scaffolds, which are amenable to high-throughput synthesis (80, 81). The first versions of synthetic non-peptidic scaffolds were oligosaccharide structures, which mimicked projections of the α -helical structure found on the transcription factor GCN4. However, limited to no success was seen with these compounds with respect to GCN4-DNA binding inhibition (82).

Other strategies for disrupting PPIs have been used successfully in targeting well-documented tumorigenic pathways including apoptosis and membrane or nuclear signaling pathways. Hamilton and colleagues developed a non-peptide-based antagonist toward the Bcl-xL protein targeting the hydrophobic cleft formed by the BH1-BH3 domains disrupting the Bcl-xL/Bak interaction (83). The mimetic was designed using a terphenyl scaffold, which in a staggered conformation closely mimics the function of an α -helix. The terphenyl scaffold is designed containing alkyl or aryl substituents at the i , $i+3$ and $i+7$ position of the α -helix mimic in addition to carboxylic acid substituents at either end to mimic the Bak α -helical structure. Treatment in HEK293 cells showed decreased binding between Bak and Bcl-xL via protein immunoprecipitation assays (84). The same group also developed benzoylurea scaffolds, which when elongated,

mimics an extended α -helical structure (85). However, thorough *in vitro* and *in vivo* studies are lacking for these compounds.

An anthracene scaffold (anthraquinone) was used to mimic the 2 faces of the α -helix of Bim-BH3. Iteration from the anthraquinone scaffold yielded an amphiphilic compound ("compound 6") with dual inhibition of the Mlc-1/Bak and Bcl-2/Bax interactions. Compound 6 was able to induce cell apoptosis in numerous cancerous cells but was innocuous in HEK293 cells (86).

Rodriguez and colleagues improved on amphiphilic helical structures with the use of pyrimidine scaffolds to develop mimics of the α -helical structure composed of the nuclear receptor interaction boxes LXXLL sequence found in nuclear receptor coactivators. A pyrimidine-based mimetic was able to mimic the LXXLL motif on p160 coactivator by forming interactions at the i , $i+3$, $i+4$ positions in the hydrophobic groove of the LBD of ER α (87). To improve torsional flexibility and allow induced fit, Hamilton and colleagues further developed diphenylindane scaffolds to mimic the i , $i+3$, $i+4$, and $i+7$ residues to cater for additional interactions from residues flanking the hydrophobic face of the helix.

To disrupt the p53/MDM2 interaction, which is a complex PPI that is deeply buried, Robinson and colleagues developed β -hairpin scaffolds. Side chains of 3 important residues, Phe19, TRp23, and Leu26, of the amphiphilic α -helix project into a hydrophobic cleft of MDM2. The design of this β -hairpin uniquely configures the spatial arrangement of the 2 C α of residues at i and $i+2$ on one strand, similar to the α -helical side chains at the i and $i+4$ residues (88). Surface plasmon resonance showed the mimetic blocked p53/MDM2 interaction.

Oligobenzamide scaffolds

Oligobenzamide scaffolds are pre-organized structures with low molecular weights and can be used to develop peptidomimetics that account for key characteristics of a protein helix. The scaffolding template comprises two or three 3-alkoxy-4-aminobenzoic acids and places 2 or 3 alkyl substituents corresponding to the side chains of amino acid residues located at the i , $i+3$, $i+4$, and $i+7$ positions in a helix. The oligobenzamide scaffold displays higher torsional flexibility due to the absence of extensive hydrogen bond networks as seen in the trispyridylamide structure despite its similar appearance (81). This facilitates superior α -helix mimicry by arranging the substituents of the oligobenzamide structure in a more staggered fashion as appears in a helix (81).

We recently developed a bisbenzamide-based peptidomimetic to block the interaction between AR and its coregulator PELP1 as a therapeutic approach to prostate cancer. The AR–PELP1 interacting structure was determined on the basis of AR X-ray crystal structure. Analysis of PELP1 revealed 10 consensus LXXLL motifs (where L is leucine and X is any amino acid including leucine) in the protein, which like other nuclear receptor box proteins is a hotspot for interaction (89). Because the LXXLL motif adopts a helical

structure, the peptidomimetic D2 was designed with the bisbenzamide scaffold based on computational and molecular docking studies. The structure of D2 was designed to accommodate 2 isobutyl groups reproducing the side chains at the i and $i+4$ positions of the LXXLL motif, creating a hydrophobic surface for interaction with AR (2).

Other approaches

Aside from α -helix mimetics, other approaches can potentially be used to design peptidomimetics. For example, tethering is an approach whereby an interacting hotspot between proteins is targeted using a cysteine mutation near the interaction site in the target protein. The mutated protein is probed with test fragments containing disulfide bonds. When a fragment meets the target area, it bonds to the cysteine residue via sulfur bonds, which can then be identified using mass spectrometry. Further fragments can subsequently be screened in this way and the fragments "stitched" together to find a potent molecule (71). Hotspots on the IL2 receptor have been identified by this approach.

A potential but somewhat "random" rational approach to peptidomimetic design includes the construction of peptide libraries using (i) synthetic or (ii) biologic methods. These can be used as lead compounds to be converted into peptidomimetics. The synthetic approach involves an iterative or position scanning process (90). This approach uses coupling chemistry to produce variants of specific peptidic conformations such as α -helices (91) or cyclic disulfide peptides (92), which are then characterized by analytical methods such as nuclear magnetic resonance (NMR) and mass spectrometry. Similarly, phage display is a method of screening a library of candidate peptides by displaying them on the surface of bacteriophage. The display is achieved by fusing a peptide-encoding gene with the gene for a capsid structural protein. In this way, billions of peptides may be screened for binding activity against target proteins. Resulting hits can be selected and the genome sequence of the bacteriophage determined to reveal the sequence of the candidate peptide (93) and binding hit peptides potentially further modified into peptidomimetics, using chemical approaches (94), such as the Smac mimetics. Smac is a mitochondrial protein, which inhibits the apoptotic activity of caspases (95). Smac peptide mimetics are synthesized using a sequence of critical residues of Smac fused with carrier peptides or administered in combination with routinely used chemotherapeutic drugs. For example, quadra- or octa- N-terminal peptides of Smac fused with penetratin, a carrier peptide from *Drosophila* inhibited PPIs with caspase-3, -7, and -9 and promoted apoptosis in MCF-7 and T47D cells (96). Apoptosis was enhanced in combination with paclitaxel and other drugs. Similarly designed N-terminal Smac mimetics have been shown to promote ubiquitination of target proteins and induce cell apoptosis (97).

Similarly, non-peptidic Smac mimetic designed by computer modeling approaches of the target-binding protein complexed with Smac. Simulation revealed 4 residues on the

N-terminus of Smac interacting with BIR3 domain of a target protein. The C-terminal of this tetrapeptide was critical for binding affinity. On the basis of this interaction, a C₂-symmetric diyne was designed to mimic C-terminal binding (98) and was shown to induce apoptosis in multiple cancer cell lines (99–101).

Improving Potency and Maintaining Specificity

A key issue in peptidomimetic design is how to present peptide pharmacophores in 3D space so that the structures obtained truly mimic the parent peptide, not just in binding affinity but *in vitro* and *in vivo* biologic function (90). Generally, specific modifications (e.g., substitutions) of the peptide backbone can improve overall binding specificity and potency. These include N-alkylation (facilitating cis-trans amide bond isomerism), C α -alkylation (stabilizing helical or extended structure), D-amino acid/proline substitution (favoring formation of β -turn structures), peptide bond isosteres (improving metabolic stability), amino acids with cyclic side chains (biasing toward β - or γ -turns), dehydro amino acids and β -alkylation (constraining conformations). Using such modifications in combination to advance the field of peptidomimetic design are type III peptidomimetics, which in principal are based on template scaffolds designed to mimic secondary structures such as α -helices. Such non-peptidic-based mimetics are designed to improve resistance to proteolytic degradation and increase bioavailability. Complex scaffolds can be designed to cater for multiple binding surfaces required to allow binding interactions on more than one side of the mimetic, thereby more accurately targeting a PPI hotspot.

An alternative to inhibiting a PPI via residue contact at an interface is to allosterically regulate a PPI at a position offset from the interface without competing with the protein binding partner to disrupt the PPI (9). This type of mechanism is successfully used by enzymes to regulate their function, that is, a ligand binds at one site (the allosteric site) and induces a conformational change at a distant location, which can cause a change in overall shape and/or conformation at the active site. This type of control can offer greater specificity (64) and its efficacy was highlighted recently with drugs that have potent effects in blocking the interaction between Runx1:CBF β found in acute myeloid lymphoma (102).

Limitations of Peptidomimetics

The primary limitation of peptidomimetic strategies is the potential for a large number of PPIs to be disrupted simultaneously. This may be the case in proteins involving a family of structurally similar domains such as that in steroid hormone receptors, where significant homology exists

(e.g., AR, ER, PR, GR, and MR; ref. 103). Interestingly, the ER promoter/enhancer recognition sequence, found upstream of ER-regulated genes, does not share a consensus sequence with AR, PR, GR, and MR promoter/enhancer recognition sequences, like that found in the "universal" MMTV-LTR sequence (104). However, the ER recruits cofactors that are in common with AR such as SRC1 (105), which may have implications for specificity using a template-based peptidomimetic design. A bisbenzamide peptidomimetic that targets a motif may enable the wider targeting of PPIs through that motif but may increase the likelihood of toxicity due to off-target effects. This bisbenzamide may have significant effects on cancer cell proliferation and be used to more broadly target the interactions using a specific motif. Alternatively, a more selective peptidomimetic may be tailored to selectively target a single PPI. Such a peptidomimetic is unlikely to have any toxicity but may not have a significant effect on the cancer cell proliferation due to redundant signaling pathways. Thus, careful refining of the peptidomimetics targeting each PPI is needed to achieve the correct balance between therapeutic efficacy, on-target specificity, and off-target toxicity.

Conclusions

Understanding cellular signaling pathways is fundamental in deciphering key PPI in normal and diseased states phenotypes. The rational design of peptide mimics likely will improve with better understanding of PPIs in cellular signaling pathways coupled with improvements in identifying key interacting motifs. These improvements may be in X-ray crystallography techniques or protein sequence mutagenesis methods. The challenge is to design specific PPI modulators that can not only target key protein interactions involved in diseases but also target only the cells displaying aberrant signaling. High-throughput approaches coupled with template-based design offer an efficient strategy for the development of peptidomimetics but target specificity remains a challenge.

Disclosure of Potential Conflicts of Interest

G.V. Raj and J.-M. Ahn have patents on peptidomimetics that have been licensed to a pharmaceutical company and have received licensing fees/laboratory support. No potential conflicts of interest were disclosed by the other authors.

Grant Support

The study was supported by Department of Defense, Prostate Cancer Foundation, and the James Thompson Research Foundation to G.V. Raj; ACS post-doctoral fellowship to D.J. DeGraff; NIH R01-DK055748 to R.J. Matusik; National Health and Medical Research Council of Australia (ID 627185), Cancer Australia (ID 11627229), and the Prostate Cancer Foundation of Australia to W.D. Tilley; and Welch Foundation AT-1595 to J.-M. Ahn.

Received November 19, 2013; revised March 6, 2014; accepted March 7, 2014; published OnlineFirst March 18, 2014.

References

1. Wang D, Garcia-Bassets I, Benner C, Li W, Su X, Zhou Y, et al. Reprogramming transcription by distinct classes of enhancers functionally defined by eRNA. *Nature* 2011;474:390–4.
2. Ravindranathan P, Lee T, Yang L, Centenera MM, Butler L, Tilley WD, et al. Peptidomimetic targeting of critical androgen receptor-co-regulator interactions in prostate cancer. *Nat Commun* 2013;4:1923.

3. Moradi S, Soltani S, Ansari AM, Sardari S. Peptidomimetics and their applications in antifungal drug design. *Anti-Infect Agent Med Chem* 2009;8:327–44.
4. Gibbons JA, Hancock AA, Vitt CR, Knepper S, Buckner SA, Brune ME, et al. Pharmacologic characterization of CHIR 2279, an N-substituted glycine peptoid with high-affinity binding for α 1-adrenoceptors. *J Pharmacol Exp Ther* 1996;277:885–99.
5. Vagner J, Qu H, Hruby VJ. Peptidomimetics, a synthetic tool of drug discovery. *Curr Opin Chem Biol* 2008;12:292–6.
6. Kharb R, Rana M, Sharma P, Yar M. Therapeutic importance of peptidomimetics in medicinal chemistry. *J Chem Pharm Res* 2011;3:173–86.
7. Ahn JM, Boyle NA, MacDonald MT, Janda KD. Peptidomimetics and peptide backbone modifications. *Mini Rev Med Chem* 2002;2:463–73.
8. Ideker T, Sharan R. Protein networks in disease. *Genome Res* 2008;18:644–52.
9. Zinzalla Giovanna, Thurston David E. Targeting protein-protein interactions for therapeutic interventions: a challenge for the future. *Future Med Chem* 2009;1:65–93.
10. Rual JF, Venkatesan K, Hao T, Hirozane-Kishikawa T, Dricot A, Li N, et al. Towards a proteome-scale map of the human protein-protein interaction network. *Nature* 2005;437:1173–8.
11. Stelzl U, Worm U, Lalowski M, Haenig C, Brembeck FH, Goehler H, et al. A human protein-protein interaction network: a resource for annotating the proteome. *Cell* 2005;122:957–68.
12. Malovannaya A, Lanz RB, Jung SY, Bulynko Y, Le NT, Chan DW, et al. Analysis of the human endogenous coregulator complexome. *Cell* 2011;145:787–99.
13. Janumyan YM, Sansam CG, Chattopadhyay A, Cheng N, Soucie EL, Penn LZ, et al. Bcl-xL/Bcl-2 coordinately regulates apoptosis, cell cycle arrest and cell cycle entry. *EMBO J* 2003;22:5459–70.
14. Decker KF, Zheng D, He Y, Bowman T, Edwards JR, Jia L. Persistent androgen receptor-mediated transcription in castration-resistant prostate cancer under androgen-deprived conditions. *Nucleic Acids Res* 2012;40:10765–79.
15. Chen CD, Welsbie DS, Tran C, Baek SH, Chen R, Vessella R, et al. Molecular determinants of resistance to antiandrogen therapy. *Nat Med* 2004;10:33–9.
16. Aveic S, Pigazzi M, Basso G. BAG1: the guardian of anti-apoptotic proteins in acute myeloid leukemia. *PLoS One* 2011;6:e26097.
17. Yang L, Ravindranathan P, Ramanan M, Kapur P, Hammes SR, Hsieh JT, et al. Central role for PELP1 in nonandrogenic activation of the androgen receptor in prostate cancer. *Mol Endocrinol* 2012;26:550–61.
18. Zhang X, Morrissey C, Sun S, Ketchandji M, Nelson PS, True LD, et al. Androgen receptor variants occur frequently in castration resistant prostate cancer metastases. *PLoS One* 2011;6:e27970.
19. Sun S, Sprenger CT, Haugk K, Mostaghel E, Plymate S. Interaction with wild-type (wt) androgen receptor (AR) alters the function of AR splice-variants and response to AR-ligand binding domain inhibition [abstract]. In: *Proceedings of the 102nd Annual Meeting of the American Association for Cancer Research*; 2011 Apr 2–6; Orlando, FL. Philadelphia (PA): AACR; 2011. Abstract nr 4537.
20. Anzick SL, Kononen J, Walker RL, Azorsa DO, Tanner MM, Guan XY, et al. AIB1, a steroid receptor coactivator amplified in breast and ovarian cancer. *Science* 1997;277:965–8.
21. Kuang SQ, Liao L, Zhang H, Lee AV, O'Malley BW, Xu J. AIB1/SRC-3 deficiency affects insulin-like growth factor I signaling pathway and suppresses v-Ha-ras-induced breast cancer initiation and progression in mice. *Cancer Res* 2004;64:1875–85.
22. Torres-Arzuay MI, Font de Mora J, Yuan J, Vazquez F, Bronson R, Rue M, et al. High tumor incidence and activation of the PI3K/AKT pathway in transgenic mice define AIB1 as an oncogene. *Cancer Cell* 2004;6:263–74.
23. Lonard DM, O'Malley BW. Nuclear receptor coregulators: judges, juries, and executioners of cellular regulation. *Mol Cell* 2007;27:691–700.
24. Louet JF, Coste A, Amazil L, Tannour-Louet M, Wu RC, Tsai SY, et al. Oncogenic steroid receptor coactivator-3 is a key regulator of the white adipogenic program. *Proc Natl Acad Sci U S A* 2006;103:17868–73.
25. Yu C, York B, Wang S, Feng Q, Xu J, O'Malley BW. An essential function of the SRC-3 coactivator in suppression of cytokine mRNA translation and inflammatory response. *Mol Cell* 2007;25:765–78.
26. Sahu B, Laakso M, Ovaska K, Mirtti T, Lundin J, Rannikko A, et al. Dual role of FoxA1 in androgen receptor binding to chromatin, androgen signalling and prostate cancer. *EMBO J* 2011;30:3962–76.
27. Lin SP, Lee YT, Wang JY, Miller SA, Chiou SH, Hung MC, et al. Survival of cancer stem cells under hypoxia and serum depletion via decrease in PP2A activity and activation of p38-MAPKAPK2-Hsp27. *PLoS One* 2012;7:e49605.
28. Darini CY, Martin P, Azoulay S, Drici MD, Hofman P, Obba S, et al. Targeting cancer stem cells expressing an embryonic signature with anti-proteases to decrease their tumor potential. *Cell Death Dis* 2013;4:e706.
29. Hassan KA, Wang L, Korkaya H, Chen G, Maillard I, Beer DG, et al. Notch pathway activity identifies cells with cancer stem cell-like properties and correlates with worse survival in lung adenocarcinoma. *Clin Cancer Res* 2013;19:1972–80.
30. Collins AT, Berry PA, Hyde C, Stower MJ, Maitland NJ. Prospective identification of tumorigenic prostate cancer stem cells. *Cancer Res* 2005;65:10946–51.
31. Wagner RT, Cooney AJ. Minireview: the diverse roles of nuclear receptors in the regulation of embryonic stem cell pluripotency. *Mol Endocrinol* 2013;27:864–78.
32. Lobo NA, Shimono Y, Qian D, Clarke MF. The biology of cancer stem cells. *Annu Rev Cell Dev Biol* 2007;23:675–99.
33. Oliver TG, Mercer KL, Sayles LC, Burke JR, Mendus D, Lovejoy KS, et al. Chronic cisplatin treatment promotes enhanced damage repair and tumor progression in a mouse model of lung cancer. *Genes Dev* 2010;24:837–52.
34. Poti Z, Mayer A. [Current methods of chemoradiotherapy for locally advanced cervical cancer. Options for reduction of side-effects]. *Orv Hetil* 2013;154:803–9.
35. Wiltshaw E. Cisplatin in the treatment of cancer. *Platinum Metals Rev* 1979;23:90–98.
36. Gaspar LE, Ding M. A review of intensity-modulated radiation therapy. *Curr Oncol Rep* 2008;10:294–9.
37. Cai Y, Jin J, Swanson SK, Cole MD, Choi SH, Florens L, et al. Subunit composition and substrate specificity of a MOF-containing histone acetyltransferase distinct from the male-specific lethal (MSL) complex. *J Biol Chem* 2010;285:4268–72.
38. Dreesen O, Brivanlou AH. Signalling pathways in cancer and embryonic stem cells. *Stem Cell Rev* 2007;3:7–17.
39. Jones S, Thornton JM. Principles of protein-protein interactions. *Proc Natl Acad Sci U S A* 1996;93:13–20.
40. Hernández-Santoyo A, Tenorio-Barajas AY, Altuzar V, Vivanco-Cid H, Mendoza-Barrera C. Protein-protein and protein-ligand docking. In: Ogawa T, editor. *Protein engineering - technology and application*; 2013. InTech.
41. Totrov M, Abagyan R. Flexible ligand docking to multiple receptor conformations: a practical alternative. *Curr Opin Struct Biol* 2008;18:178–84.
42. Welch W, Ruppert J, Jain AN. Hammerhead: fast, fully automated docking of flexible ligands to protein binding sites. *Chem Biol* 1996;3:449–62.
43. Mangoni M, Roccatano D, Di Nola A. Docking of flexible ligands to flexible receptors in solution by molecular dynamics simulation. *Proteins* 1999;35:153–62.
44. Kotzke G, Schutt M, Missler U, Moller DE, Fehm HL, Klein HH. Binding of human, porcine and bovine insulin to insulin receptors from human brain, muscle and adipocytes and to expressed recombinant alternatively spliced insulin receptor isoforms. *Diabetologia* 1995;38:757–63.
45. Pugliese A. Peptide-based treatment for autoimmune diseases: learning how to handle a double-edged sword. *J Clin Invest* 2003;111:1280–2.
46. Edwards CMB, Cohen MA, Bloom SR. Peptides as drugs. *QJM* 1999;92:1–4.

47. Crawford ED, Hou AH. The role of LHRH antagonists in the treatment of prostate cancer. *Oncology (Williston Park)* 2009;23:626–30.
48. Thundimadathil J. Cancer treatment using peptides: current therapies and future prospects. *J Amino Acids* 2012;2012:967347.
49. Broqua P, Riviere PJ, Conn PM, Rivier JE, Aubert ML, Junien JL. Pharmacological profile of a new, potent, and long-acting gonadotropin-releasing hormone antagonist: degarelix. *J Pharmacol Exp Ther* 2002;301:95–102.
50. Debruyne F, Bhat G, Garnick MB. Abarelix for injectable suspension: first-in-class gonadotropin-releasing hormone antagonist for prostate cancer. *Future Oncol* 2006;2:677–96.
51. Chrvala CA. The changing landscape of treatment options for metastatic castrate-resistant prostate cancer: challenges and solutions for physicians and patients. *P T* 2012;37:453–63.
52. Kwekkeboom D, Krenning EP, de Jong M. Peptide receptor imaging and therapy. *J Nucl Med* 2000;41:1704–13.
53. Kwekkeboom DJ, de Herder WW, Kam BL, van Eijck CH, van Essen M, Kooij PP, et al. Treatment with the radiolabeled somatostatin analog [177 Lu-DOTA 0,Tyr3]octreotate: toxicity, efficacy, and survival. *J Clin Oncol* 2008;26:2124–30.
54. Nicolas G, Giovacchini G, Muller-Brand J, Forrer F. Targeted radiotherapy with radiolabeled somatostatin analogs. *Endocrinol Metab Clin North Am* 2011;40:187–204.
55. Yoshimura K, Minami T, Nozawa M, Uemura H. Phase I clinical trial of human vascular endothelial growth factor receptor 1 peptide vaccines for patients with metastatic renal cell carcinoma. *Br J Cancer* 2013;108:1260–6.
56. Schally AV, Nagy A. Cancer chemotherapy based on targeting of cytotoxic peptide conjugates to their receptors on tumors. *Eur J Endocrinol* 1999;141:1–14.
57. Engel J, Emons G, Pinski J, Schally AV. AEZS-108: a targeted cytotoxic analog of LHRH for the treatment of cancers positive for LHRH receptors. *Expert Opin Investig Drugs* 2012;21:891–9.
58. Schally AV, Engel JB, Emons G, Block NL, Pinski J. Use of analogs of peptide hormones conjugated to cytotoxic radicals for chemotherapy targeted to receptors on tumors. *Curr Drug Deliv* 2011;8:11–25.
59. Sharma A, Kapoor P, Gautam A, Chaudhary K, Kumar R, Chauhan JS, et al. Computational approach for designing tumor homing peptides. *Sci Rep* 2013;3:1607.
60. Hatakeyama S, Sugihara K, Shibata TK, Nakayama J, Akama TO, Tamura N, et al. Targeted drug delivery to tumor vasculature by a carbohydrate mimetic peptide. *Proc Natl Acad Sci U S A* 2011;108:19587–92.
61. Sun L. Peptide based drug development. *Mod Chem Appl* 2013;1:1–2.
62. Zhong S, Macias AT, MacKerell AD Jr. Computational identification of inhibitors of protein-protein interactions. *Curr Top Med Chem* 2007;7:63–82.
63. Block P, Weskamp N, Wolf A, Klebe G. Strategies to search and design stabilizers of protein-protein interactions: a feasibility study. *Proteins* 2007;68:170–86.
64. Gonzalez-Ruiz D, Gohlke H. Targeting protein-protein interactions with small molecules: challenges and perspectives for computational binding epitope detection and ligand finding. *Curr Med Chem* 2006;13:2607–25.
65. Gallet X, Charleatoux B, Thomas A, Brasseur R. A fast method to predict protein interaction sites from sequences. *J Mol Biol* 2000;302:917–26.
66. Kini RM, Evans HJ. Prediction of potential protein-protein interaction sites from amino acid sequence. Identification of a fibrin polymerization site. *FEBS Lett* 1996;385:81–6.
67. Pazos F, Helmer-Citterich M, Ausiello G, Valencia A. Correlated mutations contain information about protein-protein interaction. *J Mol Biol* 1997;271:511–23.
68. Casari G, Sander C, Valencia A. A method to predict functional residues in proteins. *Nat Struct Biol* 1995;2:171–8.
69. Yan C, Honavar V, Dobbs D. Identification of interface residues in protease-inhibitor and antigen-antibody complexes: a support vector machine approach. *Neural Comput Appl* 2004;13:123–9.
70. Sprinzak E, Altuvia Y, Margalit H. Characterization and prediction of protein-protein interactions within and between complexes. *Proc Natl Acad Sci U S A* 2006;103:14718–23.
71. Buckingham S. Picking the pockets of protein-protein interactions. In *Horizon symposia*. Nature; 2004.
72. Azzarito V, Long K, Murphy NS, Wilson AJ. Inhibition of alpha-helix-mediated protein-protein interactions using designed molecules. *Nat Chem* 2013;5:161–73.
73. Henchey LK, Jochim AL, Arora PS. Contemporary strategies for the stabilization of peptides in the alpha-helical conformation. *Curr Opin Chem Biol* 2008;12:692–7.
74. Dolle RE, Prasad CV, Prouty CP, Salvino JM, Awad MM, Schmidt SJ, et al. Pyridazinodiazepines as a high-affinity, P2-P3 peptidomimetic class of interleukin-1 beta-converting enzyme inhibitor. *J Med Chem* 1997;40:1941–6.
75. Eguchi M, Shen RY, Shea JP, Lee MS, Kahn M. Design, synthesis, and evaluation of opioid analogues with non-peptidic beta-turn scaffold: enkephalin and endomorphin mimetics. *J Med Chem* 2002;45:1395–8.
76. Rasetti V, Cohen CN, Rueger H, Göschke R, Maibaum J, Cumin F, et al. Bioactive hydroxyethylene dipeptide isosteres with hydrophobic (P3-P1)-moieties. A novel strategy towards small non-peptide renin inhibitors. *Bioorg Med Chem Lett* 1996;6:1589–94.
77. Goschke R, Stutz S, Rasetti V, Cohen NC, Rahuel J, Rigollier P, et al. Novel 2,7-dialkyl-substituted 5(S)-amino-4(S)-hydroxy-8-phenyl-octanecarboxamide transition state peptidomimetics are potent and orally active inhibitors of human renin. *J Med Chem* 2007;50:4818–31.
78. Kritzer JA, Lear JD, Hodsdon ME, Schepartz A. Helical beta-peptide inhibitors of the p53-hDM2 interaction. *J Am Chem Soc* 2004;126:9468–9.
79. Walensky LD, Kung AL, Escher I, Malia TJ, Barbuto S, Wright RD, et al. Activation of apoptosis *in vivo* by a hydrocarbon-stapled BH3 helix. *Science* 2004;305:1466–70.
80. Lee TK, Ahn JM. Solid-phase synthesis of tris-benzamides as alpha-helix mimetics. *ACS Comb Sci* 2011;13:107–11.
81. Ahn JM. Oligo-Benzamides: versatile scaffolds to mimic protein helical surfaces. In: *Proceedings of the 22nd American Peptide Symposium*; 2011; San Diego, CA. American Peptide Society. pp. 178–9.
82. Xuereb H, Maletic M, Gildersleeve J, Pelczar I, Kahne D. Design of an oligosaccharide scaffold that binds in the minor groove of DNA. *J Am Chem Soc* 2000;122:1883–90.
83. Kutzki O, Park HS, Ernst JT, Orner BP, Yin H, Hamilton AD. Development of a potent Bcl-x(L) antagonist based on alpha-helix mimicry. *J Am Chem Soc* 2002;124:11838–9.
84. Yin H, Lee GI, Sedey KA, Kutzki O, Park HS, Orner BP, et al. Terphenyl-Based Bak BH3 alpha-helical proteomimetics as low-molecular-weight antagonists of Bcl-xL. *J Am Chem Soc* 2005;127:10191–6.
85. Rodriguez JM, Hamilton AD. Benzoylurea oligomers: synthetic foldamers that mimic extended alpha helices. *Angew Chem Int Ed Engl* 2007;46:8614–7.
86. Zhang Z, Li X, Song T, Zhao Y, Feng Y. An anthraquinone scaffold for putative, two-face Bim BH3 alpha-helix mimic. *J Med Chem* 2012;55:10735–41.
87. Rodriguez AL, Tamrazi A, Collins ML, Katzenellenbogen JA. Design, synthesis, and *in vitro* biological evaluation of small molecule inhibitors of estrogen receptor alpha coactivator binding. *J Med Chem* 2004;47:600–11.
88. Fasan R, Dias RLA, Moehle K, Zerbe O, Vrijbloed JW, Obrecht D, et al. Using a beta-hairpin to mimic an alpha-helix: cyclic peptidomimetic inhibitors of p53-MDM2 protein-protein interaction. *Angew Chem-Int Edit* 2004;43:2109–12.
89. Vadlamudi RK, Kumar R. Functional and biological properties of the nuclear receptor coregulator PELP1/MNAR. *Nucl Recept Signal* 2007;5:e004.
90. Hruby VJ, Ahn JM, Liao S. Synthesis of oligopeptide and peptidomimetic libraries. *Curr Opin Chem Biol* 1997;1:114–9.

91. Perez-Paya E, Houghten RA, Blondelle SE. Functionalized protein-like structures from conformationally defined synthetic combinatorial libraries. *J Biol Chem* 1996;271:4120–6.
92. McBride JD, Freeman N, Domingo GJ, Leatherbarrow RJ. Selection of chymotrypsin inhibitors from a conformationally-constrained combinatorial peptide library. *J Mol Biol* 1996;259:819–27.
93. Molek P, Strukelj B, Bratkovic T. Peptide phage display as a tool for drug discovery: targeting membrane receptors. *Molecules* 2011;16:857–87.
94. Franklin MC, Kadkhodayan S, Ackerly H, Alexandru D, Distefano MD, Elliott LO, et al. Structure and function analysis of peptide antagonists of melanoma inhibitor of apoptosis (ML-IAP). *Biochemistry* 2003;42:8223–31.
95. Du C, Fang M, Li Y, Li L, Wang X. Smac, a mitochondrial protein that promotes cytochrome c-dependent caspase activation by eliminating IAP inhibition. *Cell* 2000;102:33–42.
96. Arnt CR, Chiorean MV, Heldebrandt MP, Gores GJ, Kaufmann SH. Synthetic Smac/DIABLO peptides enhance the effects of chemotherapeutic agents by binding XIAP and cIAP1 *in situ*. *J Biol Chem* 2002;277:44236–43.
97. Yang QH, Du C. Smac/DIABLO selectively reduces the levels of c-IAP1 and c-IAP2 but not that of XIAP and livin in HeLa cells. *J Biol Chem* 2004;279:16963–70.
98. Li L, Thomas RM, Suzuki H, De Brabander JK, Wang X, Harran PG. A small molecule Smac mimic potentiates TRAIL- and TNFalpha-mediated cell death. *Science* 2004;305:1471–4.
99. Petersen SL, Wang L, Yalcin-Chin A, Li L, Peyton M, Minna J, et al. Autocrine TNFalpha signaling renders human cancer cells susceptible to Smac-mimetic-induced apoptosis. *Cancer Cell* 2007;12:445–56.
100. Bockbrader KM, Tan M, Sun Y. A small molecule Smac-mimic compound induces apoptosis and sensitizes TRAIL- and etoposide-induced apoptosis in breast cancer cells. *Oncogene* 2005;24:7381–8.
101. Petrucci E, Pasquini L, Petronelli A, Saulle E, Mariani G, Riccioni R, et al. A small molecule Smac mimic potentiates TRAIL-mediated cell death of ovarian cancer cells. *Gynecol Oncol* 2007;105:481–92.
102. Gorczynski MJ, Grembecka J, Zhou Y, Kong Y, Roudaia L, Douvas MG, et al. Allosteric inhibition of the protein-protein interaction between the leukemia-associated proteins Runx1 and CBFbeta. *Chem Biol* 2007;14:1186–97.
103. Falkenstein E, Tillmann HC, Christ M, Feuring M, Wehling M. Multiple actions of steroid hormones—a focus on rapid, nongenomic effects. *Pharmacol Rev* 2000;52:513–56.
104. Akram ON, Bursill C, Desai R, Heather AK, Kazlauskas R, Handelsman DJ, et al. Evaluation of androgenic activity of nutraceutical-derived steroids using mammalian and yeast *in vitro* androgen bioassays. *Anal Chem* 2011;83:2065–74.
105. Powell SM, Christiaens V, Voulgaraki D, Waxman J, Claessens F, Bevan CL. Mechanisms of androgen receptor signalling via steroid receptor coactivator-1 in prostate. *Endocr Relat Cancer* 2004;11:117–30.

The social network of PELP1 and its implications in breast and prostate cancers

Vijay K Gonugunta, Lu Miao, Gangadhara R Sareddy¹, Preethi Ravindranathan, Ratna Vadlamudi¹ and Ganesh V Raj

Department of Urology, UT Southwestern Medical Center at Dallas, 5323 Harry Hines Boulevard J8130, Dallas, Texas 75390, USA

¹Department of Obstetrics and Gynecology, UT Health Science Center, San Antonio, Texas, USA

Correspondence should be addressed to G V Raj

Email
ganesh.raja@utsouthwestern.edu

Abstract

Proline, glutamic acid- and leucine-rich protein 1 (PELP1) is a multi-domain scaffold protein that serves as a platform for various protein–protein interactions between steroid receptors (SRs) and signaling factors and cell cycle, transcriptional, cytoskeletal, and epigenetic remodelers. PELP1 is known to be a coregulator of transcription and participates in the nuclear and extranuclear functions of SRs, ribosome biogenesis, and cell cycle progression. The expression and localization of PELP1 are dysregulated in hormonal cancers including breast and prostate cancers. This review focuses on the interactive functions and therapeutic and prognostic significance of PELP1 in breast and prostate cancers.

Key Words

- ▶ PELP1
- ▶ interactome
- ▶ network
- ▶ coregulator
- ▶ steroid receptors
- ▶ genomic signaling
- ▶ nongenomic signaling
- ▶ epigenetics
- ▶ hormonal cancers

Endocrine-Related Cancer
(2014) 21, T79–T86

Introduction

Proline-, glutamic acid- and leucine-rich protein 1 (PELP1), also referred to as modulator of nongenomic activity of estrogen receptor (MNAR) (Greger *et al.* 2006), is a promiscuous coregulator of steroid receptors (SRs) and exhibits corepressor or coactivator activity (Choi *et al.* 2004). PELP1 may be classified as a scaffolding protein (Vadlamudi & Kumar 2007), and it serves as a ‘mediator’ for protein–protein interactions in different cellular processes such as cell cycle regulation, transcription, cytoskeletal and epigenetic modifications, and ribosome biogenesis (Choi *et al.* 2004, Nair *et al.* 2007, 2010a, Chakravarty *et al.* 2010a, 2011, Gonugunta *et al.* 2011, Mann *et al.* 2013). PELP1 is widely expressed in various tissues, with the highest levels being measured in the brains, testes, ovaries, and uteri of mice (Vadlamudi

et al. 2001). Dysregulation of PELP1 expression has been observed in breast, ovarian, endometrial, brain, and prostate cancers (Dimple *et al.* 2008, Chakravarty *et al.* 2011, Cortez *et al.* 2012, Kefalopoulou *et al.* 2012, Wan & Li 2012, Yang *et al.* 2012, Ravindranathan *et al.* 2013). PELP1 is involved in both genomic and extranuclear signaling pathways (Boonyaratankornkit 2011, Girard *et al.* 2013, Renoir *et al.* 2013). The functions of PELP1 can be attributed to its multiple unique structural domains, which allow it to bind to different SRs to modulate their activity (Vadlamudi & Kumar 2007, Girard *et al.* 2013). This review focuses on the structure, function, and genomic and extranuclear signaling of PELP1, associated signaling pathways, and its role as a target for therapeutic modulation in breast and prostate cancers.

PELP1 structural features

The *PELP1* gene is located on chromosome 17 on the short arm at region 13.2. The cDNA-translated protein comprises 1130 amino acids with a pI value of 4.3. However, due to the high content of proline and glutamic acid, the protein migrates as a 160 kDa form on SDS-PAGE gels (predicted 120 kDa) (Vadlamudi & Kumar 2007). Two alternatively spliced isoforms of PELP1 have been reported: a long (3.9 kb) form and a short (3.5 kb) form, both of which map to the same chromosomal region, 17p13.2, and encode the same protein. The longer isoform represents an immature transcript that contains an additional 435 bp intronic region. Of the two, the short isoform is widely expressed in patients with hormonally driven cancers (Vadlamudi *et al.* 2001, Balasenthil & Vadlamudi 2003).

PELP1 protein has multiple structural domains or discrete structural units made up of a complex of secondary structures such as α -helices and β -sheets. These short peptide recognition domains may function in an independent context and enable the binding of PELP1 to different steroid hormone receptors and proteins. These domains may be found in multiple copies, but each domain may have its own unique interactome, depending on the structural context in which it is presented. Multiple domains may be involved in the binding between PELP1 and a specific protein partner: in these interactions, each PELP1 domain independently interacts with the target protein and cooperatively increases both its binding affinity to the target protein and the likelihood of PELP1–target protein complex formation. This built-in redundancy ensures interaction between PELP1 and critical protein cofactors. Furthermore, each PELP1 domain may modulate the activity and function of other domains on PELP1 and thus influence PELP1–protein interactions by modifying the secondary structure of the PELP1 domain. Proteins that

bind to a PELP1 domain may in turn directly or indirectly interact with other proteins that bind to another domain on PELP1: thus PELP1 serves as a scaffolding protein enabling large-scale protein–protein interactions. The interactive domains on PELP1 thus promote cross talk between both proteins and signaling pathways. By virtue of its large interactome, PELP1 plays a critical role in cell signaling and cellular processes.

A domain scan using the online tool (<http://scansite.mit.edu>) has revealed several protein-interacting domains on PELP1 including multiple copies of the nuclear receptor (SR) box-interacting domains (LxxLL domains: L is leucine; x is any residue), PxxP (P=proline) domains, SH2 domains, a long unusual stretch (70 amino acids) of glutamic acids flanked by two proline-rich regions as well as three nucleolar domains, and a single nuclear localization sequence (Fig. 1; Girard *et al.* 2013). Each of these regions is described in greater detail below.

LxxLL domains

The acidic LxxLL domain is conserved in more than 300 coregulators and is a known hot spot for SR interactions (Fuchs *et al.* 2013). Although the LxxLL domains have an α -helical propensity, many factors, including the proper presentation of the LxxLL surface in the 3D structure, the availability of the domains for interaction, and the composition of the residues flanking the LxxLL core domain contribute to the determination of binding affinity and enable discrimination between binding partners. PELP1 has ten distinct LxxLL domains with unique flanking residues and structural presentation (Vadlamudi & Kumar 2007). The interaction with SRs is typically enhanced by ligand binding, which induces conformational changes in the helix 12 (H12) region with the activation function 2 (AF-2) domain of the receptor facilitating the interaction with the short-helix LxxLL

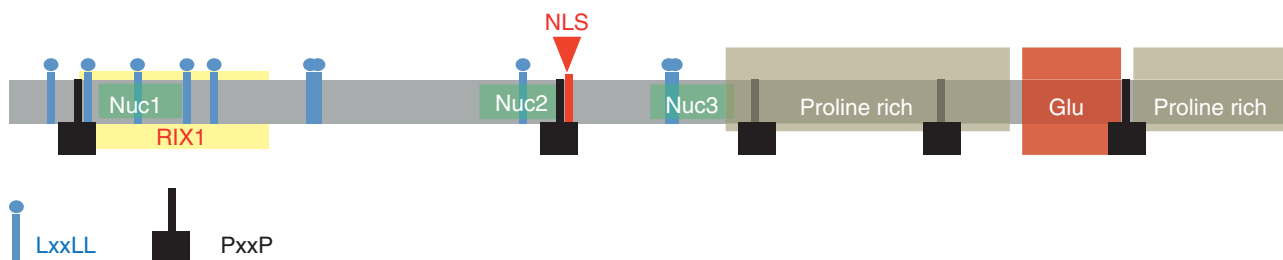


Figure 1

Schematic representation of the domains and sequences of PELP1 primary structure. PELP1 has ten LxxLL domains (blue lollipops), five PxxP domains (black hanging boxes), one nuclear localization sequence (NLS, red funnel),

three nucleolar domains (Nuc1, Nuc2, and Nuc3, green boxes), and a glutamic-acid-rich region (Glu, dark red square) flanked by two proline-rich regions (ash-colored boxes) at its C-terminal end.

domain (Folkertsma *et al.* 2007). The LxxLL domains of PELP1 have distinct binding specificities: for example, estrogen receptor- α (ER α) preferentially interacts with the fourth and fifth LxxLL domains to mediate PELP1 signaling (Barletta *et al.* 2004). Although the specific LxxLL domains of PELP1 that interact with androgen receptor (AR), progesterone receptor (PR), glucocorticoid receptor (GR), or other SRs have not been characterized, they are distinct from the fourth LxxLL domain of PELP1 (Barletta *et al.* 2004, Yang *et al.* 2012, Ravindranathan *et al.* 2013).

PxxP domains

The PxxP domains were initially described as high-affinity binding sites for proteins with a SRC homology 3 (SH3) motif. The PxxP domains are often clustered in proline-rich stretches of proteins, and the bulky prolines are important for interaction with the SH3 motif, with its characteristic β -barrel fold of five to six β -strands being arranged in two tightly packed anti-parallel β -sheets (Vanhaesebroeck *et al.* 2001). Residues flanking the core PxxP domain may enhance the stability and binding specificity of proteins with SH3 domains, by forming additional contacts with the binding partner. Mechanistic studies have shown that PELP1 interacts with the SH3 motif of c-Src via its N-terminal PxxP domain and ER interacts with the SRC homology 2 (SH2) motif of Src at phosphotyrosine 537; the PELP1–ER interaction further stabilizes this trimeric complex, leading to the activation of the Src kinase, further activating the Ras/MAPK pathway (Barletta *et al.* 2004).

SH2 domains

Several SH2-binding domains within PELP1 may enable its interaction with kinases such as Abl and Src. The SH2 domains are complex structures with an anti-parallel β -sheet between flanking α -helices, which results in a positively charged β -sheet pocket and enables high-affinity physical interactions with target proteins containing short peptides with phosphorylated tyrosines. Interestingly, the N- and C-termini of the SH2 domains are very close to each other, enabling their introduction without disturbing the existing folding of the host protein. Tyrosine phosphorylation of PELP1 may recruit SH2 effectors: the phosphorylation of PELP1 at Tyr920 by Src kinase creates a binding site for the SH2 domain of p85 subunit of PI3K, leading to the activation of the PI3K pathway (Barletta *et al.* 2004, Dimple *et al.* 2008). Furthermore, the SH2 domains on PELP1 enable its interaction with STAT3 (Manavathi *et al.* 2005).

Glutamic-acid-rich region

PELP1 has an unusual C-terminal stretch of glutamic acids (amino acids 887–960), with 61/74 glutamic acid residues and 4/74 aspartic acid residues. This sequence has a pI value of 2.18, making it an extremely acidic stretch. Unsurprisingly, this glutamic-acid-rich region is optimal for the interaction of PELP1 with basic-amino-acid-rich chromatin proteins such as histones H1 and H3 (Nair *et al.* 2004). Through the glutamic acid-rich region, PELP1 plays a role in chromatin remodeling by displacing histone H1 and by blocking hypoacetylated histones H3 and H4 from becoming the substrates of histone acetyltransferases (Choi *et al.* 2004). Furthermore, the glutamic-acid-rich region of PELP1 can function as a reader of histone dimethyl modification and facilitates the recruitment of histone demethylases such as lysine demethylase 1 (KDM1) to the DNA (Nair *et al.* 2010b). The glutamic-acid-rich region of PELP1 is further flanked on both sides by proline-rich domains, which may enable further recruitment and interaction with additional chromatin-modifying enzymes.

Nucleolar and RIX1 domains

PELP1 has three nucleolar domains (Nuc1: amino acids 79–160; Nuc2: amino acids 423–489; and Nuc 3: amino acids 569–642), which are important not only for the nuclear and nucleolar localization of PELP1, but also for rRNA processing and the activation of rDNA transcription and subsequent ribosome biogenesis (Gonugunta *et al.* 2011). PELP1 has a single RIX1 (rRNA processing/ribosome biogenesis) (amino acids 73–224) domain that enables complex formation with proteins IPI1 (TEX10), IPI3 (WDR18), and LASL1 and allows Rea1 AAA ATPase to associate with the 60S ribosomal subunit, a critical step in rRNA processing and ribosome assembly. PELP1 is also a component of the SENP3 complex, a key complex in rRNA processing (Finkbeiner *et al.* 2011a,b).

PELP1 signaling

With respect to subcellular localization, PELP1 is expressed in both the nuclei and nucleoli of cells, but at lower amounts in the cytosol and plasma membrane (Vadlamudi *et al.* 2001, 2004, 2005, Dou *et al.* 2005, Gonugunta *et al.* 2011). PELP1 is involved in several critical cellular functions, including DNA and histone modification, ribosome synthesis, and genomic and nongenomic signaling. PELP1 is modified by several posttranslational mechanisms including phosphorylation

(Vadlamudi & Kumar 2007), glutamylation (Kashiwaya *et al.* 2010), and SUMOylation (Finkbeiner *et al.* 2011a). Several cytosolic and nuclear kinases such as EGFR, Src, PKA, ATM, Cdk2, and Cdk4 have been reported to phosphorylate PELP1 (Girard *et al.* 2013). The association of PELP1 with SRs in hormonal cancers has been explored extensively, and it forms the molecular basis of much of the initial interest in PELP1.

Interaction with SRs

The interactions of PELP1 with SRs such as ER α / β , AR, GR, PR, and vitamin D3 and mineralocorticoid (MR) receptors (Vadlamudi *et al.* 2001, Kayahara *et al.* 2008, Yang *et al.* 2012) involve the SR ligand-binding domain, and the binding is significantly enhanced by the addition of ligand. PELP1, by virtue of its function as a scaffolding protein, enables cross talk between different SRs (e.g., between AR and ER) and between SRs and a variety of cellular proteins involved in histone and DNA modification (e.g., HDAC2 and KDM1 (KDM1A), as shown for ER in breast cancer cells) (Nair *et al.* 2010b). PELP1 is a critical coregulator of the transcriptional activity of SRs.

Role in genomic signaling

PELP1 does not have a known DNA-binding domain and nor does it bind to DNA directly or function as a canonical transcriptional coactivator. Nonetheless, it plays a critical role in genomic regulation induced by SRs by virtue of its recruitment of coregulators. PELP1 enables cross talk between SRs including ER α / β , PR, and AR (Yang *et al.* 2012). Data from our laboratory demonstrated that PELP1 acts as a bridge between ER α and AR to activate AR-responsive genes in the absence of androgen (Yang *et al.* 2012). Interestingly, PELP1 binds to AR and ER α through distinct LxxLL domains (Haas *et al.* 2005). In addition, recent data indicate that PELP1 may be involved in AR nuclear trafficking upon the activation of ligand (Ravindranathan *et al.* 2013).

Through distinct structural domains, PELP1 binds to critical cofactors involved in the modulation of chromatin structure and cooperatively influences gene expression (Choi *et al.* 2004, Gururaj *et al.* 2007, Nair *et al.* 2010b, Mann *et al.* 2013). For example, through its N-terminal LxxLL domain, PELP1 interacts with HDAC2 to repress chromatin decondensation (Choi *et al.* 2004). The C-terminal glutamic-acid-rich region enables the binding of PELP1 to hypoacetylated histones H3 and H4 to prevent further acetylation (Choi *et al.* 2004) and with

KDM1 to remove inhibitory histone methyl marks (Nair *et al.* 2010b). Furthermore, at the ER α target gene promoters, the association of PELP1 with CARM1 enhances its transactivation function by altering the histone H3 arginine methylation status (Mann *et al.* 2013). Together, these data clearly indicate that PELP1 has a role in the modulation of chromatin accessibility of critical target genes.

In addition, PELP1 interacts with several transcriptional activators including HDAC2, STAT3, SUMO2, MLL1/MLL, WDR5, SENP3, HCFC1/HCF1, RBBP5, ASH2L, and 5FMC complex to promote either optimal or aberrant conditions for the activity of SRs or transcription factors (Fanis *et al.* 2012).

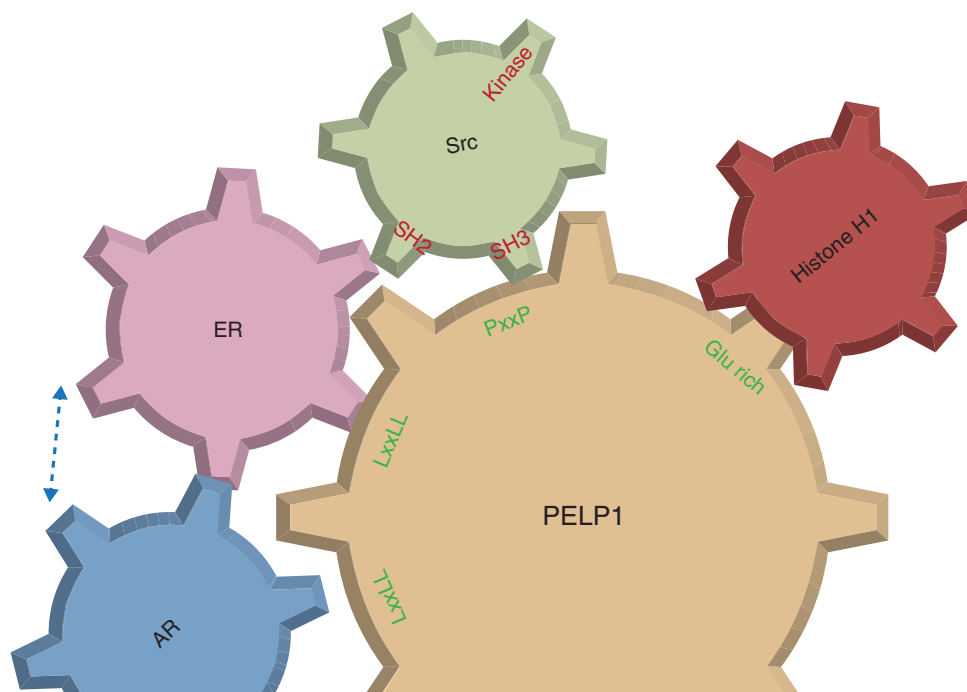
Altogether, PELP1 is involved in SR-mediated genomic signaling both directly by interacting with SRs and their coregulators and indirectly by influencing the transcriptional milieu promoting the accessibility of SRs to the promoter.

Role in nongenomic signaling

PELP1 has no known enzymatic activity. However, PELP1 couples with SRs involved in efferent signaling pathways, through its ability to form complexes. PELP1 enables membrane-mediated signaling for membrane-bound ER α through the activation of cytosolic tyrosine kinase Src (c-Src) and PI3K in the cytosol via growth-factor-mediated membrane receptor signaling (Fig. 2; Barletta *et al.* 2004). The critical scaffolding function of PELP1 was confirmed in experiments using an estrogen dendrimer conjugate that uniquely activates ER extranuclear signaling and *PELP1* knockdown, which blocks the activation of the ER-Src-PI3K-ILK1 pathway (Chakravarty *et al.* 2010b). PELP1-mediated activation of cytosolic kinases in turn influences PELP1-influenced SR genomic function. For example, membrane-bound ER α is able to activate c-Src by complexing with PELP1: c-Src subsequently phosphorylates and activates coactivator proteins in the cytoplasm, which then travel to the nucleus where they modulate PELP1-mediated ER α transcriptional events (Barletta *et al.* 2004).

Similarly, PELP1 is critical for cytosolic ER-mediated nongenomic signaling (Fig. 2). Knockdown of *PELP1* or mutation of its PxxP domain, critical for Src interaction, disrupts estradiol-induced activation of the MAP kinase pathway. PELP1 also interacts with STAT3 and enhances its activity in a Src-mitogen-activated protein kinase-sensitive manner (Manavathi *et al.* 2005).

In addition, PELP1 interacts with several growth factor receptors such as EGFR and HER2 to mediate signaling cross talk with SRs (Vadlamudi *et al.* 2005). Collectively,

**Figure 2**

Schematic representation of the interactome of PELP1 through distinct domains: PELP1 functions as a scaffold enabling the interaction between various nuclear receptors and their cellular mediators. PELP1 interacts with SRs such as AR and ER through its LxxLL domains. PELP1 interacts with the SH3 motif on c-Src through its PxxP domain and through its SH2 domain:

the involvement of two distinct domains of PELP1 is a built-in redundancy to ensure PELP1–c-Src interaction. Furthermore, c-Src and ER when docked on PELP1 may interact through the SH2 motif of c-Src. Finally, histones and histone-modifying enzymes interact with the Glu-rich motif on PELP1.

these findings indicate that the primary role of PELP1 in nongenomic signaling is to enable the formation of multifunctional protein complexes that play critical roles in cell survival and migration and growth factor signaling cross talk with SRs.

PELP1 in cancers

The role of PELP1 as a key core coregulator of SR signaling has led to an examination of its role in hormonal cancers (Girard *et al.* 2013). The expression of PELP1 is dysregulated in a spectrum of hormonal cancers, including 60–80% of breast cancer cases, 60–70% of ovarian cancer cases, and 80–95% of prostate cancer cases, with higher expression profiles being correlated with adverse pathological features including more aggressive tumor types, higher tumor grades, and higher proliferative indices. The overexpression of PELP1 is correlated with adverse clinical outcomes such as nodal positivity, distant metastasis, and therapy resistance (Rajhans *et al.* 2007). In a large cohort of breast cancer specimens ($n=1162$), the expression of PELP1 is an independent predictor of shorter breast-cancer-specific survival and shorter disease-free

survival and its elevated expression is positively associated with poorer outcome (Habashy *et al.* 2010).

In aggressive, therapy-resistant breast and prostate cancers, PELP1 has been shown to play an important role in cell migration and metastasis via its ability to modulate miRNA, epithelial-to-mesenchymal transition (EMT), and mesenchymal-to-epithelial transition (MET) genes and mediate effective cross talk between SRs (Roy *et al.* 2013). The role of PELP1 in ribosome biogenesis also has implications in the progression of cancer by virtue of the importance of ribosomes in protein synthesis and cell growth and functioning. Defective signaling within these cellular processes may disrupt the physiological role of PELP1, contributing to oncogenic phenotypes, and these are discussed below.

PELP1 in cell cycle progression

Knockdown of *PELP1* decreases the proliferation of both ER-positive and ER-negative breast cancer cells. Conversely, the overexpression of PELP1 is sufficient for cellular transformation and accelerated tumorigenesis. In *Xenopus* oocytes, PELP1 appears to mediate the inhibition of

meiosis via G β γ signaling (Haas *et al.* 2005). These data indicate that PELP1 functions as a proto-oncogene.

In breast cancer cells, PELP1 is important for estrogen-mediated cell cycle progression to S phase. The interaction of PELP1 with the cell-cycle-regulating protein retinoblastoma 1 (RB1) may be important for this cell cycle progression as PELP1 may sequester RB and relieve pRB-mediated repression (Balasenthil & Vadlamudi 2003). Furthermore, PELP1 is a cell-cycle-dependent kinase (CDK) substrate, is hyperphosphorylated during cell cycle progression, and recruited to pRB/E2F target genes (Nair *et al.* 2010a).

PELP1 in ribosome biogenesis

The cross talk between ribosome biogenesis and cell division regulated by PELP1 has recently emerged as a key mechanism via its interaction with CDKs. CDK phosphorylation of PELP1 allows PELP1 to localize to the nucleolus, where it regulates rDNA transcription. The inhibition of CDKs dramatically reduces the localization of PELP1 to the nucleolus and has been shown to decrease rDNA promoter activity (Gonugunta *et al.* 2011). This indicates that PELP1 has an overarching role not only in SR-mediated gene regulation but also in cell division. As the nucleolus is seen as the hub of ribosomal DNA transcription and ribosomal subunit processing, increased expression of PELP1 in the nucleolus allows increased protein synthesis, cell survival, and tumorigenic phenotype levels (Finkbeiner *et al.* 2011a,b, Gonugunta *et al.* 2011, Castle *et al.* 2012).

PELP1 and metastasis

Enhanced expression of PELP1 has been correlated with increased motility and invasion of tumor cells (Chakravarty *et al.* 2010b, Roy *et al.* 2013). In contrast, knockdown of *PELP1* results in decreased cell migration via down-regulation of the ER α -Src-PELP1-PI3K-ILK1 pathway, which disrupts cytoskeletal organization (Chakravarty *et al.* 2010b). The overexpression of PELP1 enhances EMT by regulating the expression of genes involved in EMT including MMPs, SNAIL (SNAIL1), TWIST (TWIST1), ZEB (ZEB1), MYC, and MTA1 as well as miR-200a and miR-141 in breast cancer patients (Chakravarty *et al.* 2010b, Roy *et al.* 2012, 2013, Wan & Li 2012).

PELP1 and therapy resistance

Several studies have indicated that the deregulation of PELP1 contributes to therapy resistance and that the

knockdown of *PELP1* or blockage of PELP1-mediated extra-nuclear signaling sensitizes cells to therapy (Vadlamudi *et al.* 2005, Nagpal *et al.* 2008, Kumar *et al.* 2009, Nair *et al.* 2011, Vallabhaneni *et al.* 2011). Interestingly, the subcellular localization of PELP1 is dysregulated in tumors with a cytosolic predominance in a subset of endometrial tumors, which exhibit resistance to tamoxifen anti-hormonal therapy. Patients whose tumors have high levels of cytoplasmic PELP1 respond poorly to tamoxifen therapy compared with patients whose tumors have low levels of cytoplasmic PELP1 (Kumar *et al.* 2009). These observations are in agreement with results from an experiment in which tamoxifen-susceptible MCF-7 cells engineered to express PELP1 in cytosol (by modification the nuclear localization sequence) were found to exhibit resistance to tamoxifen (Vadlamudi *et al.* 2005, Kumar *et al.* 2009, Gonugunta VK, Sareddy GR, Krishnan SR, Cortez V, Roy SS, Tekmal RR & Vadlamudi RK, 2014, unpublished observations). The subcellular localization of PELP1 could be used as a biomarker of hormone sensitivity or vulnerability.

Targeting PELP1 in hormonal cancers

The role of PELP1 in a number of cellular processes and signaling pathways via its various domains makes PELP1 both an attractive and a daunting target for therapeutic modulation. Genetic intervention studies have shown *PELP1* knockout to be lethal during embryonic development, which indicates the importance of PELP1 in development (Vadlamudi, unpublished data). Initial attempts targeted blocking PELP1 downstream signaling pathways such as the PELP1-Src axis, PELP1-CDK2 axis, and PELP1-KDM1 axis. The Src inhibitor dasatinib has been found to exhibit therapeutic utility in blocking the PELP1 signaling axis (Vallabhaneni *et al.* 2011). The CDK inhibitor roscovitine has been found to be effective at reducing the oncogenic processes mediated by PELP1 (Nair *et al.* 2011). KDM1 and CARM1 inhibitors have also been found to substantially inhibit tumorigenic functions of PELP1 (Cortez *et al.* 2012, Mann *et al.* 2013). Even though these studies have established the therapeutic potential of the PELP1 axis in treating hormone-related-cancer patients, these drugs are not specific to PELP1 and new drugs directly targeting PELP1 interactions with increased specificity are required. One such strategy involves targeting specific functions of PELP1 as a coregulator and scaffolding protein. Our recent study has demonstrated the feasibility of targeting the interface between PELP1 and AR interactions with small peptidomimetics that compete for AR binding to

PELP1 and effectively disrupt AR–PELP1 interactions (Ravindranathan et al. 2013). Consequently, the peptidomimetics result in decreased AR uptake into the nucleus, effectively blocking ligand-driven AR activation, with reduced expression of canonical AR-regulated genes, decreased cancer cell proliferation, and inhibition of tumor growth in xenograft and *ex vivo* cultures of primary prostate tumor cells (Ravindranathan et al. 2013). The results of these studies indicate that specific targeting of PELP1 in tumors may serve as a viable therapeutic strategy.

Conclusions and future directions

PELP1 functions as a scaffolding protein and enables critical protein–protein interactions due to its various structural domains. Although bereft of known enzymatic activity or ability to bind to DNA, PELP1 is a critical cellular protein that influences cellular signaling cascades and the cellular transcriptional machinery. Knockdown of *PELP1* is lethal during embryonic development, indicating its importance in cellular functions. The overexpression of PELP1 portends a poor prognosis for patients with hormone-related cancers. Novel approaches to selectively disrupt the interaction of PELP1 with specific protein partners or to selectively knockdown *PELP1* in tumor cells may enable effective targeting of cancers.

Declaration of interest

The authors declare that there is no conflict of interest that could be perceived as prejudicing the impartiality of the review.

Funding

This work was funded by the Department of Defense, the Prostate Cancer Foundation, and the James Thompson Research Foundation.

References

- Balasenthil S & Vadlamudi RK 2003 Functional interactions between the estrogen receptor coactivator PELP1/MNAR and retinoblastoma protein. *Journal of Biological Chemistry* **278** 22119–22127. (doi:10.1074/jbc.M212822200)
- Barletta F, Wong CW, McNally C, Komm BS, Katzenellenbogen B & Cheskis BJ 2004 Characterization of the interactions of estrogen receptor and MNAR in the activation of cSrc. *Molecular Endocrinology* **18** 1096–1108. (doi:10.1210/me.2003-0335)
- Boonyaratanakornkit V 2011 Scaffolding proteins mediating membrane-initiated extra-nuclear actions of estrogen receptor. *Steroids* **76** 877–884. (doi:10.1016/j.steroids.2011.02.017)
- Castle CD, Cassimere EK & Denicourt C 2012 LAS1L interacts with the mammalian Rix1 complex to regulate ribosome biogenesis. *Molecular Biology of the Cell* **23** 716–728. (doi:10.1091/mbc.E11-06-0530)
- Chakravarty D, Tekmal RR & Vadlamudi RK 2010a PELP1: a novel therapeutic target for hormonal cancers. *IUBMB Life* **62** 162–169. (doi:10.1002/iub.287)
- Chakravarty D, Nair SS, Santhamma B, Nair BC, Wang L, Bandyopadhyay A, Agyin JK, Brann D, Sun LZ, Yeh IT et al. 2010b Extracellular functions of ER impact invasive migration and metastasis by breast cancer cells. *Cancer Research* **70** 4092–4101. (doi:10.1158/0008-5472.CAN-09-3834)
- Chakravarty D, Roy SS, Babu CR, Dandamudi R, Curiel TJ, Vivas-Mejia P, Lopez-Berestein G, Sood AK & Vadlamudi RK 2011 Therapeutic targeting of PELP1 prevents ovarian cancer growth and metastasis. *Clinical Cancer Research* **17** 2250–2259. (doi:10.1158/1078-0432.CCR-10-2718)
- Choi YB, Ko JK & Shin J 2004 The transcriptional corepressor, PELP1, recruits HDAC2 and masks histones using two separate domains. *Journal of Biological Chemistry* **279** 50930–50941. (doi:10.1074/jbc.M406831200)
- Cortez V, Mann M, Tekmal S, Suzuki T, Miyata N, Rodriguez-Aguayo C, Lopez-Berestein G, Sood AK & Vadlamudi RK 2012 Targeting the PELP1–KDM1 axis as a potential therapeutic strategy for breast cancer. *Breast Cancer Research* **14** R108. (doi:10.1186/bcr3229)
- Dimple C, Nair SS, Rajhans R, Pitcheswara PR, Liu J, Balasenthil S, Le XF, Burow ME, Auersperg N, Tekmal RR et al. 2008 Role of PELP1/MNAR signaling in ovarian tumorigenesis. *Cancer Research* **68** 4902–4909. (doi:10.1158/0008-5472.CAN-07-5698)
- Dou Y, Milne TA, Tackett AJ, Smith ER, Fukuda A, Wysocka J, Allis CD, Chait BT, Hess JL & Roeder RG 2005 Physical association and coordinate function of the H3 K4 methyltransferase MLL1 and the H4 K16 acetyltransferase MOF. *Cell* **121** 873–885. (doi:10.1016/j.cell.2005.04.031)
- Fanis P, Gillemans N, Aghajani-refah A, Pourfarzad F, Demmers J, Esteghamat F, Vadlamudi RK, Grosveld F, Philipsen S & van Dijk TB 2012 Five friends of methylated chromatin target of protein-arginine-methyltransferase[prmt]-1 (chtop), a complex linking arginine methylation to desumoylation. *Molecular and Cellular Proteomics* **11** 1263–1273. (doi:10.1074/mcp.M112.017194)
- Finkbeiner E, Haindl M & Muller S 2011a The SUMO system controls nucleolar partitioning of a novel mammalian ribosome biogenesis complex. *EMBO Journal* **30** 1067–1078. (doi:10.1038/emboj.2011.33)
- Finkbeiner E, Haindl M, Raman N & Muller S 2011b SUMO routes ribosome maturation. *Nucleus* **2** 527–532. (doi:10.4161/nucl.2.6.17604)
- Folkertsma S, van Noort PI, de Heer A, Carati P, Brandt R, Visser A, Vriend G & de Vlieg J 2007 The use of *in vitro* peptide binding profiles and *in silico* ligand–receptor interaction profiles to describe ligand-induced conformations of the retinoid X receptor α ligand-binding domain. *Molecular Endocrinology* **21** 30–48. (doi:10.1210/me.2006-0072)
- Fuchs S, Nguyen HD, Phan TT, Burton MF, Nieto L, de Vries-van Leeuwen IJ, Schmidt A, Goodarzifard M, Agten SM, Rose R et al. 2013 Proline primed helix length as a modulator of the nuclear receptor–coactivator interaction. *Journal of the American Chemical Society* **135** 4364–4371. (doi:10.1021/ja311748r)
- Girard BJ, Daniel AR, Lange CA & Ostrander JH 2013 PELP1: a review of PELP1 interactions, signaling, and biology. *Molecular and Cellular Endocrinology* **382** 642–651. (doi:10.1016/j.mce.2013.07.031)
- Gonugunta VK, Nair BC, Rajhans R, Sareddy GR, Nair SS & Vadlamudi RK 2011 Regulation of rDNA transcription by proto-oncogene PELP1. *PLoS ONE* **6** e21095. (doi:10.1371/journal.pone.0021095)
- Gonugunta VK, Sareddy GR, Krishnan SR, Cortez V, Roy SS, Tekmal RR & Vadlamudi RK 2014 Inhibition of mTOR signaling reduces PELP1-mediated tumor growth and therapy resistance. *Molecular Cancer Therapeutics* **13** 1578–1588. (doi:10.1158/1535-7163.MCT-13-0877)
- Greger JG, Guo Y, Henderson R, Ross JF & Cheskis BJ 2006 Characterization of MNAR expression. *Steroids* **71** 317–322. (doi:10.1016/j.steroids.2005.09.016)
- Gururaj AE, Peng S, Vadlamudi RK & Kumar R 2007 Estrogen induces expression of BCAS3, a novel estrogen receptor- α coactivator, through proline-, glutamic acid-, and leucine-rich protein-1 (PELP1). *Molecular Endocrinology* **21** 1847–1860. (doi:10.1210/me.2006-0514)
- Haas D, White SN, Lutz LB, Rasar M & Hammes SR 2005 The modulator of nongenomic actions of the estrogen receptor (MNAR) regulates

- transcription-independent androgen receptor-mediated signaling: evidence that MNAR participates in G protein-regulated meiosis in *Xenopus laevis* oocytes. *Molecular Endocrinology* **19** 2035–2046. (doi:10.1210/me.2004-0531)
- Habashy HO, Powe DG, Rakha EA, Ball G, Macmillan RD, Green AR & Ellis IO 2010 The prognostic significance of PELP1 expression in invasive breast cancer with emphasis on the ER-positive luminal-like subtype. *Breast Cancer Research and Treatment* **120** 603–612. (doi:10.1007/s10549-009-0419-9)
- Kashiwaya K, Nakagawa H, Hosokawa M, Mochizuki Y, Ueda K, Piao L, Chung S, Hamamoto R, Eguchi H, Ohigashi H et al. 2010 Involvement of the tubulin tyrosine ligase-like family member 4 polyglutamylase in PELP1 polyglutamylation and chromatin remodeling in pancreatic cancer cells. *Cancer Research* **70** 4024–4033. (doi:10.1158/0008-5472.CAN-09-4444)
- Kayahara M, Ohanian J, Ohanian V, Berry A, Vadlamudi R & Ray DW 2008 MNAR functionally interacts with both NH2- and COOH-terminal GR domains to modulate transactivation. *American Journal of Physiology. Endocrinology and Metabolism* **295** E1047–E1055. (doi:10.1152/ajpendo.90429.2008)
- Kefalopoulou Z, Tzelepi V, Zolota V, Grivas PD, Christopoulos C, Kalofonos H, Maraziotis T & Sotiropoulou-Bonikou G 2012 Prognostic value of novel biomarkers in astrocytic brain tumors: nuclear receptor co-regulators AIB1, TIF2, and PELP1 are associated with high tumor grade and worse patient prognosis. *Journal of Neuro-Oncology* **106** 23–31. (doi:10.1007/s11060-011-0637-y)
- Kumar R, Zhang H, Holm C, Vadlamudi RK, Landberg G & Rayala SK 2009 Extranuclear coactivator signaling confers insensitivity to tamoxifen. *Clinical Cancer Research* **15** 4123–4130. (doi:10.1158/1078-0432.CCR-08-2347)
- Manavathi B, Nair SS, Wang RA, Kumar R & Vadlamudi RK 2005 Proline-, glutamic acid-, and leucine-rich protein-1 is essential in growth factor regulation of signal transducers and activators of transcription 3 activation. *Cancer Research* **65** 5571–5577. (doi:10.1158/0008-5472.CAN-04-4664)
- Mann M, Cortez V & Vadlamudi R 2013 PELP1 oncogenic functions involve CARM1 regulation. *Carcinogenesis* **34** 1468–1475. (doi:10.1093/carcin/bgt091)
- Nagpal JK, Nair S, Chakravarty D, Rajhans R, Pothana S, Brann DW, Tekmal RR & Vadlamudi RK 2008 Growth factor regulation of estrogen receptor coregulator PELP1 functions via protein kinase A pathway. *Molecular Cancer Research* **6** 851–861. (doi:10.1158/1541-7786.MCR-07-2030)
- Nair SS, Mishra SK, Yang Z, Balasenthil S, Kumar R & Vadlamudi RK 2004 Potential role of a novel transcriptional coactivator PELP1 in histone H1 displacement in cancer cells. *Cancer Research* **64** 6416–6423. (doi:10.1158/0008-5472.CAN-04-1786)
- Nair SS, Guo Z, Mueller JM, Koochekpour S, Qiu Y, Tekmal RR, Schule R, Kung HJ, Kumar R & Vadlamudi RK 2007 Proline-, glutamic acid-, and leucine-rich protein-1/modulator of nongenomic activity of estrogen receptor enhances androgen receptor functions through LIM-only coactivator, four-and-a-half LIM-only protein 2. *Molecular Endocrinology* **21** 613–624. (doi:10.1210/me.2006-0269)
- Nair BC, Nair SS, Chakravarty D, Challa R, Manavathi B, Yew PR, Kumar R, Tekmal RR & Vadlamudi RK 2010a Cyclin-dependent kinase-mediated phosphorylation plays a critical role in the oncogenic functions of PELP1. *Cancer Research* **70** 7166–7175. (doi:10.1158/0008-5472.CAN-10-0628)
- Nair SS, Nair BC, Cortez V, Chakravarty D, Metzger E, Schule R, Brann DW, Tekmal RR & Vadlamudi RK 2010b PELP1 is a reader of histone H3 methylation that facilitates oestrogen receptor- α target gene activation by regulating lysine demethylase 1 specificity. *EMBO Reports* **11** 438–444. (doi:10.1038/embor.2010.62)
- Nair BC, Vallabhaneni S, Tekmal RR & Vadlamudi RK 2011 Roscovitine confers tumor suppressive effect on therapy-resistant breast tumor cells. *Breast Cancer Research* **13** R80. (doi:10.1186/bcr2929)
- Rajhans R, Nair S, Holden AH, Kumar R, Tekmal RR & Vadlamudi RK 2007 Oncogenic potential of the nuclear receptor coregulator proline-, glutamic acid-, leucine-rich protein 1/modulator of the nongenomic actions of the estrogen receptor. *Cancer Research* **67** 5505–5512. (doi:10.1158/0008-5472.CAN-06-3647)
- Ravindranathan P, Lee TK, Yang L, Centenera MM, Butler L, Tilley WD, Hsieh JT, Ahn JM & Raj GV 2013 Peptidomimetic targeting of critical androgen receptor–coregulator interactions in prostate cancer. *Nature Communications* **4** 1923. (doi:10.1038/ncomms2912)
- Renoir JM, Marsaud V & Lazennec G 2013 Estrogen receptor signaling as a target for novel breast cancer therapeutics. *Biochemical Pharmacology* **85** 449–465. (doi:10.1016/j.bcp.2012.10.018)
- Roy S, Chakravarty D, Cortez V, De Mukhopadhyay K, Bandyopadhyay A, Ahn JM, Raj GV, Tekmal RR, Sun L & Vadlamudi RK 2012 Significance of PELP1 in ER-negative breast cancer metastasis. *Molecular Cancer Research* **10** 25–33. (doi:10.1158/1541-7786.MCR-11-0456)
- Roy SS, Gonugunta VK, Bandyopadhyay A, Rao MK, Goodall GJ, Sun LZ, Tekmal RR & Vadlamudi RK 2013 Significance of PELP1/HDAC2/miR-200 regulatory network in EMT and metastasis of breast cancer. *Oncogene* (In Press). (doi:10.1038/nc.2013.332)
- Vadlamudi RK & Kumar R 2007 Functional and biological properties of the nuclear receptor coregulator PELP1/MNAR. *Nuclear Receptor Signaling* **5** e004. (doi:10.1621/nrs.05004)
- Vadlamudi RK, Wang RA, Mazumdar A, Kim Y, Shin J, Sahin A & Kumar R 2001 Molecular cloning and characterization of PELP1, a novel human coregulator of estrogen receptor α . *Journal of Biological Chemistry* **276** 38272–38279. (doi:10.1074/jbc.M103783200)
- Vadlamudi RK, Balasenthil S, Broadus RR, Gustafsson JA & Kumar R 2004 Deregulation of estrogen receptor coactivator proline-, glutamic acid-, and leucine-rich protein-1/modulator of nongenomic activity of estrogen receptor in human endometrial tumors. *Journal of Clinical Endocrinology and Metabolism* **89** 6130–6138. (doi:10.1210/jc.2004-0909)
- Vadlamudi RK, Manavathi B, Balasenthil S, Nair SS, Yang Z, Sahin AA & Kumar R 2005 Functional implications of altered subcellular localization of PELP1 in breast cancer cells. *Cancer Research* **65** 7724–7732. (doi:10.1158/0008-5472.CAN-05-0614)
- Vallabhaneni S, Nair BC, Cortez V, Challa R, Chakravarty D, Tekmal RR & Vadlamudi RK 2011 Significance of ER- α axis in hormonal therapy resistance. *Breast Cancer Research and Treatment* **130** 377–385. (doi:10.1007/s10549-010-1312-2)
- Vanhaesebroeck B, Leeyers SJ, Ahmadi K, Timms J, Katso R, Driscoll PC, Woscholski R, Parker PJ & Waterfield MD 2001 Synthesis and function of 3-phosphorylated inositol lipids. *Annual Review of Biochemistry* **70** 535–602. (doi:10.1146/annurev.biochem.70.1.535)
- Wan J & Li X 2012 PELP1/MNAR suppression inhibits proliferation and metastasis of endometrial carcinoma cells. *Oncology Reports* **28** 2035–2042. (doi:10.3892/or.2012.2038)
- Yang L, Ravindranathan P, Ramanan M, Kapur P, Hammes SR, Hsieh JT & Raj GV 2012 Central role for PELP1 in nonandrogenic activation of the androgen receptor in prostate cancer. *Molecular Endocrinology* **26** 550–561. (doi:10.1210/me.2011-1101)

Received in final form 15 May 2014

Accepted 21 May 2014

Made available online as an Accepted Preprint
22 May 2014

NFI Transcription Factors Interact with FOXA1 to Regulate Prostate-Specific Gene Expression

Magdalena M. Grabowska, Amicia D. Elliott, David J. DeGraff, Philip D. Anderson, Govindaraj Anumanthan, Hironobu Yamashita, Qian Sun, David B. Friedman, David L. Hachey, Xiuping Yu, Jonathan H. Sheehan, Jung-Mo Ahn, Ganesh V. Raj, David W. Piston, Richard M. Gronostajski, and Robert J. Matusik

Department of Urologic Surgery (M.M.G., G.A. H.Y., Q.S., X.Y., R.J.M.), Department of Molecular Physiology and Biophysics (A.D.E., D.W.P.), and Vanderbilt-Ingram Cancer Center (R.J.M.), Vanderbilt University Medical Center, Nashville, Tennessee 37232; Department of Pathology (D.J.D.), Penn State University College of Medicine, Hershey, Pennsylvania 17033; Department of Biological Sciences (P.D.A.), Salisbury University, Salisbury, Maryland 21801; Mass Spectrometry Research Center (D.B.F., D.L.H.), Department of Biochemistry, Department of Biochemistry and Center for Structural Biology (J.H.S.), and Department of Cell and Developmental Biology (R.J.M.), Vanderbilt University, Nashville, Tennessee 37232; Department of Chemistry (J.-M.A.), University of Texas Dallas, Dallas, Texas 75080; Department of Urology (G.V.R.), University of Texas Southwestern, Dallas, Texas 75390; and Department of Biochemistry (R.M.G.), Developmental Genomics Group, NY State Center of Excellence in Bioinformatics and Life Sciences, University at Buffalo, Buffalo, New York 14203

Androgen receptor (AR) action throughout prostate development and in maintenance of the prostatic epithelium is partly controlled by interactions between AR and forkhead box (FOX) transcription factors, particularly FOXA1. We sought to identify additional FOXA1 binding partners that may mediate prostate-specific gene expression. Here we identify the nuclear factor I (NFI) family of transcription factors as novel FOXA1 binding proteins. All four family members (NFIA, NFIB, NFIC, and NFIX) can interact with FOXA1, and knockdown studies in androgen-dependent LNCaP cells determined that modulating expression of NFI family members results in changes in AR target gene expression. This effect is probably mediated by binding of NFI family members to AR target gene promoters, because chromatin immunoprecipitation (ChIP) studies found that NFIB bound to the prostate-specific antigen enhancer. Förster resonance energy transfer studies revealed that FOXA1 is capable of bringing AR and NFIX into proximity, indicating that FOXA1 facilitates the AR and NFI interaction by bridging the complex. To determine the extent to which NFI family members regulate AR/FOXA1 target genes, motif analysis of publicly available data for ChIP followed by sequencing was undertaken. This analysis revealed that 34.4% of peaks bound by AR and FOXA1 contain NFI binding sites. Validation of 8 of these peaks by ChIP revealed that NFI family members can bind 6 of these predicted genomic elements, and 4 of the 8 associated genes undergo gene expression changes as a result of individual NFI knock-down. These observations suggest that NFI regulation of FOXA1/AR action is a frequent event, with individual family members playing distinct roles in AR target gene expression. (*Molecular Endocrinology* 28: 949–964, 2014)

ISSN Print 0888-8809 ISSN Online 1944-9917
Printed in U.S.A.
Copyright © 2014 by the Endocrine Society
Received July 19, 2013. Accepted April 18, 2014.
First Published Online May 6, 2014

Abbreviations: AR, androgen receptor; ARE, androgen response element; ChIP, chromatin immunoprecipitation; ChIP-Seq, chromatin immunoprecipitation-sequencing; DHT, dihydrotestosterone; DBD, DNA-binding domain; ER, estrogen receptor; EtOH, ethanol; FBS, fetal bovine serum; FOX, forkhead box; FRET, Förster resonance energy transfer; GR, glucocorticoid receptor; GST, glutathione S-transferase; HA, hemagglutinin; LC-MS/MS, liquid chromatography-tandem mass spectrometry; mCer3, mCerulean3; NFI, nuclear factor I; PDB, Protein Data Bank; PSA, prostate-specific antigen; Q-RT-PCR, quantitative real-time PCR; siRNA, small interfering RNA; TF, transcription factor.

It is well recognized that signaling by the androgen receptor (AR) has important roles in normal prostate development, growth, and differentiation (1–3), as well as in benign and neoplastic conditions of the prostate (4). However, AR alone is not sufficient to mediate tissue-specific gene expression. Rather, it is the combinatorial control (5, 6) and activity of multiple factors that determine tissue-specific gene expression. Specifically, the ability of AR to engage other transcription factors (TFs) in a physical complex dictates tissue-specific gene expression in the prostate (7). In addition to the prostate, the AR is expressed in various tissues where it exhibits a distinct role for normal gene expression and physiology. For example, the AR in the skeletal muscle dictates anabolism of that tissue (8). Therefore, in addition to epigenetic mechanisms, it is the ability of AR to interact with other TFs that determines AR function in a given tissue.

Our interest in identifying factors that mediate tissue specificity of AR target gene expression led to identification of forkhead box (FOX) A1 (FOXA1) as an AR interacting protein (9, 10) and showed that this interaction is essential for the expression of AR-regulated, prostate-specific genes (for review, see Ref. 11). The FOXA family of proteins (FOXA1, FOXA2, and FOXA3) bind with differing affinity to the consensus DNA sequence [(A/C)AA(C/T)] and have been implicated in various developmental, homeostatic, and disease processes (12–14). Our focus has been on FOXA1 because FOXA2 is expressed only in neuroendocrine cells of the adult prostate and FOXA3 is not expressed in adult prostate (15). FOXA1 works as a “pioneer factor” and acts to increase TF accessibility to the DNA by displacing linker histones from nucleosomes, allowing for chromatin unfolding (16). Further studies by us and others have validated the importance of this AR/FOXA1 interaction in prostate cancer (14, 17–20) and demonstrated the interaction between FOXA1 and other steroid receptors (21–24).

The loss of FOXA1 in prostate cancer cell lines that express AR results in dramatic reprogramming of AR to different binding sites (20, 25). The ability of FOXA1 to interact with AR and specify binding to specific androgen response elements (AREs) suggests that other TFs involved with the AR/FOXA1 complex may further regulate tissue-specific gene expression. To identify novel TFs involved in the AR/FOXA1 transcription complex, we expressed a dual-tagged FOXA1 construct in an androgen-regulated prostatic cell line, LNCaP, and performed tandem affinity purification and mass spectrometry to identify a novel set of FOXA1 interacting proteins. Sixteen proteins were identified, only one of which, nuclear factor IX (NFIX), was a TF.

The NFI family of TFs contains 4 genes (*NFIA*, *NFIB*, *NFIC*, and *NFIX*) encoding proteins that bind to the con-

sensus DNA sequence TTGGCN₃GCCAA (26). NFI family members can form either homodimers or heterodimers with each other, and these dimers have comparable affinity for DNA, stability, and specificity (27), suggesting that dimer combinations will be dictated by tissue-specific expression. Indeed, NFIX has been identified as a stromal-specific factor in the human prostate, whereas NFIB has been classified as basal-specific (28). Knockout studies of individual NFI genes in mice have revealed a variety of phenotypes, including corpus callosum agenesis (NFIA) (29), lung hypoplasia (NFIB) (30), tooth defects (NFIC) (31), and neurological and skeletal defects (NFIX) (32, 33). Thus, each NFI has nonredundant roles during development.

Although an unidentified NFI (34) and NFIX (17) have been identified as FOXA1 interacting partners, little is known about the role of individual family members in the prostate gland. Therefore, we set out to identify the specific NFI family members that interact with FOXA1 and determine the role of NFI family members on prostate-specific gene expression. Our studies have revealed that the NFI family provides an elaborate and well-balanced TF set that can provide AR, FOXA1, and the AR/FOXA1 complex precise control over tissue-specific gene expression.

Materials and Methods

Cell culture and establishment of LNCaP cells stably expressing FOXA1

All cell lines used were obtained from American Type Culture Collection and were maintained in RPMI 1640 medium (Invitrogen/Gibco), supplemented with 10% (v/v) fetal bovine serum (FBS) (Atlanta Biologicals). LNCaP cells express AR and FOXA1 and engage effectively in androgen-regulated prostate-specific gene expression. We therefore chose LNCaP cells to ectopically express dual affinity tagged FOXA1 for our binding partner studies. Tandem FLAG and 6xHis affinity tags were added to the N termini of FOXA1 via a standard PCR approach, followed by subsequent cloning into a pCR-TOPO 2.1 vector (Invitrogen) to generate FLAG-6xHis-FOXA1. After restriction enzyme digestion with *Xho*I and *Hind*II (New England Biolabs), FLAG-6xHis-FOXA1 was cloned into the retroviral vector pLPCX (Clontech), resulting in LNCaP-pLPCX-FOXA1. The sequence was confirmed by DNA sequencing. LNCaP cells were next infected with virus purified from Phoenix retroviral packaging cells transfected with either pLPCX-FOXA1 or pLPCX empty vector. Cells were selected and maintained in puromycin antibiotic (5 μ g/mL).

Tandem affinity purification and mass spectrometry for the identification of FOXA1 binding partners

Nuclear extracts were prepared as described previously (35) from $\sim 10^9$ LNCaP-pLPCX-FOXA1 cells and LNCaP-pLPCX

cells maintained in RPMI 1640 medium containing 10% FBS. Nuclear extracts were first subjected to TALON resin purification (BD Biosciences) according to the manufacturer's instructions to isolate FLAG-6xHis-FOXA1 via its His tags. This was followed by purification with anti-FLAG M2 affinity gel (Sigma-Aldrich) to purify FLAG-6xHis-FOXA1 by its FLAG tag, as well as FOXA1 binding partners. Fractions isolated from each step were subjected to Western blotting analysis for FOXA1 to verify purification success. In addition, Western blotting for the known FOXA1 binding partner, AR, was performed as a positive control after the use of anti-FLAG M2 affinity gel to verify the success of our purification approach. Purified protein was subjected to SDS-PAGE electrophoresis followed by band excision and tryptic digestion according to standard procedures. Peptide hydrolysate was then analyzed by C18 reverse-phase liquid chromatography-tandem mass spectrometry (LC-MS/MS) using a Thermo LTQ ion trap mass spectrometer equipped with a Thermo MicroAS autosampler and Thermo Surveyor HPLC pump system, nanospray source, and Xcalibur 2.0 instrument control using standard data-dependent methods. MS/MS data were analyzed with the SEQUEST algorithm against the International Protein Index (IPI) human database (135 674 entries, October 2007 release) including a concatenated reverse database for calculating the false-discovery rate. The presence of at least 2 peptides from 2 separate runs was used as the criteria for a positive hit.

Coimmunoprecipitation studies

JEG-3 cells are reported to be NFI deficient (36, 37) and do not express FOXA1, making them an ideal cell line to test the ability of these proteins to interact. After transfection with FOXA1 and hemagglutinin (HA)-tagged individual mouse NFI constructs or vector plasmid (PCH), JEG-3 cells were washed 3 times with cold PBS and lysed with 1 mL of nondenaturing lysis buffer (50 mM Tris, 150 mM NaCl, 10 mM EDTA, 0.02% NaN₃, 50 mM NaF, 1 mM Na₃VO₄, 1% NP-40, 1 mM phenylmethylsulfonylfluoride, 0.5 mM dithiothreitol, and 1× concentration of complete protease inhibitor cocktail [Roche]). After sonication, centrifugation, and preclearing, 1 mg of total cell lysate for each reaction was incubated at 4°C overnight with 20 μ L (dry volume) of protein G-Sepharose beads (Amersham Biotech) conjugated with 1 μ g of experimental antibody. Immunoprecipitation was performed in the presence of ethidium bromide (100 μ g/mL; Sigma-Aldrich) to disrupt DNA-protein interactions, and BSA was added to reduce nonspecific binding. After overnight incubation, samples were centrifuged, and the pelleted protein G-Sepharose beads were washed 4 times with lysis buffer and once with PBS followed by protein dissociation and Western blotting analysis. The mouse monoclonal HA antibody (clone 12CA5; Roche) was used to immunoprecipitate HA-tagged NFI family members. Anti-HNF-3 (C-20; Santa Cruz Biotechnology) was used to immunoprecipitate FOXA1.

Glutathione S-transferase (GST)-fusion assays

Primer pairs containing *Eco*R1 and *Xho*I restriction enzyme sequences were used to amplify and subclone the NFIX coding sequence into the pGEX6p-1 vector, resulting in GST-NFIX for use in GST pull-down assays. T7 promoter-driven expression vectors encoding for FOXA1 deletion constructs were described previously (9) and were transcribed and translated in vitro using

the TnT T7 Quick Coupled Transcription/Translation System (Promega). A standard reaction involved a 90-minute incubation at 30°C with 40 μ L of TnT Quick Master Mix, 2 μ L of cold 2 mM methionine, and 2 μ g of plasmid DNA in a final volume of 50 μ L. In vitro translated recombinant FOXA1 proteins were labeled with a C-terminal V5 epitope and were used immediately for in vitro binding reactions. For GST pull-down assays, 50 μ L of swelled glutathione agarose beads (G-4510; Sigma-Aldrich) were incubated with 20 μ g of GST or GST-NFIX fusion proteins for each reaction. GST-bound beads were equilibrated with PBS-T binding buffer (1× PBS [pH 7.4], 1% Tween 20, and protease inhibitors) and incubated for 2 hours at 4°C with 5 to 10 μ L of products from the TnT reactions. Complexes were washed 4 times with 1.5 mL of cold binding buffer, heated for 10 minutes at 70°C in 1× SDS loading buffer, and separated by SDS-PAGE, after which V5-horseradish peroxidase antibody was used in a standard Western blot to determine which domain of FOXA1 is required for interactions with NFIX in vitro. Cell lysates and IP reactions were run in different orders on their respective gels. For clarity, input Western blot images have been reordered. A comparison of the original and reordered original can be found in http://press.endocrine.org/doi/suppl/10.1210/me.2013-12139/suppl_file/me-13-1213-1.pdf Supplemental Figure 1.

ARR₂PB and prostate-specific antigen (PSA) reporter gene assays

Transient transfection to determine the influence of NFI overexpression on androgen-regulated ARR₂PB and PSA reporter gene constructs was performed using Lipofectamine 2000 (Invitrogen) according to the manufacturer's recommendation and as reported previously (7). JEG-3 cells were plated at an initial density of 150 000 cells/well in 24-well tissue culture plates (BD Falcon) and allowed to attach overnight in RMPI medium 1640 supplemented with 10% FBS. On the following day, 0.25 μ g of mouse NFIA, NFIB, NFIC, or NFIX plasmid, 0.25 μ g of rat AR expression vector, and/or FOXA1 expression vector, 0.0125 μ g of pRL-CMV (Promega) were mixed in serum-free Opti-Free MEM medium (Invitrogen) and subsequently combined with Opti-Free MEM containing Lipofectamine 2000 (Invitrogen) and incubated at room temperature per the manufacturer's instructions. Medium was aspirated from target cells for transfection, which were then incubated with the DNA-Lipofectamine mixture for 6 hours, followed by removal of the medium and addition of 0.5 mL/well of Opti-Free medium supplemented at a final concentration of 10 nM dihydrotestosterone (DHT) or ethanol vehicle control (Sigma). After DHT treatment for 24 hours, cells were harvested by removing the medium, washing the cells once with PBS, and incubating with 100 μ L of passive lysis buffer (Promega) for 30 minutes at room temperature. Both firefly and *Renilla* luciferase activities were determined in a lumicounter (LUM/star; BMG LabTechnologies, Inc) by using the Dual-Luciferase reporter assay system (Promega) to control for transfection efficiency. Experiments were performed in triplicate and repeated at least twice.

Knockdown studies

LNCaP cells were transiently transfected with either ON-TARGETplus SMART pool human small interfering

siRNA (siRNA) NFIA, NFIB, NFIC, or NFIX constructs or ON-TARGETplus Non-Targeting siRNA no. 2 (Dharmacon RNAi Technologies) as described previously (38) at a working concentration of 100 nM. After 48 hours of transfection in complete medium (10% FBS in RPMI medium 1640), quantitative real-time PCR (Q-RT-PCR) was used to determine the extent of individual NFI knockdown, and the influence of individual NFI knockdown on the prostate-specific genes *PSA*, *TMPRSS2*, *FKBP5*, and *NKX3-1*. Primer sequences and associated annealing temperatures used in this study are as follows: for *NFIA*, 55°C, forward 5'-CCTCTACGAGCTCCACAAAGC-3' and reverse 5'-ATTGAGGAACCCACCTGTCC-3'; for *NFIB*, 55°C, forward 5'-AGAGATCAAGATATGTCTTC-3' and reverse 5'-CTGGCTGGTTTGTGGACTGGA-3'; for *NFIC*, 55°C, forward 5'-CCTGGACCGTTAAATGGA-3' and reverse 5'-GATAC-CAGGACTGTCCTG-3'; for *NFIX*, 58°C, forward 5'-CTGCCCAACGGGCACTTAA-3' and reverse 5'-CTGTCAATCGATGGACTTGGG-3'; for *PSA*, 58°C, forward 5'-GCAGTCTGCGGCGGTGTTCT-3' and reverse 5'-GCGGGTGTGGGAAGCTGTGG-3'; for *NKX3-1*, 62°C, forward 5'-CCGAGACGCTGGCAGAGACC-3' and reverse 5'-GCTTAGGGGTTTGGGGAAG-3'; for *TMPRSS2*, 58°C, forward 5'-GCACAGCCCACTGTGGTCCC-3' and reverse 5'-CAGAGTAGGCCAGCGGCCAG-3'; for *FKBP5*, 60°C, forward 5'-CTGGAAGGCCGCTGTGGTGG-3' and reverse 5'-TGCATAGGGACTCACACACCTTGA-3'; and for *GAPDH*, 58°C, forward 5'-GGCATGGACTGTGGTCATGAG-3' and reverse 5'-TGCACCACCAACTGCTTAGC-3'.

Primers used to validate chromatin immunoprecipitation (ChIP)-sequencing (ChIP-Seq) data mining and ChIP studies are the following: for *CLU*, forward 5'-CCCACACTTCTGACTCGGAC-3' and reverse 5'-ACTCCTCCCGGTGCTTTTTG-3'; for *OR9A2*, forward 5'-GTCTGCAGTCCCCATGTAT-3' and reverse 5'-CCATGGTCCCACAGGAAAAGT-3'; for *GREB1*, forward 5'-CGTGTGGTGACTGGAGTAGCTG-3' and reverse 5'-TGGCATCTCAGATTCGGTGC-3'; for *SOX6*, forward 5'-CTGCGGAGAAGAATGTCTTCCAA-3' and reverse 5'-TGCATTATGGGGTGCAGAGG-3'; for *SMAD2*, forward 5'-GCTCCCTCCGTCTTCCATAC-3' and reverse 5'-CTTGATC-GAACCTCCCGGC-3'; for *SYPL1*, forward 5'-TGGC GCCCAACATCTACTTG-3' and reverse 5'-AGAAGCAATC-CACTCGAGGAC-3'; and for *IL-8*, forward 5'-CAGAGACAGCA-GAGCACACA-3' and reverse 5'-GGCAAAACTGCACC TTCACA-3'.

ChIP

LNCaP cells were used to determine the ability of NFI TFs to bind to AR target genes. ChIP assays were performed according to the manufacturer's instructions for the SimpleChIP Enzymatic Chromatin IP kit with magnetic beads (Cell Signaling Technology). Antibodies used for ChIP assays were as follows: ChIP-grade rabbit anti-AR (2 µg, 74272; Abcam), ChIP-grade rabbit anti-FOXA1 (2 µg, 23738; Abcam), rabbit anti-pan NF-1 N-20 (5 µg, sc-870; Santa Cruz Biotechnology), rabbit anti-NFIB (5 µg, HPA003956; Sigma-Aldrich), and normal rabbit IgG (5 µg, 2729; Cell Signaling Technology). LNCaP cells were treated with either ethanol (EtOH) control or 10 nM DHT for 2 hours, which represents the time required for peak AR recruitment to the PSA enhancer after DHT treatment (39). Cells were cross-linked for 9 minutes with formaldehyde and processed according to the manufacturer's instructions. ChIP DNA

was analyzed by Q-RT-PCR. The primer set for ChIP analysis was hChIP PSA 206 (forward 5'-ACAGACCTACTCTGGAGGAA-3' and reverse 5'-AAGACAGCAACACCTTTTTTTTC-3') used at an annealing temperature of 52°C. Results from PCR normalized to EtOH IgG are depicted. Primers used for ChIP validation are as follows: for *TMPRSS2* ChIP, forward 5'-TGGTGTGT-TAGGGATCTGGAG-3' and reverse 5'-CACGCCCC GCTTCTTTTTTA-3'; for *CLU* ChIP, forward 5'-GCCTGGTT-GTGCACTCATCTA-3' and reverse 5'-TCCTGGTACACAG-CAGTTCA-3'; for *OR9A2* ChIP, forward 5'-CCCTAGCTGC-TATGCTCCAA-3' and reverse 5'-AGGTGGGA-AGACTGAGTGGA-3'; for *GREB1* ChIP, forward 5'-GTAGTCCTTCGGAGGCAAGC-3' and reverse 5'-GTTTT-GCTGGGTCACAGTGC-3'; for *SOX6* ChIP, forward 5'-CAACATTACTGTGTCCCTGGC-3' and reverse 5'-CTGTCTCCCTGAGTGGGTCT-3'; for *SMAD2* ChIP, forward 5'-ACTGGAGTTCAGCGTGGAAG-3' and reverse 5'-TGACTTTCCATCCAGTGGGAC-3'; and for *IL-8* ChIP, forward 5'-TGCTCACCCAAATGGCAGAT-3' and reverse 5'-ACATAGGAAAACGCTGTAGGTCA-3'.

Förster resonance energy transfer (FRET) construct development

The AR-Cerulean construct was created by amplifying the gene encoding AR with primers (forward 5'-AAAGCTAGCGC-CACCATGGAAGTGCAGTTAGGGC-3' and reverse 5'-AAAACCGGTCCACGCGTCTGGGTGTGGAAA-3') and sequential digestion/ligation of the product and mCerulean3 (mCerulean3)-C1 vector using *NheI* and *AgeI* restriction enzymes. NFIX-Venus was created similarly with primers (forward 5'-AAAAGATCTATGTATAGCCCGTACTGCCTCACC-3' and reverse 5'-AAAGGTACCTTCAGAAAGTTGCCGTCCC-3') for the NFIX gene and an mVenus-C1 vector was used with *NheI* and *AgeI* restriction enzymes. Finally, the FOXA1-Venus construct was created with amplifying primers (forward 5'-AAAGCTAGCGCCACCATGTTAGGAAGTGTGAAG-3' and reverse 5'-AAAACCGGTCCGGAAGTGTGTTAGGACGGG-3') for FOXA1 and an mVenus-C1 vector using *BglII* and *KpnI* restriction enzymes. Sequences of the constructs were verified using the Vanderbilt Genome Sciences Sanger DNA sequencing laboratory.

Cellular sample preparation for FRET studies

HeLa cells were transiently transfected with plasmid DNA encoding mCerulean3-tagged AR, mVenus-tagged NFIX, and/or mVenus-tagged FOXA1; FRET8 (a dimer of enhanced cyan fluorescent protein and enhanced yellow fluorescent protein) or mCerulean3 and mVenus were used as controls. Transfection was accomplished using Lipofectamine 2000 (Invitrogen) transfection reagent according to the manufacturer's instructions. Cells were seeded onto no. 1 coverslip bottom dishes (MatTek) and cultured in DMEM (Invitrogen/Gibco) supplemented with 10% FBS (Invitrogen/Gibco), 100 U/mL penicillin (Mediatech), and 100 µg/mL streptomycin (Mediatech) at 37°C under 5% humidified CO₂. At 24 hours after transfection, samples were fixed with 4% paraformaldehyde, washed in Dulbecco's PBS (Invitrogen/Gibco), and mounted with Gelvatol. For samples containing the AR plasmid, 24 hours after transfection cells were incubated overnight with medium containing charcoal-stripped

serum and then treated with DHT (Sigma-Aldrich) for 4 hours before fixing as stated above.

Fluorescence microscopy for FRET

FRET imaging was performed using a Zeiss LSM780 confocal microscope with excitation provided by a Coherent chameleon 2-photon laser at 800 nm with emission collected in spectral mode from 465 to 692 nm with 8.7-nm spectral resolution. In addition, images were collected with an argon laser at 514 nm to confirm cells expressing the mVenus-tagged constructs. Data were analyzed using ImageJ and GraphPad Prism software. FRET ratios were expressed as mVenus/mCerulean after linear unmixing and normalized to the vehicle-treated AR + FOXA1 control ratios. A total of 70 to 100 cells/dish were quantified for mean intensity, and the experiments were repeated in 3 cellular preparations. *P* values are the result of repeated-measures ANOVA compared with NFIX + AR.

Identification NFI binding sites in proximity to AR/FOXA1 binding sites

Previously published ChIP-Seq data (20, 40) was downloaded from the National Center for Biotechnology Information (NCBI) and converted to the FASTQ format using the Sequence Read Archive (SRA) toolkit (41), analyzed for quality using FastQC (42), aligned to the human genome using Bowtie (43), and interrogated using HOMER (44) for AR/FOXA1 adjacent peaks in LNCaP and VCaP cells. From this list, we searched for predicted NFI binding sites within 100 bp in either direction of the AR/FOXA1 region. Based on this list, several candidate genomic elements and their corresponding genes were arbitrarily selected and validated by ChIP and Q-RT-PCR. For programming specifics, please see the http://press.endocrine.org/doi/suppl/10.1210/me.2013-1213/suppl_file/me-13-1213-2.pdf Supplemental Methods.

Modeling of TF interactions

The model was constructed from the 3-dimensional structures of DNA-binding domains (DBDs) of 3 TFs bound to DNA. The atomic coordinates of the homodimeric DBD of AR were taken from crystal structure 1R4I (Protein Data Bank [PDB] ID; Ref. 45). The coordinates of the FOXA1 DBD are from the Nucleic Acid Database (NDB ID PDT013; Ref. 46), and the structure of the NFIX DBD was modeled on the dimeric Smad MH1 domain 1MHD (PDB ID; Ref. 47), using the 3D-Jury server at <http://bioinfo.pl/> (48). These 3 DNA-bound protein structures were then aligned, using University of California, San Francisco (UCSF) Chimera (49), to a model of the probasin promoter region (−140 to −65) generated in idealized B-form by NAB (50) at the University of Southern California (USC) make-na server (51). Ovals representing the attached N- and C-terminal non-DBDs were added to illustrate potential inter-domain contacts. The ovals are scaled roughly to the size of the non-DBDs. The locations of the ovals are consistent with their attachment points on the DBDs, but the orientations are speculative.

Statistical analysis

Statistical analysis was performed using GraphPad Prism 6, and specific tests are identified in the figure legends.

Results

Tandem affinity purification and mass spectrometry identify a novel set of FOXA1-interacting proteins

In an effort to identify additional novel FOXA1 binding partners, we used a retroviral-based approach to establish LNCaP cells that stably overexpress dual affinity tagged FOXA1 (LNCaP-FOXA1) or empty vector (LNCaP-pLPCX). Although LNCaP cells express FOXA1, dual affinity tagged FOXA1 (FLAG-6xHis-FOXA1) was significantly overexpressed in these cells (Figure 1A), enabling the purification of FOXA1 and associated binding partners. To purify FLAG-6xHis-FOXA1 and associated binding partners, nuclear extracts from LNCaP-FOXA1 and LNCaP-pLPCX cells were subjected to purification via tandem TALON and FLAG purification. Western blotting analysis using antibodies specific for both FOXA1 and the His tag reveal significant enrichment for FOXA1 (Figure 1B) after purification. Importantly, Western blotting for AR revealed that this approach was capable of purifying AR, the known FOXA1 binding partner (Figure 1C). Total purified protein was subjected to SDS-PAGE and colloidal blue staining (Figure 1D), followed by tryptic digestion and LC-MS/MS analysis. Analysis of MS/MS data via the Sequest algorithm against the IPI human database identified a total of 16 proteins that appear to interact with FOXA1 (Table 1). Of the 16 proteins meeting the “hit” criteria, 6 have been reported previously to interact with AR by a direct or an indirect link (52–57). In addition to these known AR interacting proteins, we identified gene products that are generally important for the maintenance of protein stability, RNA processing, cell cycle control, and chromatin regulation. We chose to focus on NFIX and its family members because NFI family members are TFs, NFI motifs have been associated with AREs and NFI can bind to FOXA1, an AR coregulator (7, 17, 34, 58).

NFI family members are expressed in prostate cancer cell lines and physically interact with FOXA1

The NFI family of TF contains four genes (*NFIA*, *NFIB*, *NFIC*, and *NFIX*) encoding proteins that bind to the consensus DNA sequence TTGGCN₅GCCAA (26). The levels of NFI family member expression in commonly used cell lines was determined by Q-RT-PCR on LNCaP, PC3, and DU145 cells (Figure 2A) and on the JEG-3 choriocarcinoma cell line, which was previously reported to express low levels of NFI (36, 37). JEG-3 cells indeed expressed virtually undetectable levels of NFI family members. On the other hand, LNCaP, PC3, and DU145

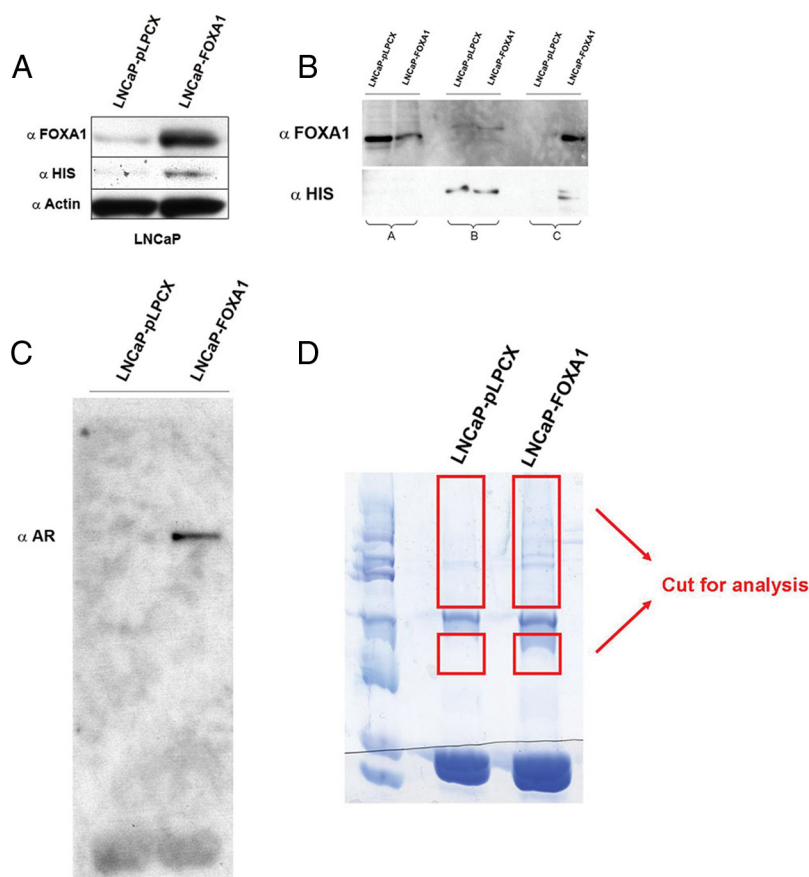


Figure 1. Purification of antigen-tagged FOXA1 and associated binding partners. A, Antigen-tagged FOXA1 was sufficiently expressed in LNCaP-FOXA1 cells. B, Western blotting analysis for FOXA1 and His affinity tag after tandem affinity purification. A lanes depict flow through of control and LNCaP-FOXA1 cells after the first purification step, B lanes depict flowthrough of LNCaP-FOXA1 and control cells from the second purification step, and C lanes depict the final eluate from LNCaP-FOXA1 and control cells. C, Western blotting analysis of purified samples for the known FOXA1 binding partner, AR indicates that the purification procedure was sufficient to identify FOXA1 binding partners. D, Final eluates from LNCaP-FOXA1 cells and control cells were separated in a 10% SDS-PAGE gel, and protein visualized by colloidal blue staining were subjected to trypsin digestion and LC-MS/MS analysis, resulting in the identification of 16 novel putative FOXA1 binding partners (Table 1).

cells expressed each NFI family member, with the highest levels of family member expression consisting of *NFIA* and *NFIB* (Figure 2A). Although *NFIC* and *NFIX* expression was detectable in these prostate cell lines, expression was relatively low compared with that for *NFIA* and *NFIB*.

Because JEG-3 choriocarcinoma cells express exceedingly low levels of NFI, we individually expressed HA-tagged NFIA, NFIB, NFIC, NFIX, or vector (PCH), along with FOXA1, in JEG-3 cells to identify the NFI family member(s) capable of interacting with FOXA1. Immunoprecipitation was performed using an anti-FOXA1 antibody, followed by Western blotting analysis with anti-HA monoclonal antibody. Immunoprecipitation results indicated that NFIA, NFIB, NFIC, and NFIX are capable of interacting with FOXA1 (Figure 2B, top panel). An unidentified protein that has previously re-

ported to occur after ectopic expression (33), perhaps an NFIA degradation product, was also capable of interacting with FOXA1 in JEG-3 cells. This could also be an NFI family member (such as NFIC or NFIB, which are similar in size) that was purified with NFIA during the immunoprecipitation. Nonetheless, reciprocal immunoprecipitation analysis confirmed the ability of each NFI family member to interact with FOXA1 (Figure 2B, bottom panel).

To confirm the interaction between NFI family members and FOXA1 and also to identify the domain in FOXA1 required for mediating this interaction, GST-fusion assays using GST-tagged full-length NFIX, as well as an assortment of FOXA1 deletion constructs, were performed (Figure 2C). NFIX was selected because it was identified by LC-MS/MS analysis and coimmunoprecipitated strongly with FOXA1 (Figure 2B, bottom panel). Full-length FOXA1 indeed interacts with GST-tagged NFIX (Figure 2D), whereas deletion of the N terminus (Δ N) or more than half of the forkhead domain of FOXA1 (NT construct) abrogated this interaction (Figure 2D). Taken together, these data indicate that FOXA1 interacts with all members of the NFI family,

and the interaction of NFIX and by extension other NFI family members with FOXA1 is mediated by the N-terminal transactivation and forkhead domains of FOXA1.

Overexpression of NFI family members represses androgenic induction of the probasin promoter and PSA enhancer

An NFI binding site has been identified within the probasin promoter (59), and a pan-NFI antibody ChIP analysis demonstrated that an NFI family member binds to the probasin promoter adjacent to the FOXA1 binding site (7). In addition, NFI binding sites exist in close apposition to AR and FOXA1 binding sites within the PSA enhancer and appear to be common in most AR-regulated genes (58). To determine the influence of individual NFI family members on the transcriptional activity of these prostate-specific regulatory sequences, we performed re-

Table 1. FOXA1 Binding Partners Identified by Tandem Affinity Purification and LC-MS/MS

Protein	Accession No.	Function	Ref. (If Associated With AR)
Known or potential AR coregulators			
Nuclear factor I/X	Q14938	TF; AR coregulator	52
Paraspeckle protein 1 α	Q8WXF1	AR coregulator	53
Splicing factor, proline- and glutamine-rich	P23246	RNA splicing; physically interacts with AR	54
Matrin-3	P43243	Nuclear matrix component; interacts with SFPQ	55
Protein polybromo-1	Q86U86	Chromatin structure regulation; AR coregulator	56
DNA-dependent protein kinase catalytic subunit	P78527	DNA-dependent protein kinase, isoform 2; phosphorylates AR	57
Protein stability			
Peptidyl-prolyl <i>cis-trans</i> isomerase-like 4	Q8WUA2	Peptidylprolyl isomerase	
Heat shock cognate 71-kDa protein	P11142	Chaperone	
RNA processing			
Splicing factor 3B subunit 3	Q15393	Subunit of splicing factor SF3B	
Heterogeneous nuclear ribonucleoprotein L	P14866	Component of the heterogeneous nuclear ribonucleoprotein complex; provides substrate for the processing events that pre-mRNAs in the cytoplasm	
Cleavage and polyadenylation specificity factor subunit 6	Q16630	Component of cleavage factor complex; plays role in 3' pre-mRNA processing	
RNA binding protein 10	P98175	Putative mRNA splicing factor	
DEAH box polypeptide 15	O43143	RNA helicase; RNA splicing factor	
Transcription initiation factor TFIID subunit 4	O00268	Component of TFIID transcriptional complex	
Miscellaneous			
Nucleostemin	Q9BVP2	Cell cycle regulation	
TOX HMG family member 4	O94842	Chromatin structure regulation	

porter gene assays using previously described probasin (ARR₂PB) and PSA luciferase reporters (7). Individual reporters were cotransfected with the AR as well as individual NFI family members either in the presence or absence of FOXA1 in JEG-3 cells (Figure 3). In the absence of FOXA1, individual NFI family members repressed androgen induction of the PSA (A) and probasin (C) reporter, and the ability of NFI family members to repress androgen-induced probasin reporter activity was maintained in the presence of FOXA1 (Figure 3, B and D). These results suggest that NFI family members can confer additional regulation to AREs.

NFI knockdown affects prostate-specific gene expression

Previous studies have examined the consequences of a pan-siRNA against NFI (siNFI) construct on AR target genes (*PSA*, *KLK2*, *TGM2*, *TMPRSS2*, and *FKBP5*) and observed gene-dependent changes (58), suggesting that NFI regulation of AR target genes may be NFI family member specific. To identify the role of individual NFI family members in prostate-specific gene expression, individual NFI family members were knocked down in LNCaP cells, and the cell line was examined by Q-RT-PCR for the known AR/FOXA1 target genes *PSA*, *TMPRSS2*, *NKX3-1*, and *FKBP5* (Figure 4). Knockdown of individual NFI family members was specific and effi-

cient (Figure 4A). Interestingly, *NFIX* knockdown resulted in up-regulation of *NFIA* and *NFIB* relative to that of nontargeting siRNA (Figure 4A, *NFIA* and *NFIB*). These observations suggest that in prostatic cells, NFI family members are capable of compensating for each other and may regulate each other as well. Adding complexity to the situation, NFI family members can be induced, repressed, or unregulated by DHT treatment (Supplemental Figure 2).

To simplify the analysis, we focused on examining the influence of individually knocking down NFI family members on AR target gene expression in LNCaP cells maintained in complete medium (Figure 4B). Knockdown of *NFIA* resulted in decreased *TMPRSS2* and *NKX3-1* expression, and increased *FKBP5* expression. *NFIB* knockdown resulted in increased expression of *NKX3-1* and *FKBP5*. *NFIC* knockdown resulted in decreased *PSA* and *NKX3-1* expression. *NFIX* knockdown resulted in increased *TMPRSS2* expression. In summary, although NFI expression levels affect the expression of androgen-regulated genes, this regulation is complex, and individual NFI family members can be redundant to each other.

NFI proteins bind to the PSA enhancer

To determine the ability of NFI proteins to bind to *cis*-regulatory regions of the human PSA enhancer and to determine whether NFI binding to this region is itself regulated by androgen, ChIP reactions were performed in

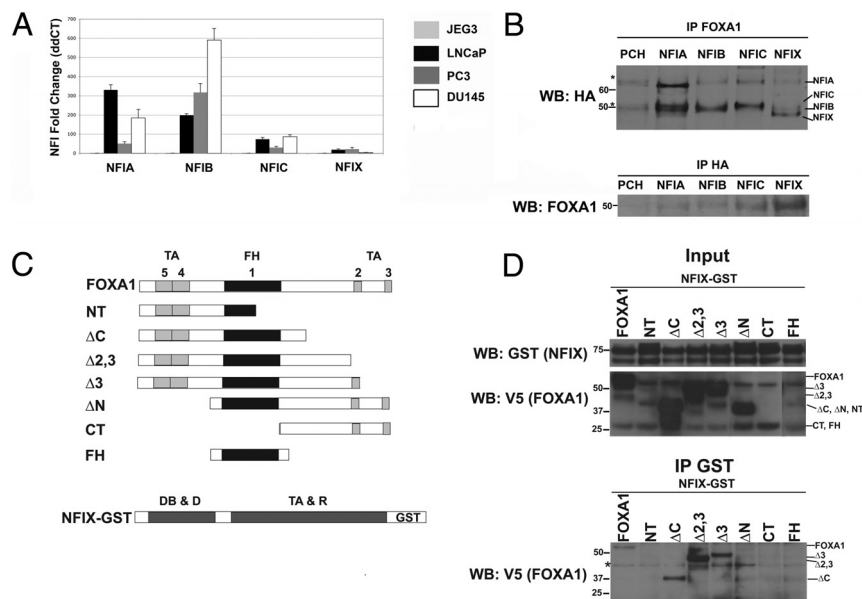


Figure 2. A, NFI family members are expressed in prostate cancer cell lines and interact with FOXA1. LNCaP, PC3, and DU145 prostate cancer cells and in JEG-3 choriocarcinoma cells were screened by Q-RT-PCR for NFI family member expression. NFI family member expression was virtually undetectable in JEG-3 cells, whereas *NFIA* and *NFIB* were relatively highly expressed in prostate cancer cell lines compared with expression of *NFIC* and *NFIX*. B, NFI family members interact with FOXA1. HA-tagged *NFIA*, *NFIB*, *NFIC*, *NFIX*, or vector (PCH; negative control) constructs were individually transfected into JEG-3 cells along with FOXA1. Immunoprecipitation (IP) with anti-FOXA1 antibody and Western blotting (WB) for HA (top panel) or the reciprocal immunoprecipitation (bottom panel) in the presence of ethidium bromide to squelch DNA-protein binding was performed. Results show that individual NFI family members interact with FOXA1. C, Schematic diagram of previously described FOXA1 deletion (38) and *NFIX* constructs used in GST-fusion assays to identify the domain of FOXA1 responsible for the interaction with *NFIX*. FH, forkhead domain (winged helix DBD), domain 1; light gray boxes 2 to 5, transactivation domains; DB & D, DNA binding and dimerization; TA & R, transactivation and repression. Schematics are based on Refs. 38, 79, and 80. D, GST-fusion experiments indicate that full-length FOXA1 interacts with GST-tagged *NFIX*. JEG-3 cells were transfected with *NFIX*-GST constructs and 1 of 8 FOXA1-V5 deletion constructs. Cells were analyzed for expression of *NFIX*-GST and FOXA1-V5 constructs (Input panels) and underwent GST pull-down assays (IP GST panel). As expected, GST pull-down successfully pulled down full-length FOXA1. Based on these studies, the N-terminal domain is required for FOXA1 binding to *NFIX*, because constructs missing the N terminus (FH, ΔN, and CT) are not pulled down by the GST immunoprecipitation. The full FH domain of FOXA1 is required in addition to the N terminus domain, because the NT construct, which contains the N terminus and half of the FH domain, cannot be pulled down by GST. Asterisks denote nonspecific binding bands.

LNcaP cells in the presence or absence of DHT. Because of the lack of specific ChIP-grade or ChIP-validated antibodies for *NFIA*, *NFIC*, and *NFIX*, only a pan-NFI and *NFIB* antibody were used. In addition, ChIP was performed using AR and FOXA1 antibodies. The Tess TF search program (<http://www.cbil.upenn.edu/cgi-bin/tess/tess>) revealed consensus NFI binding sites within AREIII, just downstream of AREIIIA, and adjacent to a FOXA1 binding site (9) within the PSA core enhancer (Figure 5A). Target sequence primers were designed to amplify a region within the PSA enhancer, encompassing AREIIIA and AREIIIB, as well as the 3 consensus NFI binding sites (9, 60). As expected, DHT treatment resulted in robust binding of AR to the PSA enhancer (Figure 5B). Antibodies for FOXA1, pan-NFI, and *NFIB* revealed that al-

though AR is recruited to the PSA enhancer, FOXA1 and *NFIB* are already occupying these regions (Figure 5B). This finding is consistent with other reports suggesting that pan-NFI occupancy of target gene promoters and enhancers is less responsive to DHT (58).

NFIX interacts with AR in the presence of FOXA1

FRET, which is facilitated by tagging the proteins of interest with fluorescent proteins as reporters, is a phenomenon useful for studying protein-protein interactions (61). Because FRET occurs only when the fluorescent proteins are within 10 nm, it is commonly used to indicate the proximity of proteins of interest. Here, we tagged FOXA1, *NFIX*, and AR with either a donor (mCerulean3) or acceptor (mVenus) fluorescent protein and assayed the relative FRET ratios in HeLa cells expressing the constructs. The *NFIX* and FOXA1 constructs localized to the nucleus constitutively, whereas the AR translocated to the nucleus only after treatment with DHT (Figure 6, A and B).

Consistent with previous reports of AR and FOXA1 interactions (9, 10), cotransfected AR-mCerulean3 and FOXA1-mVenus exhibited a high FRET ratio of 0.93 ± 0.052 in cells treated with DHT (Figure 6C), compared with both positive (mCerulean3-mVenus dimer) and negative (cotransfection of single mCerulean3- and mVenus-expressing plasmids) controls (quantified in Figure 6G). To determine whether *NFIX* and FOXA1 are close enough to interact directly, cells were cotransfected with a *NFIX*-mCerulean3 donor and FOXA1-mVenus acceptor construct. This pair exhibited nuclear localization and a FRET ratio of 0.59 ± 0.026 (Figure 6, D and G). Importantly, when we performed this experiment with FOXA1-mCerulean3 as the donor and *NFIX*-mVenus as the acceptor, the FRET ratio was comparable to that of the negative control (data not shown). This result demonstrates that the folding and orientation of the proteins with fluorescent protein tags is critical for FRET to occur. Because of the constitutive localization of the

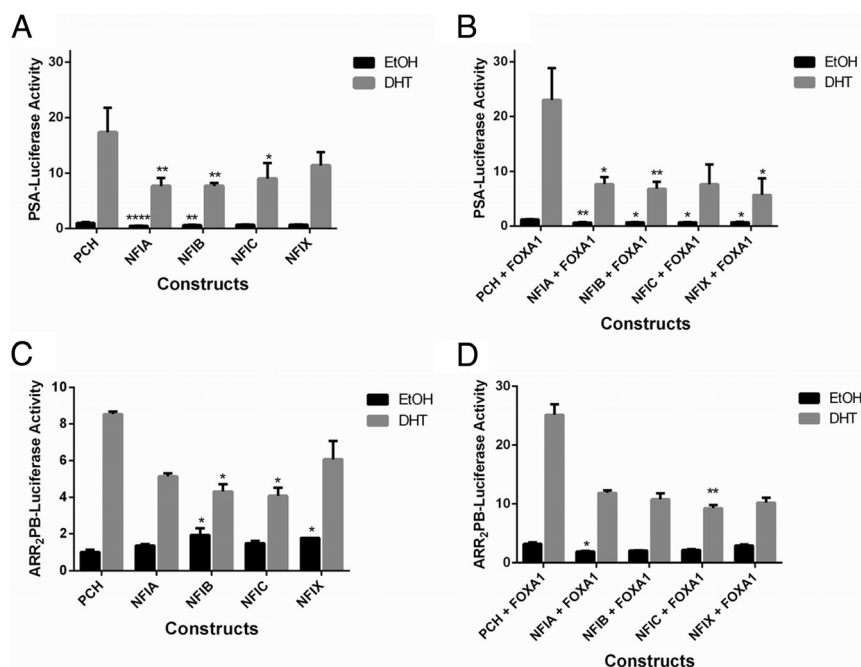


Figure 3. Influence of individual NFI family members in the presence or absence of FOXA1 on prostate-specific reporter activity. PSA (A and B) and ARR₂PB (C and D) androgen-induced reporter activity in JEG-3 cells. Cells were transiently transfected with PCH (empty vector) or individual NFI family members and treated in the presence of EtOH (vehicle) or DHT to examine changes in luciferase activity (A and C). The influence of NFI on androgen responsive reporter gene activity in JEG-3 cells was also tested in the presence or absence of transiently transfected FOXA1 (B and D), because JEG-3 cells do not express endogenous FOXA1. The addition of NFIs decreases luciferase activity, even in the presence of FOXA1, suggesting that NFI family members add another element of regulation to the probasin and PSA promoters. All data are normalized to PCH EtOH. Asterisks over columns indicate statistically significant values compared with values for PCH (EtOH or DHT, as appropriate). A representative experiment is shown. Statistical analysis was performed by the Kruskal-Wallis test. *, $P \leq .05$; **, $P \leq .01$; ***, $P \leq .001$; ****, $P \leq .0001$.

NFIX-mCer3 donor and FOXA1-mVenus acceptor to the nucleus, a FRET signal of comparable strength can also be detected in HeLa cells cultured in charcoal-stripped serum medium without DHT treatment (Supplemental Figure 3).

The AR-mCer3 and NFIX-mVenus FRET ratio of 0.23 ± 0.021 was significantly lower (Figure 6, E and G), suggesting that these proteins are further away from each other than the AR and FOXA1. To test the hypothesis that overexpressing FOXA1 could bridge the interaction between NFIX and AR, we cotransfected cells with AR-mCer3, NFIX-mVenus, and untagged FOXA1. After treatment with DHT, the FRET ratio of AR-mCer3 and NFIX-mVenus was increased to 0.53 ± 0.058 , a level intermediate between those for the FOXA1/AR and NFIX/AR samples (Figure 6, F and G). This result suggests that FOXA1 can either serve as a bridge to bring NFIX and AR together or alter the relative orientation of NFIX and AR, which may result in AR-mediated gene transcription.

NFI motif discovery and validation at AR and FOXA1 binding sites

ChIP-Seq has become a routine technique to investigate the spatial and temporal patterns of DNA occupancy by TFs and provides insight into the mechanisms of coregulation by TF complexes. Because the LNCaP cell line is one of the few AR-dependent prostate cancer cell lines, ChIP-Seq for AR and FOXA1 (Supplemental Figure 4) has been performed by several groups (20, 25, 40, 62). We took advantage of high-quality AR and FOXA1 ChIP-Seq data (20, 40) to explore AR/FOXA1 and NFI complex formation. From the ChIP-Seq data, we identified the genome-wide set of loci bound by AR and FOXA1 in LNCaP cells (Supplement 1). For these sets, we applied a computational algorithm, HOMER, to identify consensus NFI full-length and half-site motifs (Figure 7A) within 100 nucleotides of AR and FOXA1 binding sites. HOMER (44) uses a more stringent consensus sequence than the Tess TF search program (<http://www.cbil.upenn.edu/cgi-bin/tess/tess>). Our in silico analysis revealed that in the 5125 loci bound by AR and FOXA1, there are 1764 (34.4%) AR/FOXA1 peaks with at least 1 NFI motif. This finding suggests that about one third of the AR/FOXA1 target genes are potentially coregulated by NFI (Figure 7B).

The presence of NFI motifs at one third of AR/FOXA1 peaks raised the possibility that NFIs may also regulate FOXA1 (FOXA1-only) and AR (AR-only) binding separately. Further analysis of the data revealed that in the 3898 loci bound by AR only, there are 1495 (38.4%) AR-only peaks with an associated NFI motif (Figure 7B). In the 17 808 loci bound by FOXA1-only, there are 5848 (32.8%) FOXA1-only peaks with an NFI motif (Figure 7B). These observations suggest that roughly one third of AR alone-, FOXA1 alone-, and AR/FOXA1-occupied peaks have the potential to be regulated by NFI family members in LNCaP cells.

To obtain a more comprehensive picture of NFI binding beyond LNCaP cells, we also analyzed AR and FOXA1 ChIP-Seq data from VCaP cells (Supplement 1).

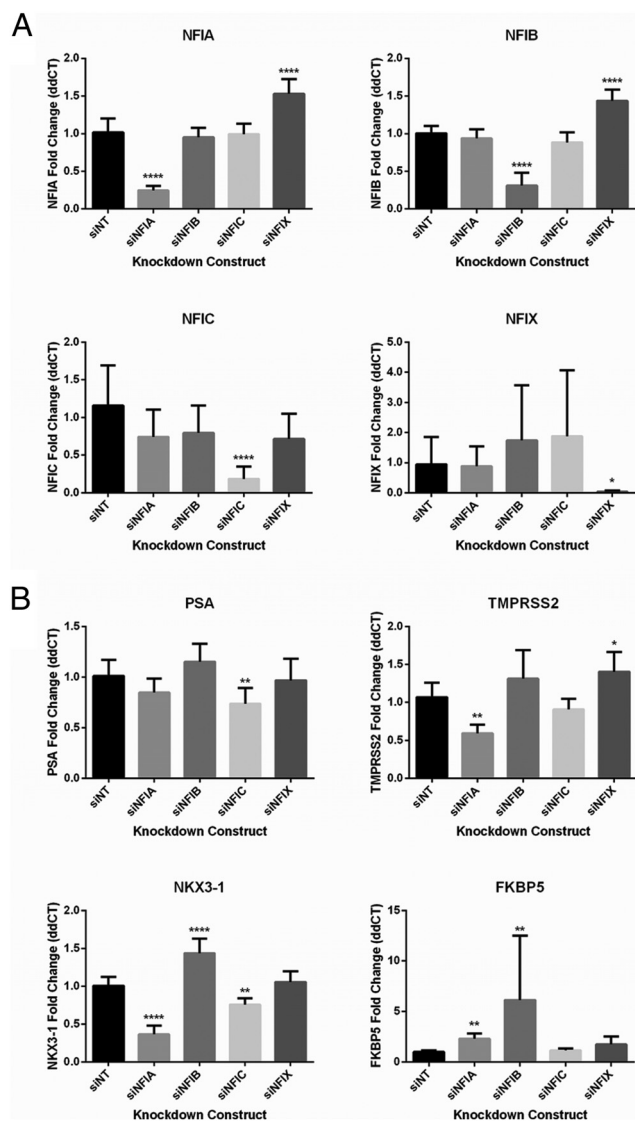


Figure 4. Knockdown of individual NFI family members reveals a role in prostate-specific gene expression. A, Efficiency and specificity of individual NFI family member knockdown was measured via Q-RT-PCR. Knockdown of *NFIX* results in increased *NFIA* and *NFIB* expression. B, Influence of NFI knockdown on the expression of *PSA*, *TMPRSS2*, *NKX3-1*, and *FKBP5*. After NFI knockdown in LNCaP cells, AR target gene expression was measured by Q-RT-PCR and normalized to nontargeting siRNA (siNT). Generally, *NFIA* and *NFIC* promote the expression of these AR-target genes, whereas *NFIB* and *NFIX* appear to be largely repressive. Two individual experiments were combined and analyzed by one-way ANOVA. *, $P \leq .05$; **, $P \leq .01$; ****, $P \leq .0001$.

At the 2016 loci bound by AR and FOXA1 in VCaP, we identified 372 (18.5%) AR/FOXA1 peaks with at least one NFI motif (Figure 7C) within 100 nucleotides. In the 2531 loci bound by AR only, there are 841 (33.2%) AR-only peaks with at least 1 NFI motif (Figure 7C). In the 11 905 loci bound by FOXA1 only, there are 3490 (29.3%) FOXA1-only peaks with at least 1 NFI motif (Figure 7C). The decrease in AR/FOXA1/NFI binding sites in VCaP cells is particularly interesting and requires

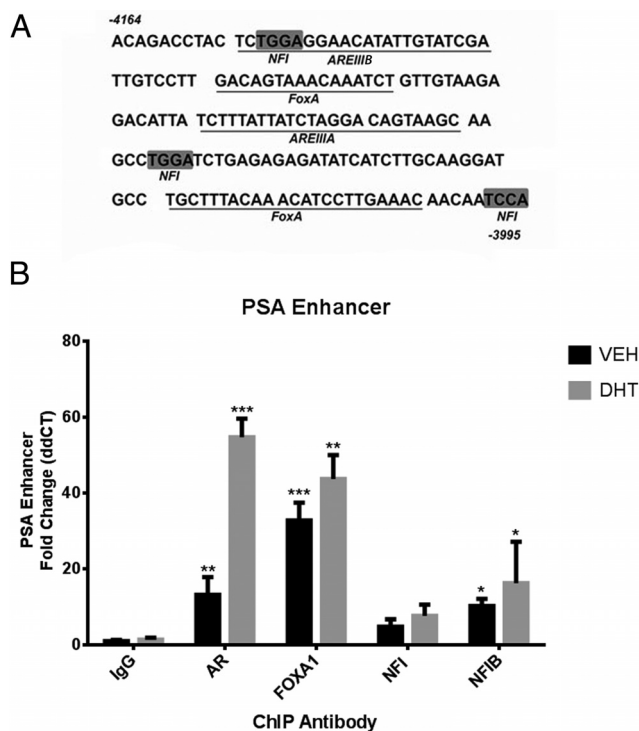


Figure 5. ChIP shows an NFI within the PSA core enhancer. A, Schematic diagram of AREIII in the PSA enhancer, highlighting previously identified AR and FOXA1 binding sites, as well as consensus NFI binding sites. B, AR, FOXA1, and NFI ChIP for the PSA enhancer. LNCaP cells were treated in the presence of the vehicle control (EtOH) or 10 nM DHT for 2 hours. After androgen treatment, cells were subjected to ChIP with anti-IgG control, AR, FOXA1, pan-NFI, and NFIB antibodies. Data were normalized to the vehicle (VEH) IgG control. Results show that recruitment of AR to the PSA enhancer increases after DHT treatment ($P < .05$), while FOXA1 and NFIB are continuously present. Asterisks over columns indicate that there is significant recruitment to the PSA enhancer vs the control (EtOH or DHT IgG as appropriate). A representative experiment is shown, with data analyzed by the Kruskal-Wallis test. *, $P \leq .05$; **, $P \leq .01$; ***, $P \leq .001$.

further investigation. Nevertheless, in silico analysis of AR and FOXA1 binding sites in both LNCaP and VCaP cells reveals that NFIs may globally regulate AR-mediated gene expression.

AR/FOXA1/NFI co-occupied regions predict NFI binding and gene expression modulation

To validate our in silico predictions, 8 genomic loci/elements identified by in silico analysis were validated by ChIP and Q-RT-PCR. Validation targets were selected based on the proximity to genes of particular interest to prostate cancer, peaks conserved between LNCaP and VCaP cells, and peaks with high peak scores. Because of the limitations of specific ChIP-validated NFI antibodies, we again limited our analysis to NFIB and the pan-NFI antibody. ChIP for NFIB and pan-NFI followed by Q-RT-PCR to genomic loci with proximity to *TMPRSS2*, *SYPL*, *CLU*, and *SMAD2* showed enrichment for pan-NFI,

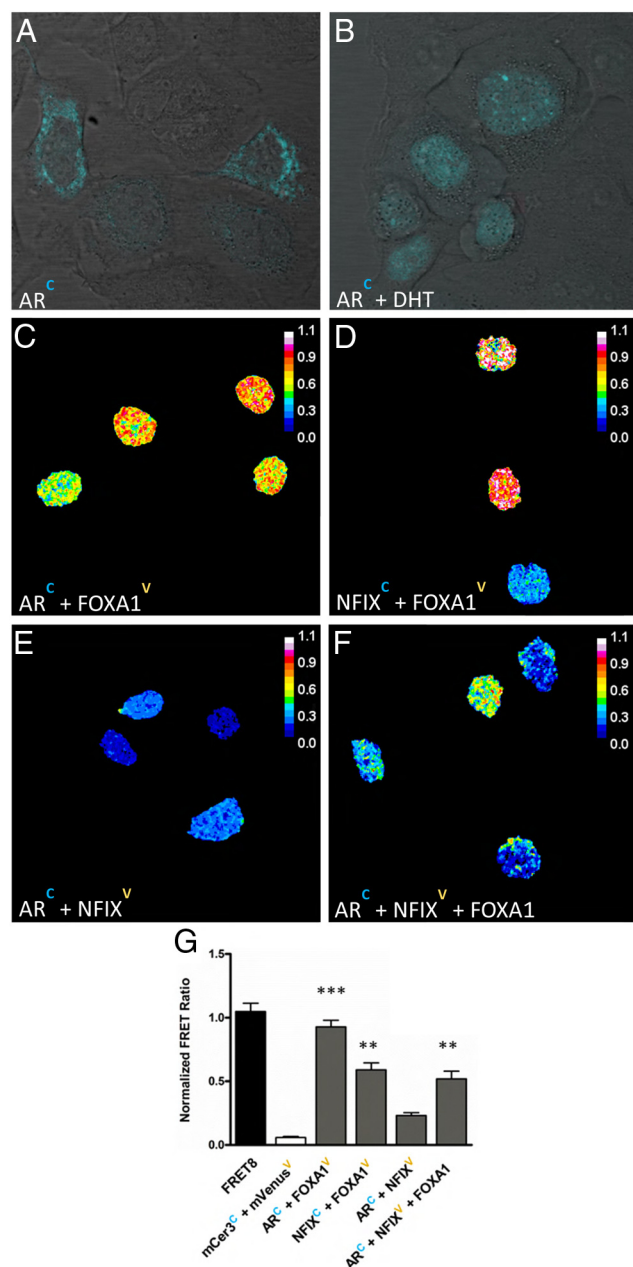


Figure 6. FRET demonstrates protein-protein interactions between NFIX, FOXA1, and AR. A–F, Cellular localization of AR-mCerulean3 transfected in HeLa cells in charcoal-stripped serum medium (A) or treated for 4 hours with DHT (B–F). C–F, Representative ratiometric images of FRET in cells transfected with AR-mCerulean3 and FOXA1-mVenus (C), FOXA1-mVenus and NFIX-mCerulean3, AR-mCerulean3 and NFIX-mVenus (E), or AR-mCerulean3, NFIX-mVenus, and untagged FOXA1 (F). G, Quantification of FRET ratios (all but FRET8 and mCerulean3 + mVenus normalized to vehicle controls) for 3 independent transfections treated with DHT ($n = 70$ – 100 cells per transfection). Statistics were performed by ANOVA and data are presented as means \pm SEM. **, $P < .01$; ***, $P < .001$, compared with NFIX + AR.

NFIB, or both at these loci compared with that for IgG (Figure 8Ai; AR and FOXA1 not shown). Q-RT-PCR analysis of these genes in response to individual NFI knockdown demonstrated NFI-specific and gene-specific changes (Figure 8Aii).

Although *OR9A2* and *SOX6* elements showed enrichment by ChIP (Figure 8Bi), their expression was unchanged by NFI knockdown (Figure 8Bii). Finally, *IL-8* and *GREB1* did not achieve significant enrichment or changes in gene expression (Figure 8C). Of our 8 candidate genomic elements/genes, 6 enriched at their predicted genomic element, and 4 had changes in gene expression in response to individual NFI knockdown. The 4 genes (*IL-8*, *OR9A2*, *GREB1*, and *SOX6*) that were unaffected by knockdown may either be unresponsive to NFI family members or they are not limited to specific homodimers or heterodimers in the presence of DHT. Regardless, validation of 6 of 8 binding sites by ChIP and gene changes in 4 of 8 of these proteins suggest that the NFI family members are broadly responsible for modulating AR/FOXA1 transcriptional activity.

Modeling the AR/FOXA1/NFI complex

Based on the significant effects of NFI knockdown on AR target gene expression, as well as the prediction that NFI may regulate approximately one third of the AR/FOXA1 target genes, a molecular model of this complex was developed using the probasin promoter. The homodimeric DBDs of AR (crystal structure 1R4I [PDB ID; Ref. 45]), FOXA1 (PDT013 [Nucleic Acid Database ID; Ref. 46]), and NFIX (modeled on the dimeric Smad MH1 domain 1MHD [PDB ID; Ref. 47]), were aligned to a model of the probasin promoter region ([140 to –65 base pairs). To illustrate potential interdomain contacts, ovals representing the attached N- and C-terminal non-DBDs were added and scaled roughly to an appropriate size. Although the locations of the ovals are consistent with their attachment points on the DBDs, their orientations are speculative. Nevertheless, the molecular model suggests that AR and FOXA1 bind directly adjacent to each other, with NFIX binding within 10 nm of the AR/FOXA1 complex (Figure 9). This model is consistent with the FRET results, which validated the AR/FOXA1 interaction, and suggests that FOXA1 can bridge the AR-NFIX interaction. Therefore, this model may be representative of the complex present on many if not most AR/FOXA1/NFI-regulated gene promoters.

Discussion

Several AR coregulators that both control and fine-tune AR activity, including FOXA1, which interacts with AR to control multiple prostate-specific genes in the epithelium, have been identified (9, 18). Recent reports have shown that AR and FOXA1 sites are commonly associated with androgen-regulated genes in prostate cancer cell

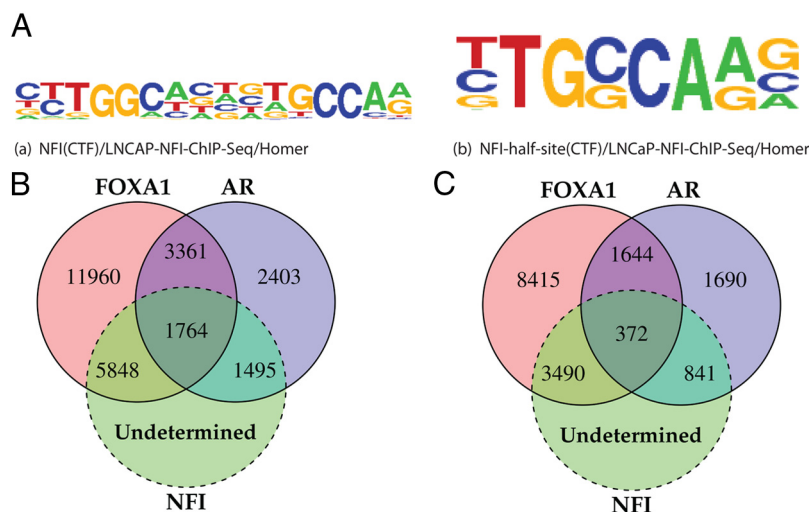


Figure 7. Analysis of NFI consensus sites within AR/FOXA1 peaks. **A**, NFI full-site and half-site motif from HOMER. **B**, Schematic representation of peaks occupied by AR, FOXA1, and NFI in LNCaP. Of the 5125 peaks co-occupied by FOXA1 and AR, 1764 of them have an NFI full- or half-site, suggesting that 34.4% of AR/FOXA1 sites have the potential to be regulated by NFIs. Predicted AR/NFI and FOXA1/NFI sites also occur at a significant frequency (38.4 and 32.8%, respectively). AR and FOXA1 sites were discovered by ChIP-Seq and are enclosed in solid circles. NFI sites are predicted and are enclosed in dashed circles. **C**, Schematic representation of peaks occupied by AR, FOXA1, and NFI in VCaP. Of the 2016 peaks co-occupied by FOXA1 and AR, 372 of them have an NFI full- or half-site, suggesting that 18.5% of AR/FOXA1 sites have the potential to be regulated by NFIs in VCaP cells. Predicted AR/NFI and FOXA1/NFI sites also occur at an appreciable frequency (33.2 and 29.3%, respectively).

lines (58, 63). In addition to AR, FOXA1 serves as a coregulator for various steroid receptors, including the glucocorticoid receptor (GR) (64) and estrogen receptor (ER) (65), suggesting that FOXA1 is a central mediator of endocrine responsive gene expression. To this end, multiple ER-responsive genes have been shown to contain FOXA1 binding sites (24) in paradigm similar to that for AR and FOXA1 sites, whereas GR binding sites are enriched for forkhead motifs (66). Unsurprisingly, both ER and GR have been reported to interact with FOXA1 (23, 24).

Much like FOXA proteins, NFI proteins are well known for their ability to regulate the activity of endocrine responsive *cis*-elements, such as the murine mammary tumor virus and the phosphoenolpyruvate carboxykinase promoters (67, 68). Furthermore, NFI activity is required to regulate expression of mammary gland-specific differentiation markers, including whey acidic protein and α -lactalbumin, among others (26). The frequent occurrence of NFI sites adjacent to AR and FOXA1 sites in multiple genes (58, 69) suggests that the NFI family is a central TF for androgen-regulated genes. Because NFI proteins bind to DNA as homodimers or heterodimers, the complexity for targeting specific genes regulated by the AR/FOXA1 complex is greatly increased. Further, preferential distribution of NFIX to prostatic stroma and NFIB to the basal cells (28), of which a subset

contain AR and all lack FOXA1, suggests unique mechanisms to regulate AR action in different prostatic cell types. The central role of each NFI family member in organ development (29–33), as well as the fact that FOXA1 expression is restricted to specific organs, suggests a fundamental role for NFI and FOXA1 in combinatorial control (5, 6), resulting in tissue-specific gene expression.

These studies have demonstrated that all 4 family members are capable of interacting with FOXA1 via transient transfection of His-tagged NFI family members, which complements other studies that have shown an unidentified NFI protein (34) or that NFIX (17) can interact with FOXA1. The interaction between FOXA1 and NFIs modulates expression of AR target genes. When we determined the influence of

knocking down individual NFI family members on the expression of *PSA*, *TMPRSS2*, *FKBP5*, and *NKX3-1*, we observed that NFIA and NFIC largely promote AR target gene expression, whereas NFIB and NFIX are mainly repressive. Subsequent ChIP analysis for the PSA enhancer, as well as 8 arbitrarily selected genomic loci identified by ChIP-Seq data mining, demonstrated that NFIs bind areas adjacent to the AR/FOXA1 peaks and can modulate the expression of genes associated with these loci. Our *in silico* analysis predicts that 34.4% of AR/FOXA1 target peaks have the potential to be regulated by NFIs. The NFIs, therefore, are potent modulators of AR-mediated gene expression in keeping with the observation they physically interact with FOXA1, which suggests that NFI family members play a critical, yet complex, role in prostate development and disease.

The frequent association of NFI binding sites with AR/FOXA1 binding sites (58, 69) suggests that this TF complex modeled on the probasin promoter (Figure 9) is not unique but represents a general model in which AR/FOXA1/NFI plays a fundamental role to regulate AR action. FRET was used to test the prediction that AR, FOXA1, and NFIX are in close proximity, resulting in the formation of a stable TF complex. The high FRET ratios shown by AR and FOXA1 were dependent on pretreatment of the cells with DHT to drive AR into the nucleus. Meanwhile, FOXA1 and NFIX FRET was independent of

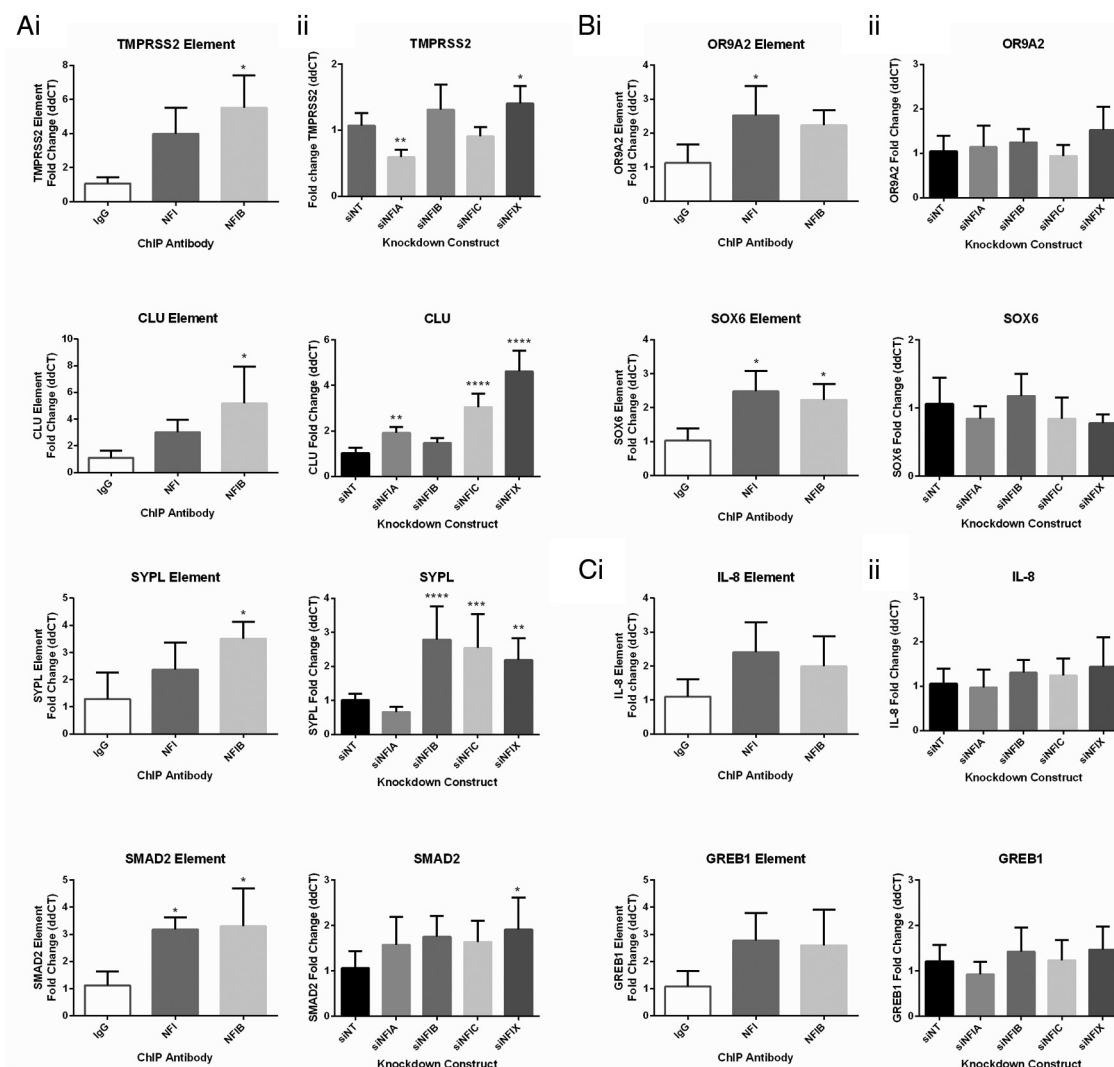


Figure 8. Validation of ChIP-Seq data mining. From the list of 438 full-site NFI/AR/FOXA1 peaks identified by ChIP-Seq data mining, 8 peaks (genomic elements) were chosen for validation with ChIP and Q-RT-PCR. A, Elements and genes that validated by ChIP (i) and Q-RT-PCR (ii). i, *TMPPRSS2*, *SYPL*, *CLU*, and *SMAD2* all showed significant enrichment for pan-NFI, NFIB, or both vs IgG. ii, Q-RT-PCR analysis revealed gene-specific changes for individual family members in response to individual family knockdown compared with those for nontargeting siRNA (siNT). *TMPPRSS2* Q-RT-PCR was originally presented in Figure 4B and is recreated here for comparison to *TMPPRSS2* element ChIP. B, Elements and genes that validated by ChIP (i) but not Q-RT-PCR (ii). *OR9A2* and *SOX6* elements showed significant enrichment for pan-NFI, NFIB, or both vs the IgG control (i); however, there was no statistically significant changes for these genes in response to NFI family knockdown as compared to siNT (ii). C, Elements and genes that failed to validate by ChIP (i) and Q-RT-PCR (ii). *IL-8* and *GREB1* elements failed to show enrichment after ChIP or changes in gene expression in response to NFI knockdown. For ChIP studies, representative data are shown with statistical analysis by Kruskal-Wallis. For Q-RT-PCR analysis, 2 independent experiments were combined and analyzed by one-way ANOVA. *, $P \leq .05$; **, $P \leq .01$; ***, $P \leq .001$; ****, $P \leq .0001$.

DHT treatment, further supporting the FOXA1 and NFI interaction. Although AR and NFIX did not exhibit a significant FRET ratio compared with that of negative controls, the additional transfection of an untagged FOXA1 significantly increased this ratio, suggesting that FOXA1 can bridge the AR-NFI interaction.

These observations are particularly interesting in the context of our data mining observations, which suggest that roughly one third of FOXA1-alone sites (ie, no AR) are associated with NFI sites, as are one third of AR-alone sites (ie, no FOXA1). For AR, this suggests

that up 36% of AR binding sites in LNCaP cells may be regulated by NFIs, which may indicate that in the absence of FOXA1, such as in the stroma, an alternative AR cofactor bridges the NFI-AR interaction. Because FOXA1 is not expressed in the stroma (18), whereas NFIX expression is high in the stroma (28), androgen-regulated genes in the stroma may use NFIX and stromal forkhead genes, such as FOXF1, FOXF2, or FOXC1 (70), to mediate AR gene transcription. Indeed, AR interaction with FOXC1 has been recently reported (71). This alternate forkhead mechanism may

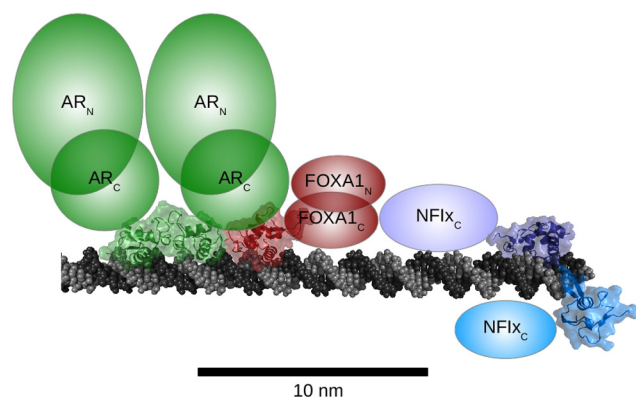


Figure 9. Model of TFs bound to the probasin promoter region. The DBDs of each protein are depicted as 3-dimensional structures bound to the probasin promoter DNA, based on known X-ray crystal structures of DBD-DNA complexes. The non-DNA-binding N- and C-terminal domains of each protein are shown as 2-dimensional ovals to indicate their relative size and location and illustrate potential physical interactions among the TFs. Dimeric AR is represented by the structure and ovals in green. FOXA1 is depicted in red. NFI is shown in blue and purple as a representative NFI family member. The 10-nm scale bar indicates the distance limit of FRET effects.

also be true for the portion of the AR-NFI peaks that occur independently of FOXA1 in LNCaP cells.

Conversely, NFIs and FOXA1 can interact independently of AR, which suggests that FOXA1/NFI may play a role independent of AR, such as that in androgen-independent neuroendocrine (small cell) or castrate-resistant prostate cancer. Neuroendocrine prostate cancer is a rare and highly aggressive form of prostate cancer, which does not express AR (72), and is therefore considered to be androgen independent. NFIB has been identified as oncogenic in small cell lung cancer (73), and a mouse model of neuroendocrine prostate cancer (synaptophysin positive and androgen independent) has chromosomal gains at locus 4qC3, which contains NFIB, and results in increased expression of NFIB in the tumors (74). Whereas the status of FOXA1 in human neuroendocrine prostate cancer has not yet been reported, FOXA2 is expressed in human neuroendocrine prostate cancer, and mouse models of neuroendocrine prostate cancer have strong FOXA1 and FOXA2 expression (18). It is possible, therefore, that in the absence of AR, NFIB and FOXA1 interact to mediate gene transcription unique to neuroendocrine prostate cancer.

Unlike neuroendocrine prostate cancers that do not express AR, castrate-resistant prostate cancers continue to express AR and depend upon AR signaling, as demonstrated by their response to second-generation antiandrogens (75–77). Because FOXA1 expression increases as prostate cancer progresses (14), it is likely that the AR/FOXA/NFI complex will continue to mediate gene transcription. However, work by Sharma et

al (69) has suggested that in castrate-resistant disease, the AR interaction shifts from FOXA1 and NFI to other cofactors such as STAT, MYC, E2F, AP-1, GATA, and NFkB. If AR is indeed being bound by other TFs or if antiandrogen therapy is interfering with AR/FOXA1/NFI complex formation, this would leave FOXA1 and NFI open to other interactions, perhaps with GR. Recent studies have indicated that FOXA1 can interact with GR (23). GR is particularly interesting because it can bind AREs and promote the expression of some AR target genes, and GR increases in castrate-resistant prostate cancer, supporting the failure of antiandrogens (78). In the presence of antiandrogens, therefore, the interaction of GR, FOXA1, and NFI may be uniquely important in driving castrate-resistant prostate cancer. Subsequent studies focusing on the NFI/FOXA1 complex in androgen-independent neuroendocrine prostate cancer, characterizing the AR/FOXA1/NFI complex in castrate-resistant prostate cancer, and identifying new coregulators that can bridge the AR-NFI divide will be particularly interesting. In summary, NFI family members interact with FOXA1, bind to AREs in an AR/FOXA1/NFI complex, and modulate AR-mediated gene transcription, implicating them as potent regulators of androgen-responsive, prostate-specific gene expression.

Acknowledgments

We thank Tom Case for his technical support, and Darlene Hancock for assistance with manuscript preparation.

Address all correspondence and requests for reprints to: Magdalena M. Grabowska, A-1302 MCN, 1161 21st Avenue South, Nashville, TN 37232-2765. E-mail: magda.grabowska@vanderbilt.edu.

R.J.M. was supported by the National Institutes of Health (Grant 2R01-DK055748-14) and the Joe C. Davis Foundation. R.M.G. was supported by the National Institutes of Health (Grant R01-HL080624-5) and NYSTEM (Grants C026429 and C026714). M.M.G. was supported by Vanderbilt University Medical Center (Integrated Biological Systems Training in Oncology Training Grant T32 CA119925). D.J.D. was supported by Vanderbilt University Medical Center (Multidisciplinary Training Grant in Molecular Endocrinology T32 DK007563-21 and Integrated Biological Systems Training in Oncology Training Grant T32 CA119925) and by a American Cancer Society Great Lakes Division-Michigan Cancer Research Fund Postdoctoral Fellowship. G.V.R. was supported by Department of Defense Institute of Defense Analyses (Grant W81XWH-12-1-0288).

Disclosure Summary: The authors have nothing to disclose.

References

- Cunha GR, Lung B, Reese B. Glandular epithelial induction by embryonic mesenchyme in adult bladder epithelium of BALB/c mice. *Invest Urol*. 1980;17:302–304.
- Cunha GR, Lung B. The possible influence of temporal factors in androgenic responsiveness of urogenital tissue recombinants from wild-type and androgen-insensitive (Tfm) mice. *J Exp Zool*. 1978;205:181–193.
- Cunha GR, Donjacour AA, Cooke PS, et al. The endocrinology and developmental biology of the prostate. *Endocr Rev*. 1987;8:338–362.
- Izumi K, Mizokami A, Lin WJ, Lai KP, Chang C. Androgen receptor roles in the development of benign prostate hyperplasia. *Am J Pathol*. 2013;182:1942–1949.
- Gierer A. Molecular models and combinatorial principles in cell differentiation and morphogenesis. *Cold Spring Harbor Symp Quant Biol*. 1974;38:951–961.
- Matusik RJ, Jin RJ, Sun Q, et al. Prostate epithelial cell fate. *Differentiation*. 2008;76:682–698.
- Zhang J, Gao N, DeGraff DJ, et al. Characterization of cis elements of the probasin promoter necessary for prostate-specific gene expression. *Prostate*. 2010;70:934–951.
- Herbst KL, Bhasin S. Testosterone action on skeletal muscle. *Curr Opin Clin Nutr Metab Care*. 2004;7:271–277.
- Gao N, Zhang J, Rao MA, et al. The role of hepatocyte nuclear factor-3 α (forkhead box A1) and androgen receptor in transcriptional regulation of prostatic genes. *Mol Endocrinol*. 2003;17:1484–1507.
- Gao N, Ishii K, Mirosevich J, et al. Forkhead box A1 regulates prostate ductal morphogenesis and promotes epithelial cell maturation. *Development*. 2005;132:3431–3443.
- DeGraff DJ, Yu X, Sun Q, et al. The role of Foxa proteins in the regulation of androgen receptor activity. In: Tindall DJ, Mohler JL, eds. *Androgen Action in Prostate Cancer*. New York, NY: Springer; 2009:587–615.
- Friedman JR, Kaestner KH. The Foxa family of transcription factors in development and metabolism. *Cell Mol Life Sci*. 2006;63:2317–2328.
- DeGraff DJ, Clark PE, Cates JM, et al. Loss of the urothelial differentiation marker FOXA1 is associated with high grade, late stage bladder cancer and increased tumor proliferation. *PLoS One*. 2012;7:e36669.
- Gerhardt J, Montani M, Wild P, et al. FOXA1 promotes tumor progression in prostate cancer and represents a novel hallmark of castration-resistant prostate cancer. *Am J Pathol*. 2012;180:848–861.
- Mirosevich J, Gao N, Matusik RJ. Expression of Foxa transcription factors in the developing and adult murine prostate. *Prostate*. 2005;62:339–352.
- Cirillo LA, Lin FR, Cuesta I, Friedman D, Jarnik M, Zaret KS. Opening of compacted chromatin by early developmental transcription factors HNF3 (FoxA) and GATA-4. *Mol Cell*. 2002;9:279–289.
- Robinson JLL, Hickey TE, Warren AY, et al. Elevated levels of FOXA1 facilitate androgen receptor chromatin binding resulting in a CRPC-like phenotype [published online ahead of print December 2, 2013]. *Oncogene*. doi: 10.1038/onc.2013.508.
- Mirosevich J, Gao N, Gupta A, Shappell SB, Jove R, Matusik RJ. Expression and role of Foxa proteins in prostate cancer. *Prostate*. 2006;66:1013–1028.
- Grasso CS, Wu YM, Robinson DR, et al. The mutational landscape of lethal castration-resistant prostate cancer. *Nature*. 2012;487:239–243.
- Sahu B, Laakso M, Ovaska K, et al. Dual role of FoxA1 in androgen receptor binding to chromatin, androgen signalling and prostate cancer. *EMBO J*. 2011;30:3962–3976.
- Sahu B, Laakso M, Pihlajamäe P, et al. FoxA1 specifies unique androgen and glucocorticoid receptor binding events in prostate cancer cells. *Cancer Res*. 2013;73:1570–1580.
- Laganière J, Deblois G, Lefebvre C, Bataille AR, Robert F, Giguère V. From the cover: Location analysis of estrogen receptor α target promoters reveals that FOXA1 defines a domain of the estrogen response. *Proc Natl Acad Sci USA*. 2005;102:11651–11656.
- Belikov S, Åstrand C, Wrangé Ö. FoxA1 binding directs chromatin structure and the functional response of a glucocorticoid receptor-regulated promoter. *Mol Cell Biol*. 2009;29:5413–5425.
- Carroll JS, Liu XS, Brodsky AS, et al. Chromosome-wide mapping of estrogen receptor binding reveals long-range regulation requiring the forkhead protein FoxA1. *Cell*. 2005;122:33–43.
- Wang D, Garcia-Bassets I, Benner C, et al. Reprogramming transcription by distinct classes of enhancers functionally defined by eRNA. *Nature*. 2011;474:390–394.
- Murtagh J, Martin F, Gronostajski RM. The nuclear factor I (NFI) gene family in mammary gland development and function. *J Mammary Gland Biol Neoplasia*. 2003;8:241–254.
- Kruse U, Sippel AE. Transcription factor nuclear factor I proteins form stable homo- and heterodimers. *FEBS Lett*. 1994;348:46–50.
- Oudes AJ, Campbell DS, Sorensen CM, Walashek LS, True LD, Liu AY. Transcriptomes of human prostate cells. *BMC Genomics*. 2006;7:92.
- Wong YW, Schulze C, Streichert T, Gronostajski RM, Schachner M, Tilling T. Gene expression analysis of nuclear factor I-A deficient mice indicates delayed brain maturation. *Genome Biol*. 2007;8:R72.
- Gründer A, Ebel TT, Mallo M, et al. Nuclear factor I-B (NfIB) deficient mice have severe lung hypoplasia. *Mech Dev*. 2002;112:69–77.
- Steele-Perkins G, Butz KG, Lyons GE, et al. Essential role for NFI-C/CTF transcription-replication factor in tooth root development. *Mol Cell Biol*. 2003;23:1075–1084.
- Driller K, Pagenstecher A, Uhl M, et al. Nuclear factor I X deficiency causes brain malformation and severe skeletal defects. *Mol Cell Biol*. 2007;27:3855–3867.
- Campbell CE, Piper M, Plachez C, et al. The transcription factor Nfix is essential for normal brain development. *BMC Dev Biol*. 2008;8:52.
- Norquay LD, Yang X, Jin Y, Detillieux KA, Cattini PA. Hepatocyte nuclear factor-3 α binding at P sequences of the human growth hormone locus is associated with pituitary repressor function. *Mol Endocrinol*. 2006;20:598–607.
- Snoek R, Rennie PS, Kasper S, Matusik RJ, Bruchovsky N. Induction of cell-free, in vitro transcription by recombinant androgen receptor peptides. *J Steroid Biochem Mol Biol*. 1996;59:243–250.
- Messina G, Biressi S, Monteverde S, et al. Nfix regulates fetal-specific transcription in developing skeletal muscle. *Cell*. 2010;140:554–566.
- Bachurski CJ, Yang GH, Currier TA, Gronostajski RM, Hong D. Nuclear factor I/thyroid transcription factor 1 interactions modulate surfactant protein C transcription. *Mol Cell Biol*. 2003;23:9014–9024.
- Sun Q, Yu X, Degraff DJ, Matusik RJ. Upstream stimulatory factor 2, a novel FoxA1-interacting protein, is involved in prostate-specific gene expression. *Mol Endocrinol*. 2009;23:2038–2047.
- Kang Z, Jänne OA, Palvimo JJ. Coregulator recruitment and histone modifications in transcriptional regulation by the androgen receptor. *Mol Endocrinol*. 2004;18:2633–2648.
- Yu J, Yu J, Mani RS, et al. An integrated network of androgen receptor, polycomb, and TMPRSS2-ERG gene fusions in prostate cancer progression. *Cancer Cell*. 2010;17:443–454.
- Leinonen R, Sugawara H, Shumway M. The sequence read archive. *Nucleic Acids Res*. 2011;39:D19–D21.
- Andrews S. FastQC: a quality control tool for high throughput

- sequence data. Babraham Institute, 2010. <http://www.bioinformatics.babraham.ac.uk/projects/fastqc/>. Accessed October 30, 2012.
43. Langmead B, Trapnell C, Pop M, Salzberg S. Ultrafast and memory-efficient alignment of short DNA sequences to the human genome. *Genome Biol.* 2009;10:R25.
44. Heinz S, Benner C, Spann N, et al. Simple combinations of lineage-determining transcription factors prime *cis*-regulatory elements required for macrophage and B cell identities. *Mol Cell.* 2010;38:576–589.
45. Shaffer PL, Jivan A, Dollins DE, Claessens F, Gewirth DT. Structural basis of androgen receptor binding to selective androgen response elements. *Proc Natl Acad Sci USA.* 2004;101:4758–4763.
46. Clark KL, Halay ED, Lai E, Burley SK. Co-crystal structure of the HNF-3/fork head DNA-recognition motif resembles histone H5. *Nature.* 1993;364:412–420.
47. Shi Y, Wang YF, Jayaraman L, Yang H, Massagué J, Pavletich NP. Crystal structure of a Smad MH1 domain bound to DNA: insights on DNA binding in TGF- β signaling. *Cell.* 1998;94:585–594.
48. Ginalski K, Elofsson A, Fischer D, Rychlewski L. 3D-Jury: a simple approach to improve protein structure predictions. *Bioinformatics.* 2003;19:1015–1018.
49. Pettersen EF, Goddard TD, Huang CC, et al. UCSF Chimera—a visualization system for exploratory research and analysis. *J Comp Chem.* 2004;25:1605–1612.
50. Macke T, Case DA. Modeling unusual nucleic acid structures. In: Leontes NB, SantaLucia J Jr, eds. *Molecular Modeling of Nucleic Acids*, Washington, DC: American Chemical Society; 1998:379–393.
51. Stroud JC. Automation of Making Nucleic Acid Helices by NAB. <http://structure.usc.edu/make-na/>. Updated August 3, 2013. Accessed August 7, 2011.
52. Darne CH, Morel L, Claessens F, et al. Ubiquitous transcription factors NF1 and Sp1 are involved in the androgen activation of the mouse vas deferens protein promoter. *Mol Cell Endocrinol.* 1997;132:13–23.
53. Kuwahara S, Ikei A, Taguchi Y, et al. PSPC1, NONO, and SFPQ are expressed in mouse Sertoli cells and may function as coregulators of androgen receptor-mediated transcription. *Biol Reprod.* 2006;75:352–359.
54. Dong X, Sweet J, Challis JR, Brown T, Lye SJ. Transcriptional activity of androgen receptor is modulated by two RNA splicing factors, PSF and p54nrb. *Mol Cell Biol.* 2007;27:4863–4875.
55. Salton M, Lerenthal Y, Wang SY, Chen DJ, Shiloh Y. Involvement of Matrin 3 and SFPQ/NONO in the DNA damage response. *Cell Cycle.* 2010;9:1568–1576.
56. Lemon B, Inouye C, King DS, Tjian R. Selectivity of chromatin-remodelling cofactors for ligand-activated transcription. *Nature.* 2001;414:924–928.
57. Shank LC, Kelley JB, Gioeli D, et al. Activation of the DNA-dependent protein kinase stimulates nuclear export of the androgen receptor in vitro. *J Biol Chem.* 2008;283:10568–10580.
58. Jia L, Berman BP, Jariwala U, et al. Genomic androgen receptor-occupied regions with different functions, defined by histone acetylation, coregulators and transcriptional capacity. *PLoS One.* 2008;3:e3645.
59. Yeung LH, Read JT, Sorenson P, Nelson CC, Jia W, Rennie PS. Identification and characterization of a prostate-specific androgen-independent protein-binding site in the probasin promoter. *Biochem J.* 2003;371:843–855.
60. Shang Y, Myers M, Brown M. Formation of the androgen receptor transcription complex. *Mol Cell.* 2002;9:601–610.
61. Piston DW, Kremers GJ. Fluorescent protein FRET: the good, the bad and the ugly. *Trends Biochem Sci.* 2007;32:407–414.
62. Tan PY, Chang CW, Chang KR, Wansa KD, Sung WK, Cheung E. Integration of regulatory networks by NKX3-1 promotes androgen-dependent prostate cancer survival. *Mol Cell Biol.* 2012;32:399–414.
63. Wang Q, Li W, Liu XS, et al. A hierarchical network of transcription factors governs androgen receptor-dependent prostate cancer growth. *Mol Cell.* 2007;27:380–392.
64. Espinás ML, Roux J, Pictet R, Grange T. Glucocorticoids and protein kinase A coordinately modulate transcription factor recruitment at a glucocorticoid-responsive unit. *Mol Cell Biol.* 1995;15:5346–5354.
65. Lupien M, Eeckhoutte J, Meyer CA, et al. FoxA1 translates epigenetic signatures into enhancer-driven lineage-specific transcription. *Cell.* 2008;132:958–970.
66. Biddie SC, John S, Sabo PJ, et al. Transcription factor AP1 potentiates chromatin accessibility and glucocorticoid receptor binding. *Mol Cell.* 2011;43:145–155.
67. Brüggemeier U, Rogge L, Winnacker EL, Beato M. Nuclear factor I acts as a transcription factor on the MMTV promoter but competes with steroid hormone receptors for DNA binding. *EMBO J.* 1990;9:2233–2239.
68. Crawford DR, Leahy P, Hu CY, et al. Nuclear factor I regulates expression of the gene for phosphoenolpyruvate carboxykinase (GTP). *J Biol Chem.* 1998;273:13387–13390.
69. Sharma NL, Massie CE, Ramos-Montoya A, et al. The androgen receptor induces a distinct transcriptional program in castration-resistant prostate cancer in man. *Cancer Cell.* 2013;23:35–47.
70. van der Heul-Nieuwenhuijsen L, Dits NF, Jenster G. Gene expression of forkhead transcription factors in the normal and diseased human prostate. *BJU Int.* 2009;103:1574–1580.
71. DeGraff DJ, Grabowska MM, Case T, et al. Foxa1 deletion in luminal epithelium causes prostatic hyperplasia and alteration of differentiated phenotype [published online May 19, 2014]. *Lab Invest.* 2014. doi:10.1038/labinvest.2014.64.
72. Helpap B, Köllermann J. Undifferentiated carcinoma of the prostate with small cell features: immunohistochemical subtyping and reflections on histogenesis. *Virchows Arch.* 1999;434:385–391.
73. Dooley AL, Winslow MM, Chiang DY, et al. Nuclear factor I/B is an oncogene in small cell lung cancer. *Genes Dev.* 2011;25:1470–1475.
74. Zhou Z, Flesken-Nikitin A, Corney DC, et al. Synergy of p53 and Rb deficiency in a conditional mouse model for metastatic prostate cancer. *Cancer Res.* 2006;66:7889–7898.
75. Scher HI, Fizazi K, Saad F, et al. Increased survival with enzalutamide in prostate cancer after chemotherapy. *N Engl J Med.* 2012;367:1187–1197.
76. Scher HI, Beer TM, Higano CS, et al. Antitumour activity of MDV3100 in castration-resistant prostate cancer: a phase 1–2 study. *Lancet.* 2010;375:1437–1446.
77. Fizazi K, Scher HI, Molina A, et al. Abiraterone acetate for treatment of metastatic castration-resistant prostate cancer: final overall survival analysis of the COU-AA-301 randomised, double-blind, placebo-controlled phase 3 study. *Lancet Oncol.* 2012;13:983–992.
78. Arora VK, Schenkein E, Murali R, et al. Glucocorticoid receptor confers resistance to antiandrogens by bypassing androgen receptor blockade. *Cell.* 2013;155:1309–1322.
79. Kaestner KH. The hepatocyte nuclear factor 3 (HNF3 or FOXA) family in metabolism. *Trends Endocrinol Metab.* 2000;11:281–285.
80. Mason S, Piper M, Gronostajski RM, Richards LJ. Nuclear factor one transcription factors in CNS development. *Mol Neurobiol.* 2009;39:10–23.